

**PARAMETRIC STUDY OF CURVED STEEL BRIDGES
SUPPORTED ON NARROW CONCRETE PIERS**

by

JASON ERIC OLSEN, B.S.C.E.

THESIS

**Presented to the Faculty of the Graduate School of
The University of Texas at Austin
in Partial Fulfillment
of the Requirements
for the Degree of**

MASTER OF SCIENCE IN ENGINEERING

THE UNIVERSITY OF TEXAS AT AUSTIN

May 1994

**PARAMETRIC STUDY OF CURVED STEEL BRIDGES
SUPPORTED ON NARROW CONCRETE PIERS**

APPROVED:

ABSTRACT

PARAMETRIC STUDY OF CURVED STEEL BRIDGES SUPPORTED ON NARROW CONCRETE PIERS

by

**JASON ERIC OLSEN, MASTER OF SCIENCE IN ENGINEERING
THE UNIVERSITY OF TEXAS AT AUSTIN, 1994
SUPERVISOR: MICHAEL ENGELHARDT**

This study investigates horizontally curved steel plate girder bridges supported on narrow concrete piers as currently used by the Texas Department of Transportation. All longitudinal girders are supported on individual bearings at the ends of the bridge, but at the intermediate supports, the girders connect to steel bent caps. Each bent cap is supported by a narrow concrete pier through two bearings spaced six to twelve feet apart.

Because the bridge is not supported across its full width at the intermediate supports, downward live loads placed on the bridge outside of the bearings tend to increase compression in the closer bearing but tend to decrease compression in the further bearing. Finite element analyses of some typical bridges were conducted to determine the load placements which maximize or minimize compression in the bearings. The results of the analyses were used to produce simplified load patterns which can be used in the design of the bearings.

Another consequence of supporting the deck on narrow piers is that such a support condition violates the assumptions of the V-load method, an analysis

technique for curved plate-girder bridges. Comparisons were made between finite element analyses and V-load analyses of some typical bridges to determine if the V-load method produces reasonably accurate girder moments and bearing reactions when some of its assumptions are violated. The V-load method was found to produce results which typically are no worse than a few percent unconservative. The V-load method was also found to produce reasonable results when the piers are offset from the centerline of the deck.

Supporting the deck on narrow piers also affects the forces in the deck's cross-frames. The V-load method gives reasonable estimates of the cross-frame forces due to the resistance of the internal torsion of the curved deck and the AASHTO equations give reasonable estimates of the cross-frame forces due to wind load. However, the critical forces in the cross-frames result from supporting the deck on narrow piers. A somewhat flexible bent cap, when supported by a narrow pier at the center, will deflect at the ends, which in turn causes the nearby cross-frames to deflect at the ends. These imposed deflections produce cross-frame forces which can be several times larger than forces due to the resistance of internal torsion or wind load. Deflection limits should be imposed on the bent caps to keep the cross-frame forces below the allowable levels.

TABLE OF CONTENTS

Chapter 1: Analysis Goals	1
Chapter 2: Description of the Bridge Systems	6
Chapter 3: Maximum Forces and Rotations at the Bearings	22
Chapter 4: Evaluation of the V-load Method	49
Chapter 5: Evaluation of Cross-frame Forces	86
Chapter 6: Summary and Conclusions	112
Appendix A: Description of the Finite Element Models	117
Appendix B: Verification of the Models	138
Appendix C: The V-load Method	159
Bibliography	169
Vita	170

CHAPTER 1

ANALYSIS GOALS

Introduction

This thesis presents the results of some analyses of horizontally curved steel plate girder bridges. The typical bridge studied herein consists of a reinforced concrete slab supported on longitudinal steel plate girders and has three spans with span lengths between 100 and 200 feet. The girders are braced against lateral load and torsion by steel cross-frames evenly spaced along the length of the bridge. At the ends of the bridge each girder rests directly on a concrete support. At intermediate supports along the length of the bridge, the girders frame into transverse steel bent caps, which in turn are supported on single, narrow reinforced concrete piers. The connections between the bent caps and the piers typically consist of rocker bearings or pot bearings to provide vertical support and rotational freedom about a transverse axis. Anchor bolts provide resistance to any uplift arising from torsion in the bridge. A more complete description of the bridge system is provided in Chapter 2.

The analyses presented herein were conducted primarily in the pursuit of four goals. The first goal was to determine reaction forces and deflections at the bearings using the finite element method. Achieving the first goal required the pursuit of the second goal of determining loading patterns which produced maximum bearing forces and deflections. The third goal was to verify the

adequacy of the V-load method for determining both the behavior of the longitudinal girders and the behavior of the bent cap and bearings. The fourth goal was to investigate the forces developed in the cross-frames.

Bearing forces and deflections

This analytical study is part of a larger study which seeks to verify the adequacy of current bearing designs and to develop and test new, more cost-effective bearing designs. The primary work of this larger study is to experimentally establish the stiffness, fatigue strength and ultimate strength of both the current and proposed new bearing designs. Determining the capacities of these connections, however, is only meaningful if the capacities can be compared to reasonable estimates of the loads to which the connections will be subjected. Thus, it is part of the first goal of this analysis portion of the project to determine the maximum forces expected in the bearings for comparison against the ultimate capacity of the bearings, and to determine the range of forces caused by cyclic loading for comparison against the fatigue capacity of the bearings.

In addition to providing adequate capacity to support the loads, the bearings are also designed to allow rotation of the longitudinal girders about a transverse axis. Providing such rotational freedom complicates the bearing design and increases the costs. Consequently, the new bearing designs under evaluation have removed the physical pin in the bearing and have replaced it with a heavy wide-flange section. To provide rotational freedom the wide-flange bearing must deform. Since the bearing rotations are cyclic, the deformations in the wide-flange bearing member may lead to fatigue problems. Thus, a part of the analysis portion of this project will determine the range of bearing rotation.

Loading patterns producing maximum bearing forces

The maximum static load or the maximum range of cyclic loading on the bearing requires the application of both dead and live loading. Once the bridge is constructed and is in service, the distribution of dead load is constant. Live load, on the other hand, varies continuously. Because of the T-shape of the bent cap and pier, simply applying the maximum live load to all parts of the bridge does not necessarily produce the largest forces in all of the bearings. As shown in Figure 1-1, a load applied to the bent cap from the exterior girder on the right increases the downward force on the right bearing but decreases the force on the left bearing. Thus such a load will be included in finding the maximum downward force for the bearing on the right but will not be included when finding the maximum downward force for the bearing on the left. In general, to determine when a load increases or decreases a bearing force, an influence surface can be created. From the influence surface, loading patterns can be selected in which the load is applied on only those areas which tend to increase forces, thus producing the maximum force in the bearing. It is the second goal of this project to determine these loading patterns.

Evaluation of the V-load method

Simplified analysis techniques are typically used for curved steel bridges. The techniques involve distributing the load from the slab to the girders by applying a fixed fraction of the total slab load to each girder. The girders are then analyzed using an approximate technique for curved bridges called the V-load method, which is described in Appendix C. From the V-load analysis, reactions at the girder supports are calculated. Where the girders are supported by a bent cap, the reactions are applied as forces on the bent cap to determine bearing forces.

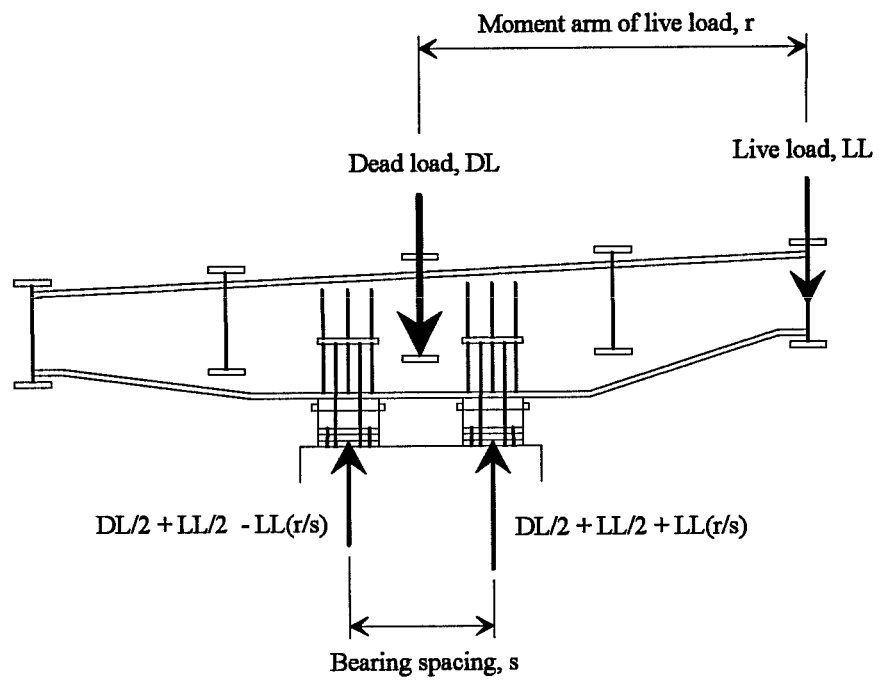


Figure 1-1: Bearing forces due to eccentric load

To determine if these simplified analysis techniques provide a reasonably accurate prediction of bearing forces, it is the third goal of this study to compare the results of the V-load method to the results of a more sophisticated analysis technique, namely the finite element method.

Investigation of the cross-frames

The cross-frames are provided to control the torsion that naturally results in curved girders subjected to vertical load. The V-load method gives an estimate of the forces applied to the cross-frames by the girders. The design of these cross-frames, then, is based on these forces from the V-load analysis and also on forces produced by transverse loads. The V-load method, however, ignores the contribution of the slab to resisting torsion in the girders and thus produces an inaccurate distribution of forces in the cross-frames. Furthermore, the flexibility of the bent cap in bending allows the exterior girders to sag relative to the interior girders, thus generating additional forces on adjacent cross-frames. It is thus the fourth goal of this study to determine more accurately the forces in the cross-frames.

Analysis method

In order to provide the most accurate analytical results possible, the bridge systems in this study were modeled using the finite element method. A commercially available general purpose finite element program, ANSYS, was used in this study. Details of the finite element models developed for this study using ANSYS are provided in Appendix A. Verification of the modeling techniques is outlined in Appendix B, where finite element analysis results are compared to closed form solutions for a simplified structure.

CHAPTER 2

DESCRIPTION OF THE BRIDGE SYSTEMS

Introduction

The focus of this study was on typical horizontally curved steel bridge systems designed by the Texas Department of Transportation (TxDOT). Three span horizontally curved bridges with span lengths between 100 and 200 feet and radii of curvature between 1000 and 2500 feet were investigated. The typical bridge consists of a reinforced concrete slab, superelevated four to six percent, supported on longitudinal steel plate girders. The girders are braced by cross-frames evenly spaced along the length of the bridge. At the ends of the bridge each girder rests directly on a concrete support. At intermediate supports along the length of the bridge, the girders frame into transverse steel bent caps, which in turn are supported on single, narrow reinforced concrete piers. Plan and elevation views of a typical bridge are shown in Figure 2-1.

Slab details

The typical reinforced concrete slab for these bridges is from 30 to 60 feet wide and is supported on four to seven longitudinal girders. The number of girders is such that the lateral center-to-center spacing of the girders is between 7 feet 6 inches and 9 feet, with the slab cantilevered an additional three feet beyond the centerlines of both the inside and outside girders. Such

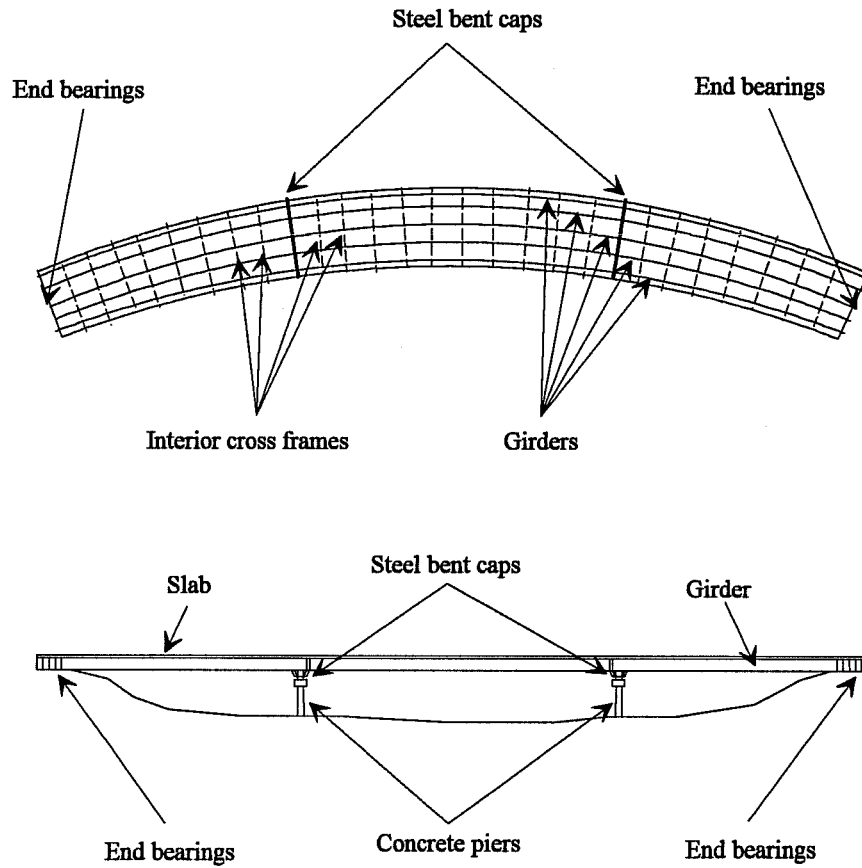


Figure 2-1: Plan and elevation views of a horizontally curved steel bridge

unsupported slab widths lead to slab thicknesses between 7-1/2 and 8 inches thick over the unsupported width. Over the girders, the slab thickness is increased to compensate for variations in top flange thickness by keeping the distance between the top of the slab and the tops of the girder webs constant. A typical detail of a slab is shown in Figure 2-2.

The slab is made composite with the girders over the positive moment regions of the bridge. Shear studs are provided at two foot intervals over most of the positive moment region with the exception of the ends of the positive moment regions where the spacing is reduced to 1 foot or less.

The 3000 psi concrete slab is poured in five stages. The first two stages entail placement of the concrete in the regions of the two end spans where dead loads produce positive moments. In the third stage, the concrete is placed in the positive moment region of the center span. Finally in the last two stages, the concrete is placed in the two negative moment regions. The bridge is continuous at all four construction joints with no provisions for thermal expansion at the joints. Some bridge plans allow the contractor the option of pouring the slab continuously, given that a minimum number of linear feet, typically 30 feet, of slab are poured and finished per hour.

Girder details

The girders are assembled from corrosion-resistant, high-strength A588 steel ($F_y = 50$ ksi) plates welded together to form wide flange sections. A common web depth, typically between 48 and 66 inches, and a common flange width, typically between 16 and 20 inches, are used for all girders of a bridge, where the larger plate widths are used for longer span bridges. For economy, the bending and shear strength provided by the girder is varied along the length of the girder according to the bending and shear forces from the moment and

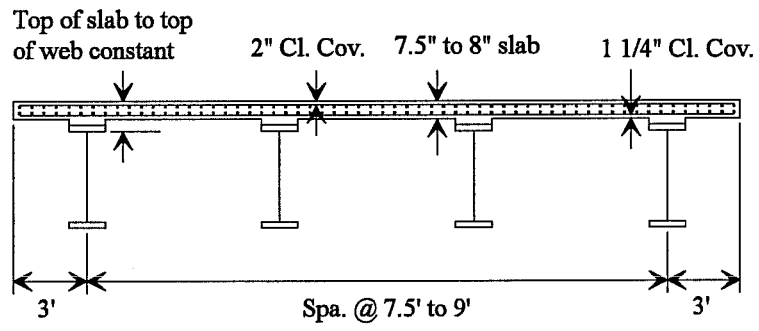


Figure 2-2: Typical slab detail

shear diagrams. This is accomplished by varying the thicknesses of the flange and web plates. The web plate thickness is typically $1/2$ inch over the middle of the spans and increases to as much as $11/16$ inch over the supports. Both the top and the bottom flange plate thicknesses are typically 1 inch over the regions with the least moment and increase to as much as 3 inches in the most highly stressed portions of the negative moment region and to as much as $1-1/4$ inches in the most highly stressed portions of the positive moment region. A typical girder detail is shown in Figure 2-3.

Cross-frame details

To distribute lateral loads and to resist torsion resulting from the curvature of the bridge, cross-frames brace the girders at intervals of 15 to 18 feet. The two end cross-frames use a standard K-brace detail as shown in Figure 2-4. The intermediate cross-frames use a standard X-brace detail as shown in Figure 2-5.

Bent cap details

The bent cap is assembled like the longitudinal girders from A588 plates welded together to form a wide-flange girder. Web depth varies along the length of the bent cap with the bent cap deepest where moment is the greatest and shallowest where moment is the least. At the center of the caps, where moments are the greatest, the web depth is greater than the depth of the longitudinal girders. At the ends of the cantilevered caps, where moments are the least, the web depth is less than the depth of the longitudinal girders. The web plate has a constant thickness typically between $3/4$ and $1-1/4$ inches, where the thicker plates are used for wider bridges. A common flange width, typically 20 to 30 inches, is used for all flange plates, where the wider flange

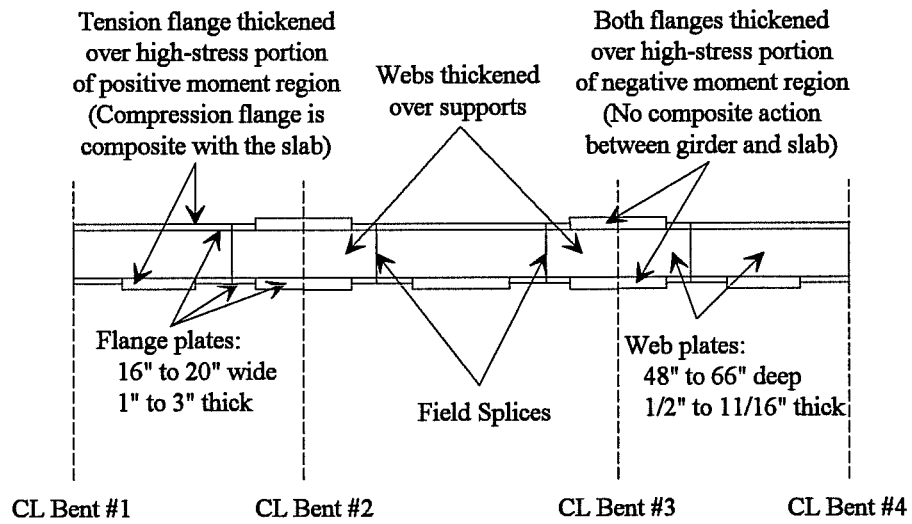


Figure 2-3: Typical girder detail

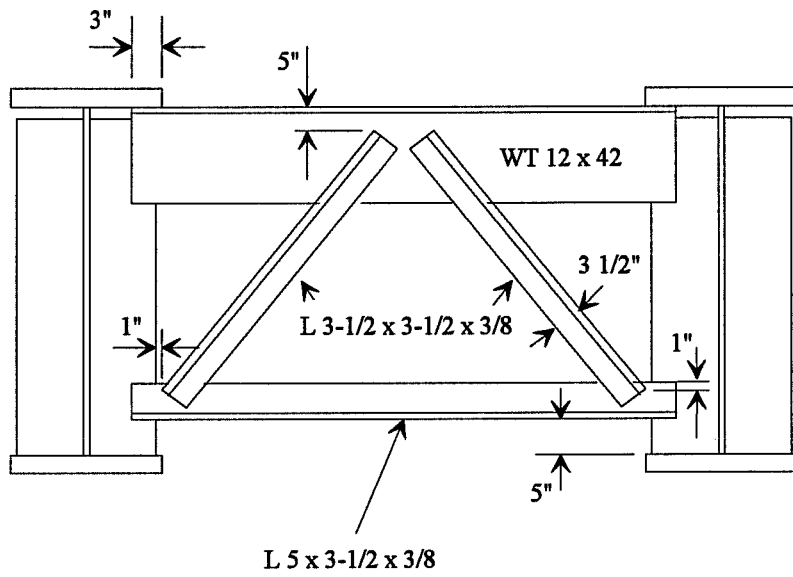


Figure 2-4: Standard K-brace detail

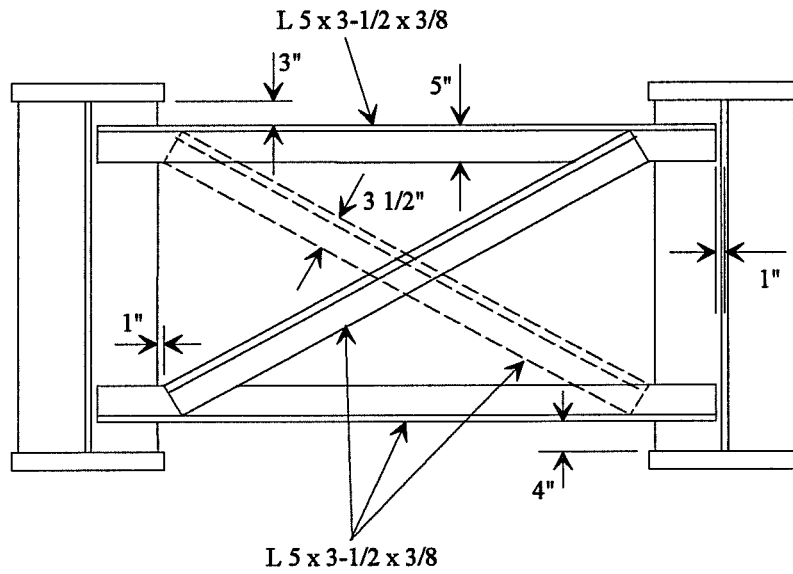


Figure 2-5: Standard X-brace detail

plates are typically used for wider bridges. A single top flange thickness of 2 to 2-1/4 inches is used over the full length of the bent cap. The bottom flange consists of plates of two thicknesses. Thinner plates of 1 to 2 inches are used at the ends of the bent cap and a thicker plate of 2-3/4 to 3 inches is used over the center of the bent cap. A typical bent cap detail is shown in Figure 2-6.

The longitudinal girders are made continuous at the bent caps by a combination of bolted and welded connection elements as shown in Figure 2-7. The tops of the longitudinal girders are coped to allow the top flange of the bent cap to pass through the tops of the webs of the longitudinal girders, thereby retaining continuity of the bent cap. To restore continuity to the top flanges of the longitudinal girders, plates connecting the discontinuous flanges are bolted onto both the tops and bottoms of the top flanges. The bottom flanges are made continuous by welding the flanges to plates which are bolted to the web of the bent cap. The webs of the longitudinal girders are bolted to the web of the bent cap using angles.

The bent cap is supported on two bearings spaced 6 to 12 feet apart. Present designs place the centerline of the pier coincidental with the centerline of the bridge, but future designs may offset the centerline of the pier from the centerline of the bridge in cases where the layout of an interchange restricts placement of the piers.

General bearing details

Currently two types of bearing details are in use: a rocker bearing and a disc bearing. The bearings are designed to allow rotation of the pier cap about an axis parallel to the axis of the bent cap, so as to approximate a pinned support for the longitudinal girders and to minimize the transfer of transverse moment into the concrete pier. This rotational freedom about the transverse

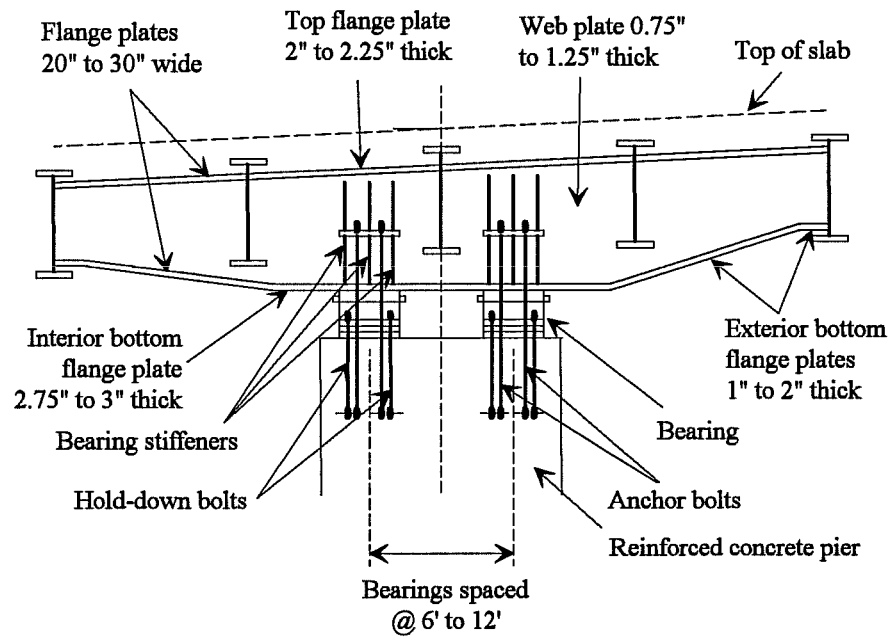


Figure 2-6: Typical bent cap detail

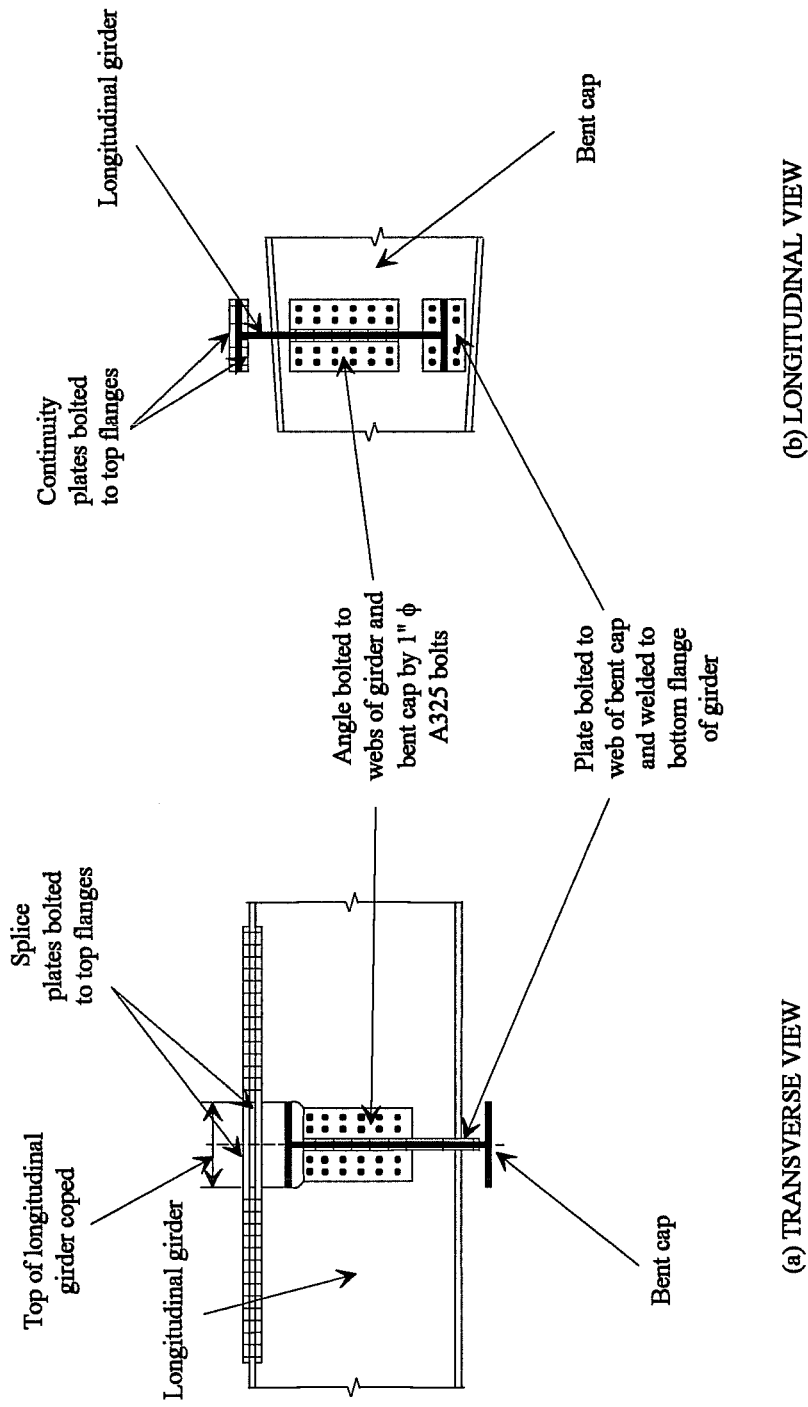


Figure 2-7: Typical girder-to-bent cap connection

axis is provided by supporting the bridge on a narrow rocker or elastomeric pad. At the same time the bearings are designed to fix the rotation of the cap about an axis parallel to the axis of the bridge. This rotational fixity about the longitudinal axis is accomplished by using a wide support consisting of two bearings spaced 6 to 12 feet apart.

In addition to providing rotational freedom and fixity as appropriate, the bearing is designed primarily to provide vertical support. The bent cap is supported against downward forces by resting the bottom flange of the bent cap on the bearings which in turn rest on the concrete pier. Stiffeners are used to prevent crippling or local yielding of the web of the bent cap at the bearing locations.

Rocker bearing details

A typical rocker bearing is shown in Figure 2-8. Rotational freedom about the transverse axis is provided by a rounded machined convex bearing surface connected to the concrete pier and the companion concave plate connected to the bottom flange of the bent cap. Thick steel plates welded to the bottom of the pin distribute vertical stresses from the narrow bearing surface to the concrete pier. To provide resistance to uplift and horizontal shear, the steel bent cap is bolted to the concrete pier by means of anchor bolts. The tops of the anchor bolts pass through horizontal plates in the bent cap which in turn bear on the web stiffener plates. The bottoms of the anchor bolts are fastened to a bolt template embedded roughly three feet below the top of the pier. Hold-down bolts also fasten the lower portion of the bearing to the bolt template embedded in the concrete pier.

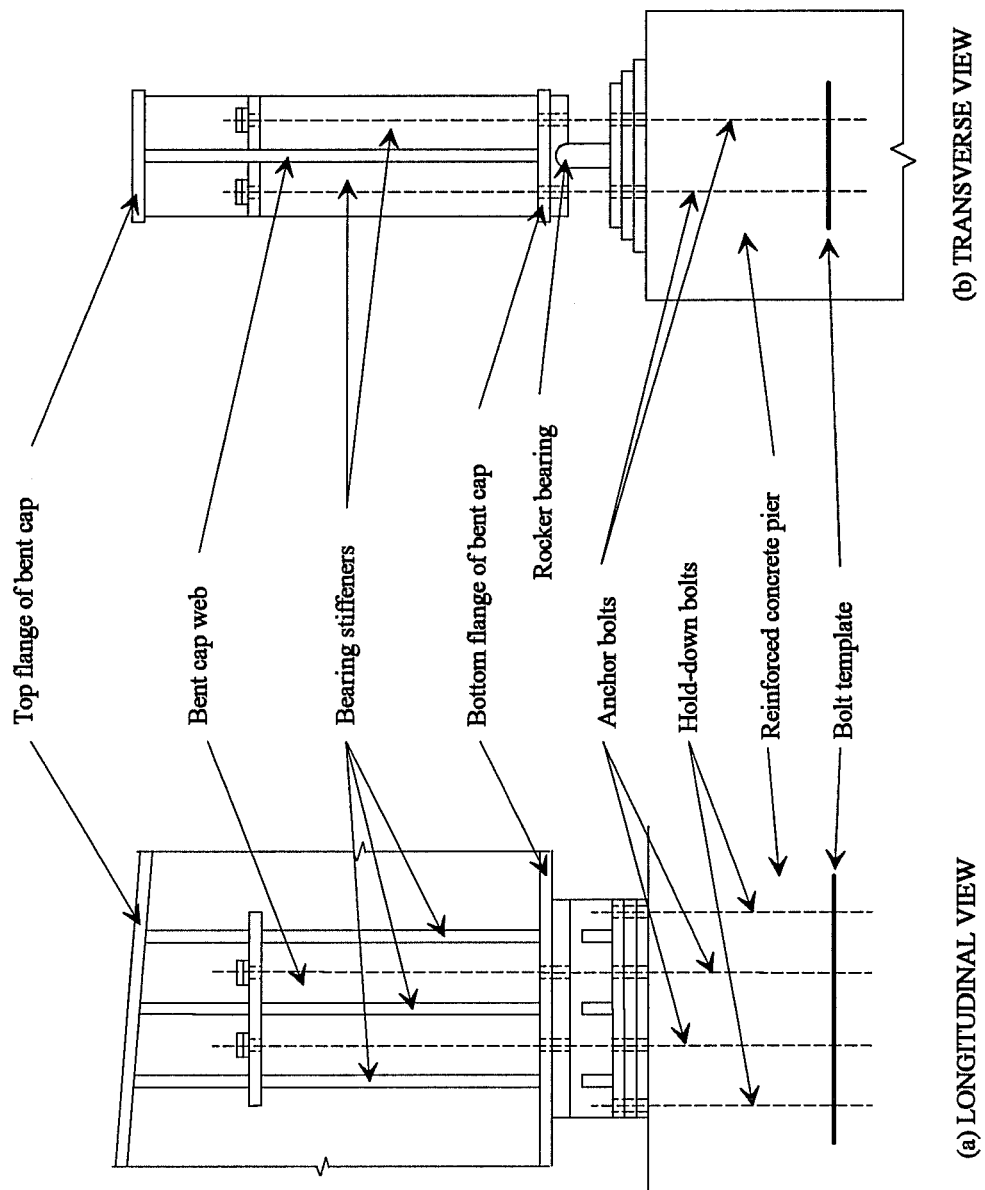


Figure 2-8: Typical rocker bearing detail

Disc bearing details

A typical disc bearing is shown in Figure 2-9. Rotational freedom about the transverse axis is provided by resting the bent cap on a flexible elastomeric disc between two steel discs attached to the bottom flange of the bent cap and to the top of the concrete pier, respectively. Horizontal shear resistance is provided by a shear key between the steel discs.

Wide-flange bearing details

A typical wide-flange bearing is shown in Figure 2-10. This bearing detail is currently under investigation as part of this research project. A heavy rolled wide-flange section is used in place of the complicated bearing elements used in the rocker and disc bearings. Such a detail should allow transverse rotational flexibility by bending of the web of the W-section and should provide vertical support by compression of the web.

Selection of bridge systems for analysis

The bridge systems analyzed in this study are based on actual designs provided by TxDOT. The analyses required the variation of several bridge parameters, such as radius of curvature, span length, and bearing spacing. In such a parametric study, it is easiest to correlate the results of the variation of a parameter with the variation of that parameter itself when only one parameter is allowed to vary at a time. Because several parameters vary from the design of one TxDOT bridge to the next, it was not feasible to use the actual TxDOT designs in this parametric study. Rather, typical details were abstracted from the TxDOT designs. These typical details, which have been described in this chapter, served as a basis for generating hypothetical bridges for analysis.

In the design of actual bridges, it is typically necessary to vary member

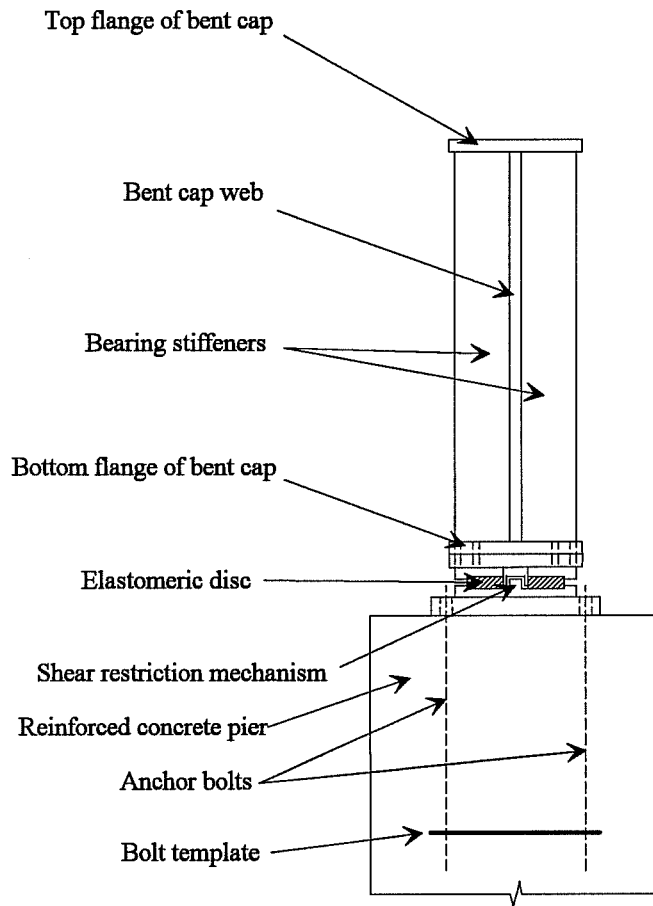


Figure 2-9: Typical disc bearing detail

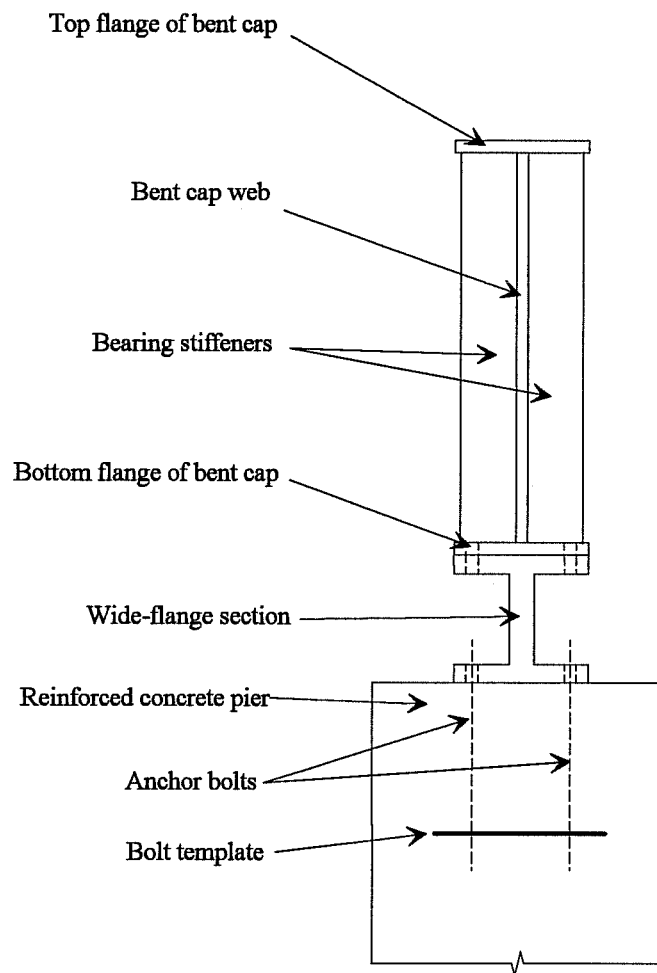


Figure 2-10: Possible wide-flange bearing detail

sizes along with particular bridge parameters. For example, increasing the span length will necessitate increasing the girder plate thicknesses. The designer, however, has countless ways to choose member sizes for a particular bridge. In designing a girder over a particular span, for example, the designer may choose to use only three different flange plate thicknesses which coarsely follow the moment diagram, or the designer may choose to use ten different flange plate thicknesses which follow the moment diagram more closely. The different choices of member sizes may lead to different distributions of stiffness in the bridge. As a result, when member sizes are varied simultaneously with the parameter under inspection, the results may be unduly affected by the particular choice of member sizes rather than simply being affected by the variation of the parameter. To avoid this problem, member sizes were not varied along with the parameters.

CHAPTER 3

MAXIMUM FORCES AND ROTATIONS

AT THE BEARINGS

Introduction

The critical reactions and deformations in the bearings are the vertical forces, either compression or uplift, and the rotations about a transverse axis. This analysis seeks to determine the range and maximum values of these forces and rotations.

The typical bridge has multiple spans and portions of the bridge are cantilevered from single piers at the interior support locations. Consequently, the live load may increase or decrease the compression in a given bearing depending on the location of the load. Likewise, the location of the load can affect the direction of the rotation at a given bearing. To determine how to place the load so as to maximize or minimize compression in a bearing or to maximize rotation in one direction or the other, influence surfaces can be created.

An influence surface is a three-dimensional contour plot of the magnitude of some response parameter, such as bearing force or rotation, projected over the surface of the bridge. The magnitude of the response parameter at a given point on the influence surface corresponds to the response that would result from applying a unit load at that point on the surface of the bridge. For design purposes the information provided by this three-dimensional

plot is typically more information than is necessary. For example, when the loading consists of a single concentrated load on the bridge, it is sufficient to know simply the two locations where the load produces the greatest positive and the least negative response. When the loading consists of a surface load, it is sufficient to know simply the sign of the parameter over the surface – whether the load applied at a given point on the surface contributes positively or negatively to the response – and not the actual magnitude of the response. Such are the loadings for bridges, where the loads are either small clusters of concentrated loads representing a single truck or surface loads representing lane loads. Consequently, rather than presenting three-dimensional contour plots, the influence surfaces will be presented as two-dimensional plots of the bridge surface indicating the two points where concentrated loads produce the peak positive and negative responses and indicating the areas over which surface loads would contribute positively or negatively to the response. All influence surfaces were developed using finite element models of bridges as described in Appendix A.

AASHTO [1] specifies two types of live loads, namely truck loads and lane loads. For the HS20-44 class of loading used for bridges exposed to heavy truck traffic, the truck load consists of six concentrated loads totaling 72 kips spaced to correspond to the wheels of a typical tractor truck with a semitrailer. The lane load consists of a uniform load over a 10 foot width of 640 pounds per linear foot and, in the case of multiple spans, either two concentrated loads of 18 kips each for determining the maximum negative moment, a single concentrated load of 18 kips for determining the maximum positive moment, or a single concentrated load of 26 kips for determining the maximum shear, placed so as to maximize the respective stress. For both truck and lane loads, the loads are placed in design lanes 12 feet wide spread across the full width of

the bridge from curb to curb. The traffic lanes are placed on the bridge, and the loads are placed within the individual traffic lanes, so as to maximize the stress in the member under consideration. Any fractional lane widths remaining after the lanes are spread across the bridge are not used. Only a single truck is placed in each lane of the bridge whereas the lane load can be applied either continuously or discontinuously over the full length of the bridge. For three or more lanes of traffic live load reduction factors are permitted.

The truck loads are intended essentially to produce maximum shears and moments in the girders of short spans. In long spans, lane loads usually control for shear and moment. Moreover, lane loads also usually control for bearing reactions. Consider a three span continuous bridge with spans of 150 feet each. A 72 kip truck load concentrated over a support produces a maximum vertical reaction of only 72 kips, whereas a 640 pound per foot lane load over two adjacent spans produces a maximum vertical reaction of 115.2 kips. Thus, to produce the maximum compression or uplift in a bearing, lane loads rather than truck loads should be applied on all regions of the bridge where those loads maximize the compression or uplift.

Influence surface for vertical reactions

A sample three-span, five-girder bridge is used to illustrate the typical shape of the influence surface for the vertical reactions at the bearings. The first sample bridge has a radius of curvature of 2000 feet and has symmetric span lengths of 150 feet – 180 feet – 150 feet. To determine whether the curvature of the bridge affects the influence surface substantially, the second bridge has only half the radius of curvature of the first bridge but also has symmetric span lengths. To determine whether differences in span length affect the influence surface, the third bridge uses asymmetric span lengths of 120 feet

– 210 feet – 150 feet but retains the original radius of curvature of 2000 feet.

The first sample bridge has a radius of curvature of 2000 feet and span lengths of 150 feet for each end span and 180 feet for the center span. The influence map for the vertical reaction in bearing #1, an interior bearing, is shown in Figure 3-1 and the influence map for the vertical reaction in bearing #2, an exterior bearing, is shown in Figure 3-2. As might be expected, placing a concentrated load at the innermost edge of the bridge at the cross-section of the bearing produces the greatest compression in the interior bearing while placing a concentrated load at the outermost edge at about the same cross-section produces the greatest uplift in that bearing. Also as might be expected, the converse is true for the exterior bearing. As for the lane loads, however, placement might not be so obvious. It might be believed that placing lane loads in all lanes and along the full length of the bridge produces the greatest bearing reactions. Such a loading pattern certainly produces the greatest total compression in all of the bearings summed together. For an individual bearing, however, the load over part of the area of the bridge produces compression in the bearing while the load on the remaining area produces uplift, so loading the entire bridge produces a lesser reaction than would be produced if the load were applied only over the area contributing to compression in the bearing.

For the two spans on either side of the bearing, the line demarcating the areas over which loads produce compression and the areas over which loads produce uplift follows roughly the centerline of the bearings where the area leading to compression bulges slightly over the centerline. Thus, in these two spans when using an analysis method which analyzes the girders individually, such as the V-load method, it would be convenient to load the interior and center girders to produce maximum compression in the interior bearing and to load the exterior girders to produce maximum uplift in the interior bearing.

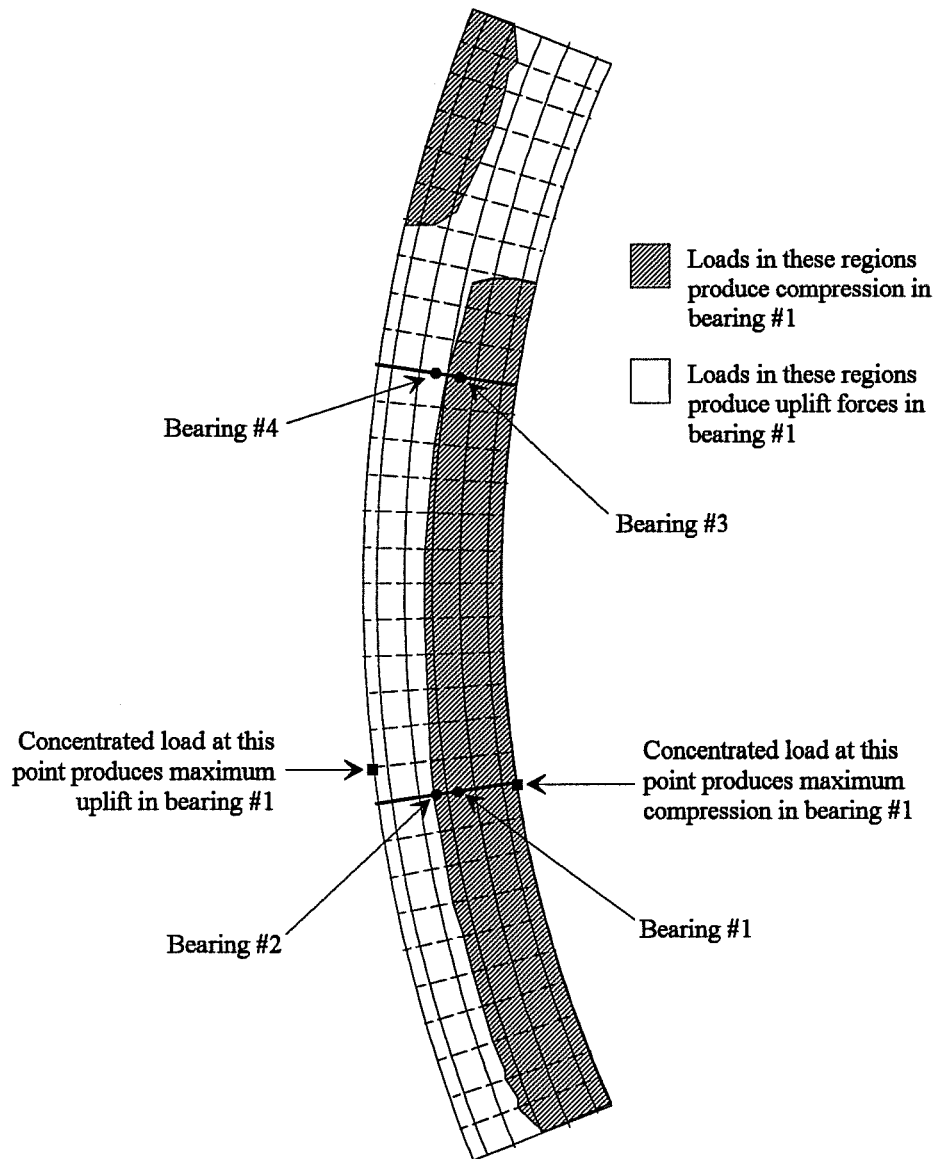


Figure 3-1: Influence surface for an interior bearing of a symmetric 2000' radius bridge

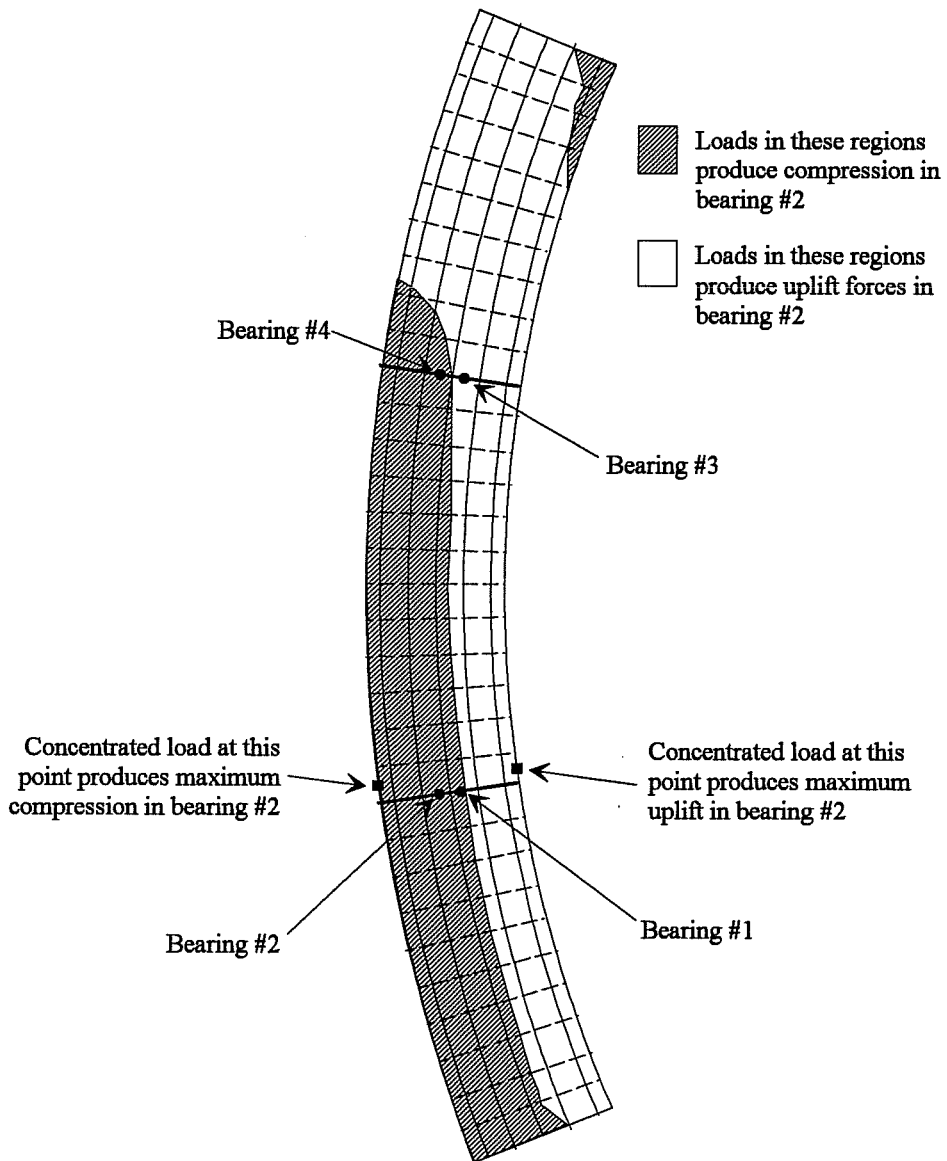


Figure 3-2: Influence surface for an exterior bearing of a symmetric 2000' radius bridge

Likewise, it would be convenient to load the exterior and center girders to produce maximum compression in the exterior bearing and to load the interior girders to produce maximum uplift in the exterior bearing.

In the far span not adjacent to the bearings, however, the loading pattern is more complicated. The pattern for the other two spans continues for a short distance into the third span, but then the pattern switches so that it roughly mirrors the original load pattern from the first two spans. This situation is analogous to a three-span continuous girder where uniform loads can be placed on each span. As shown in Figure 3-3, loading the spans adjacent to a bearing puts the bearing into compression whereas loading the far span puts the bearing into uplift. It should be added, however, that the contribution of the load in the far span to the reaction in a bearing is typically very small compared to the contributions from the adjacent spans – usually loading the far span changes the reaction in a bearing by less than two percent. Figure 3-4 shows the three dimensional plot of the same influence surface shown in Figure 3-1. As the figure shows, forces in the far span from bearing #1 contribute very little to the reaction in bearing #1. Thus, it may be sufficient to disregard the contribution of loads in the far span and load only the adjacent spans to produce the worst-case compression and uplift reactions in a bearing.

Figures 3-5 and 3-6 show the influence surfaces when the radius of curvature of the bridge is halved. The locations for the concentrated loads have not changed, nor have the surface load patterns in the two spans adjacent to the bearings under consideration. Slight changes appear in the far span, but again, the loads in the far span do not significantly affect the bearing reactions.

Figures 3-7 and 3-8 show the influence surfaces when the span lengths are made asymmetric. The surface load patterns have not changed appreciably, but the locations for the two concentrated loads have moved slightly.

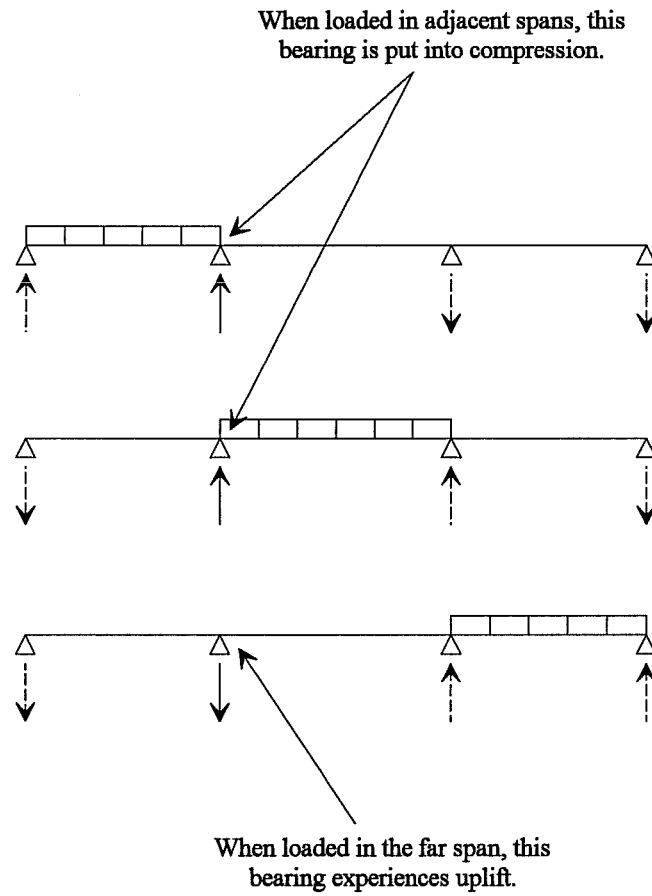
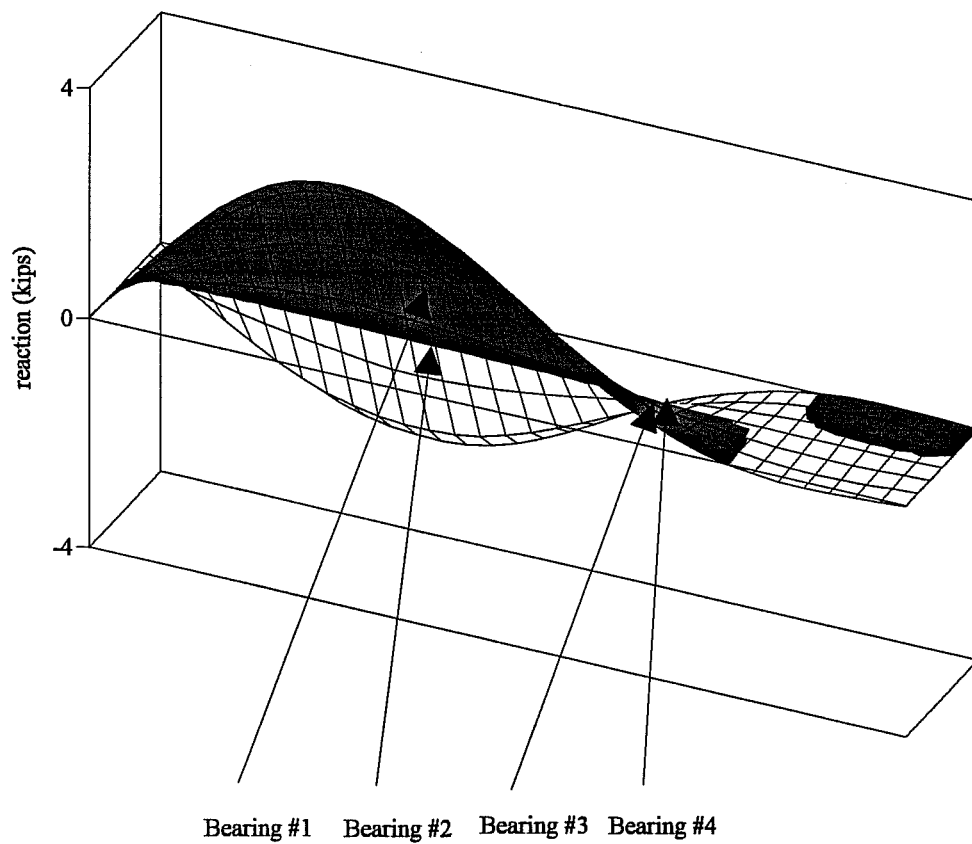


Figure 3-3: Effects of the placement of loads on the reactions in a continuous girder

Figure 3-4: Influence surface for the vertical reaction at an interior support of a symmetric 2000' radius bridge



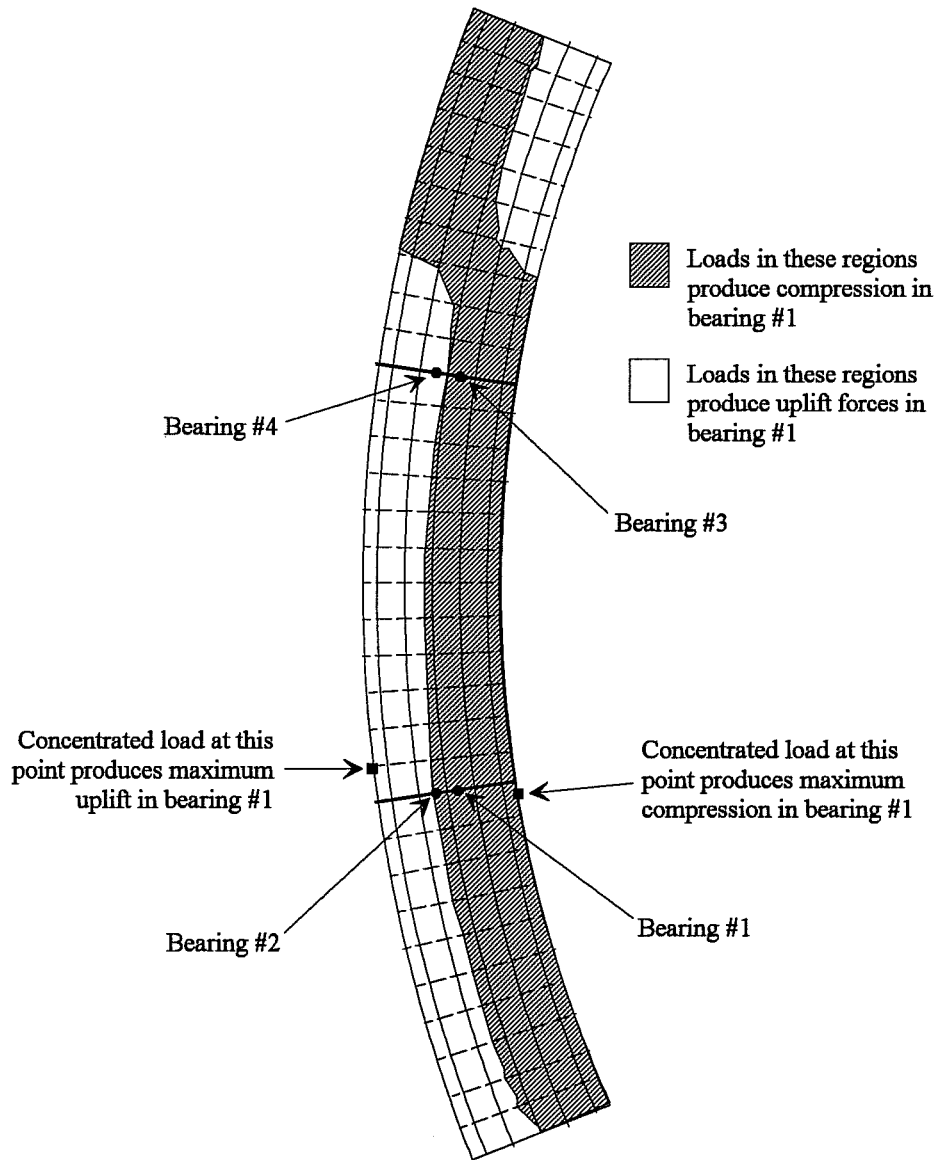


Figure 3-5: Influence surface for an interior bearing of a symmetric 1000' radius bridge

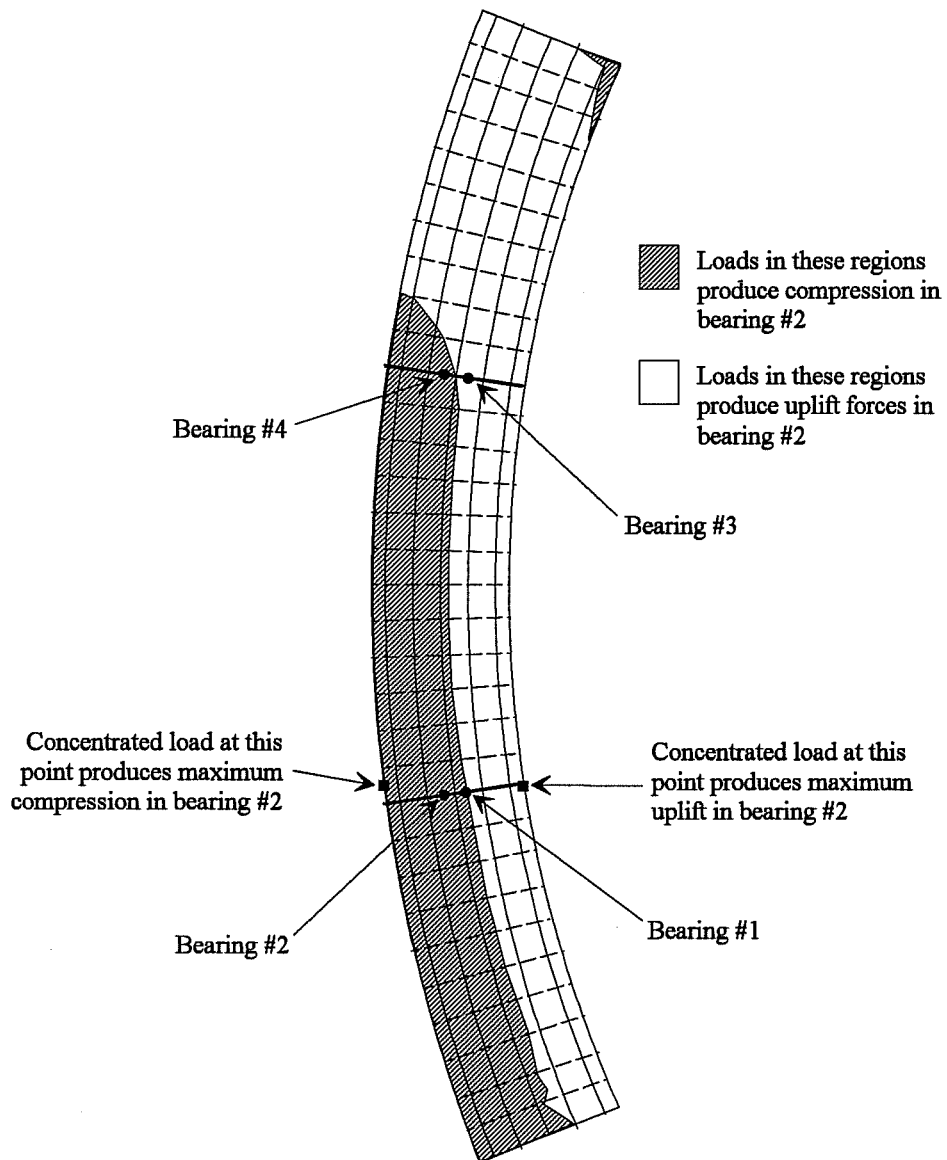


Figure 3-6: Influence surface for an exterior bearing of a symmetric 1000' radius bridge

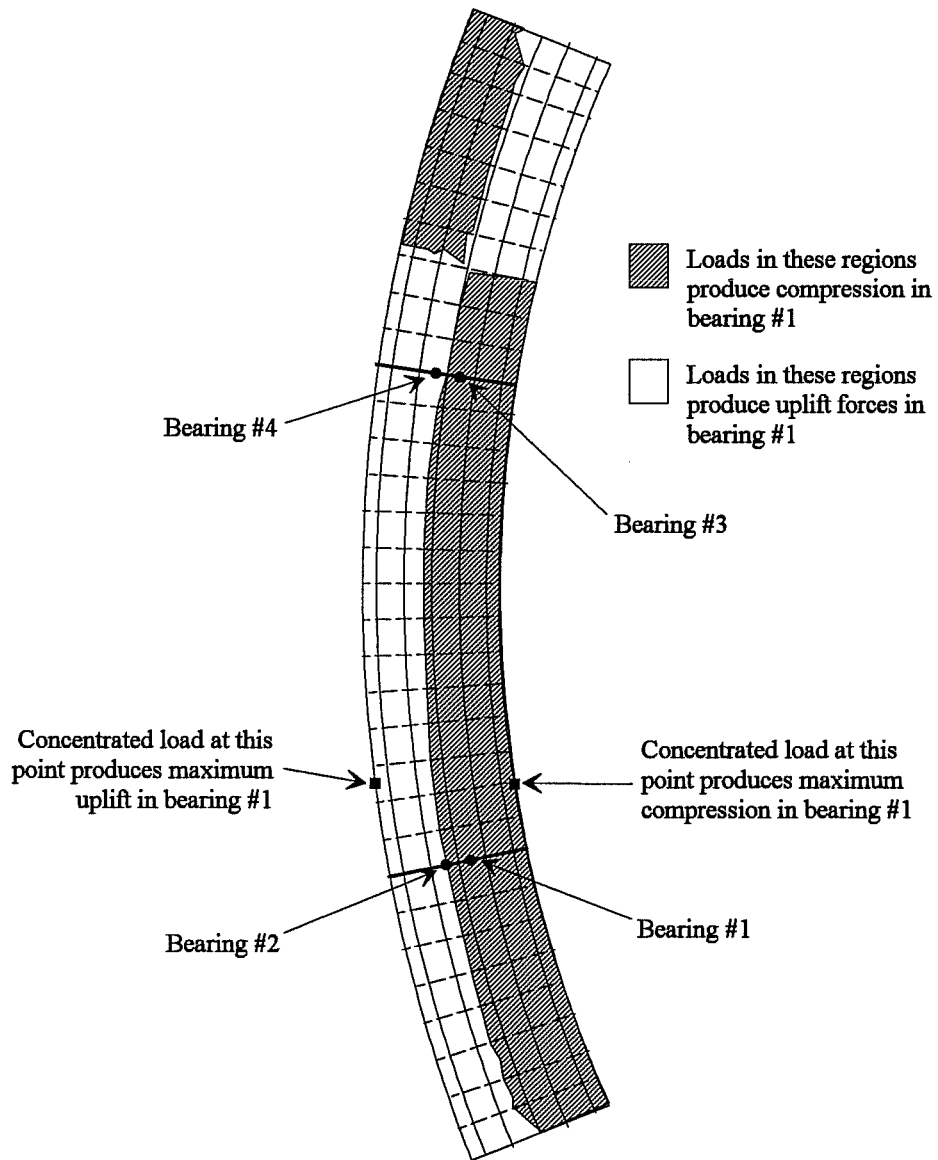


Figure 3-7: Influence surface for an interior bearing of an unsymmetric 2000' radius bridge

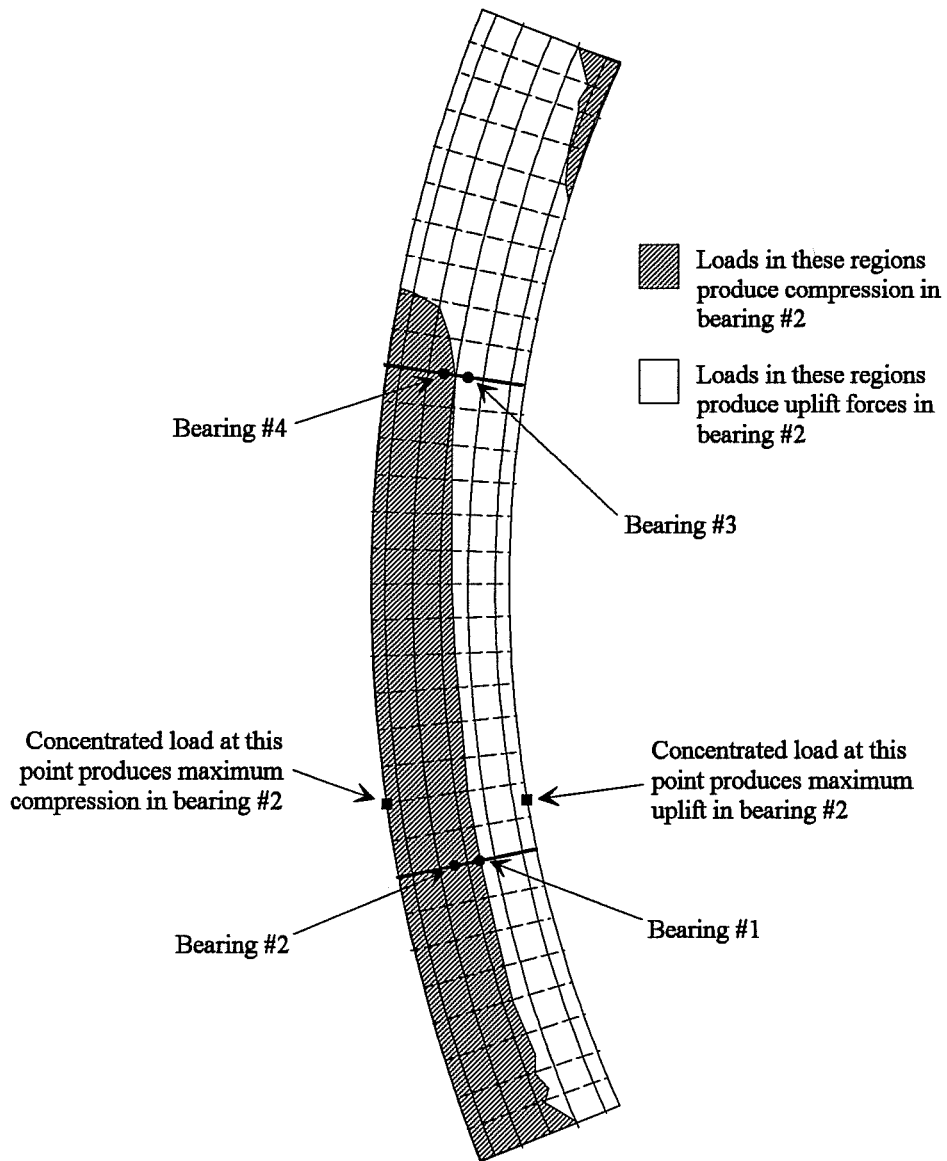


Figure 3-8: Influence surface for an exterior bearing of an unsymmetric 2000' radius bridge

Influence surface for rotations about a transverse axis

A sample three-span, five-girder bridge is also used to illustrate the typical shape of the influence surface for the rotation about a transverse axis at the bearings. Like before, the first sample bridge has a radius of curvature of 2000 feet and has symmetric span lengths of 150 feet – 180 feet – 150 feet. To determine whether the curvature of the bridge affects the influence surface substantially, the second bridge has only half the radius of curvature of the first bridge but also has symmetric span lengths. To determine whether differences in span length affect the influence surface, the third bridge uses asymmetric span lengths of 120 feet – 210 feet – 150 feet but retains the original radius of curvature of 2000 feet.

The first sample bridge has a radius of curvature of 2000 feet and span lengths of 150 feet for each end span and 180 feet for the center span. The influence map for the rotation about a transverse axis at bearing #1, an interior bearing, is shown in Figure 3-9 and the influence map for the rotation about a transverse axis at bearing #2, an exterior bearing, is shown in Figure 3-10. As might be expected, all of the loads placed in the end span adjacent to bearings #1 and #2 tend to rotate the bearings such that the end span deflects downward while the center span deflects upward, and likewise, all of the loads placed in the center span tend to rotate the bearings such that the center span deflects downward while the end span deflects upward. As for the loads in the far end span, loads over some areas of the far span tend to rotate the bearings in one direction while loads over other areas of the far span tend to rotate the bearings in the opposite direction. If each girder is individually supported by the bearings at the piers, all of the loads in the far span tend to rotate the bearings such that the end span deflects downward while the center span deflects upward. Because the bent cap is supported by only two closely-spaced

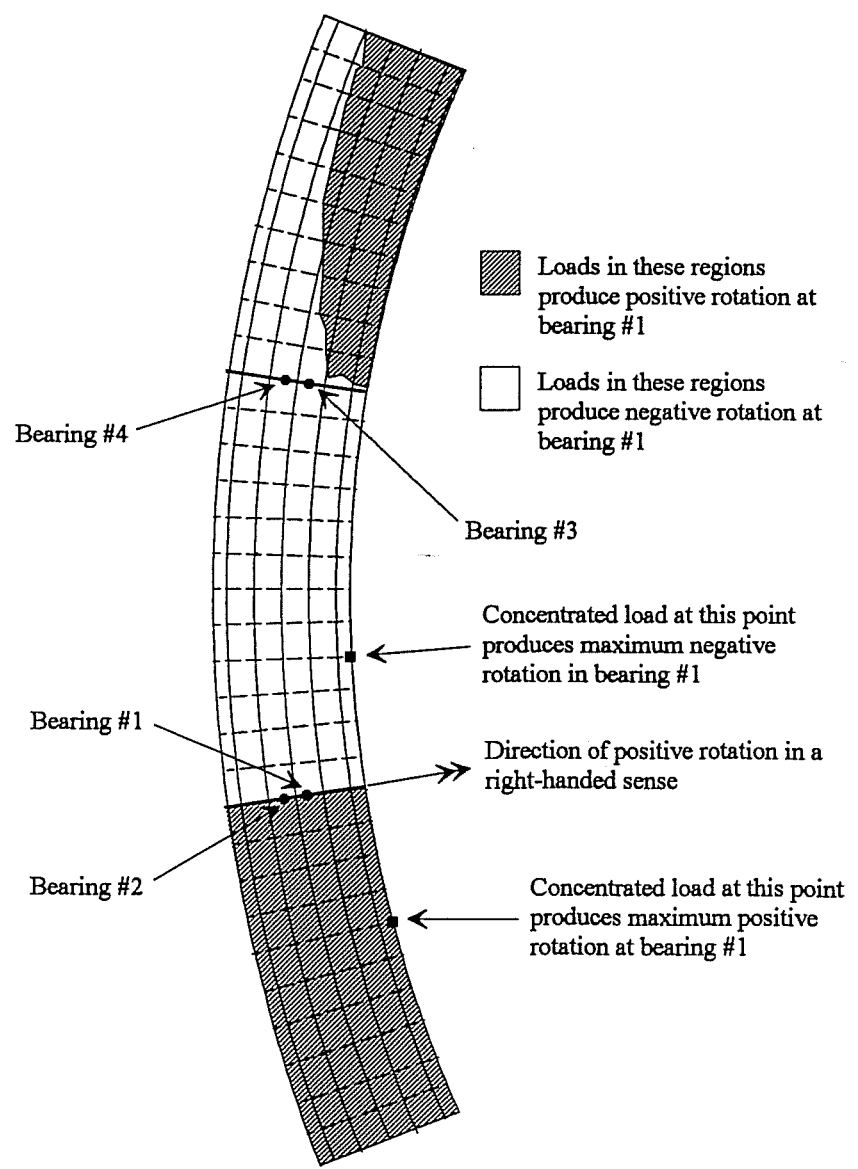


Figure 3-9: Influence surface for the rotation at an interior bearing of a symmetric 2000' radius bridge

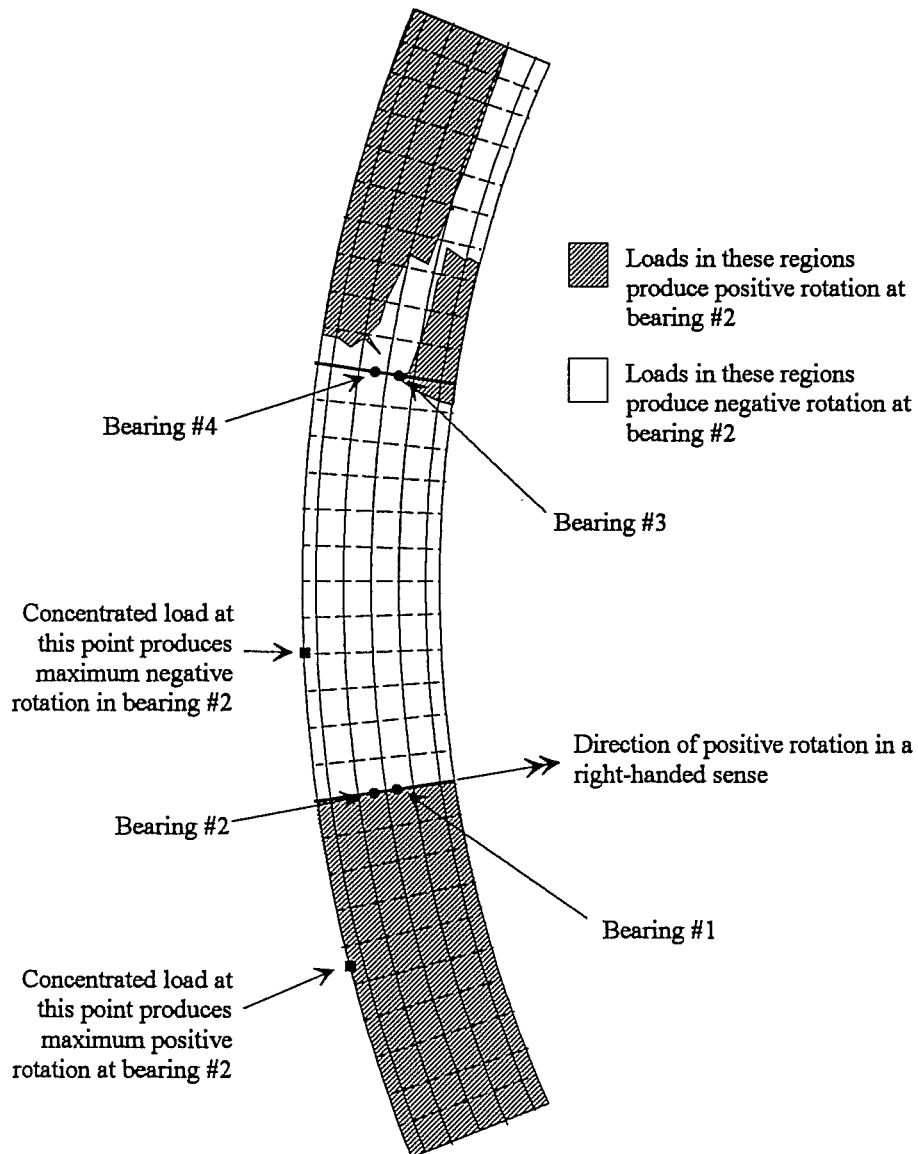


Figure 3-10: Influence surface for the rotation at an exterior bearing of a symmetric 2000' radius bridge

bearings, however, the exact shapes of these influence areas depends on the stiffness of the bent cap-support system. As with the influence of loads applied to the far span on the vertical reactions in the bearings, however, the influence of the loads applied to the far span is negligible – less than ten percent of the influence of the loads applied to the two adjacent spans – on the rotation in the bearings.

Effect of offsetting the pier from the centerline of the bridge

When the pier is offset from the centerline of the bridge, the same general properties appear in the influence surfaces as when the piers are centered beneath the bridge. For the two spans on either side of a bearing, the line demarcating the areas over which loads produce compression and the areas over which loads produce uplift in that bearing follows roughly the centerline of the bearings where the area leading to compression bulges slightly over the centerline. To show this, the piers of the 2000 foot radius bridge were moved outward six feet. The influence surfaces for the interior and exterior bearing reactions are shown in Figures 3-11 and 3-12, respectively.

Design Recommendations: maximum reactions and rotations

Influence surfaces for bearing reactions and rotations were developed for a variety of cases, such as those discussed in the previous sections. From these analyses simplified influence surfaces were developed. Boundaries of the exact influence surfaces were simplified, and portions of the influence surfaces that have only a minor effect on bearing reaction or rotation were eliminated. In general it is anticipated the bearing reactions and rotations computed in the finite element model using the simplified influence surfaces will be within five percent of the values based on the exact influence surfaces.

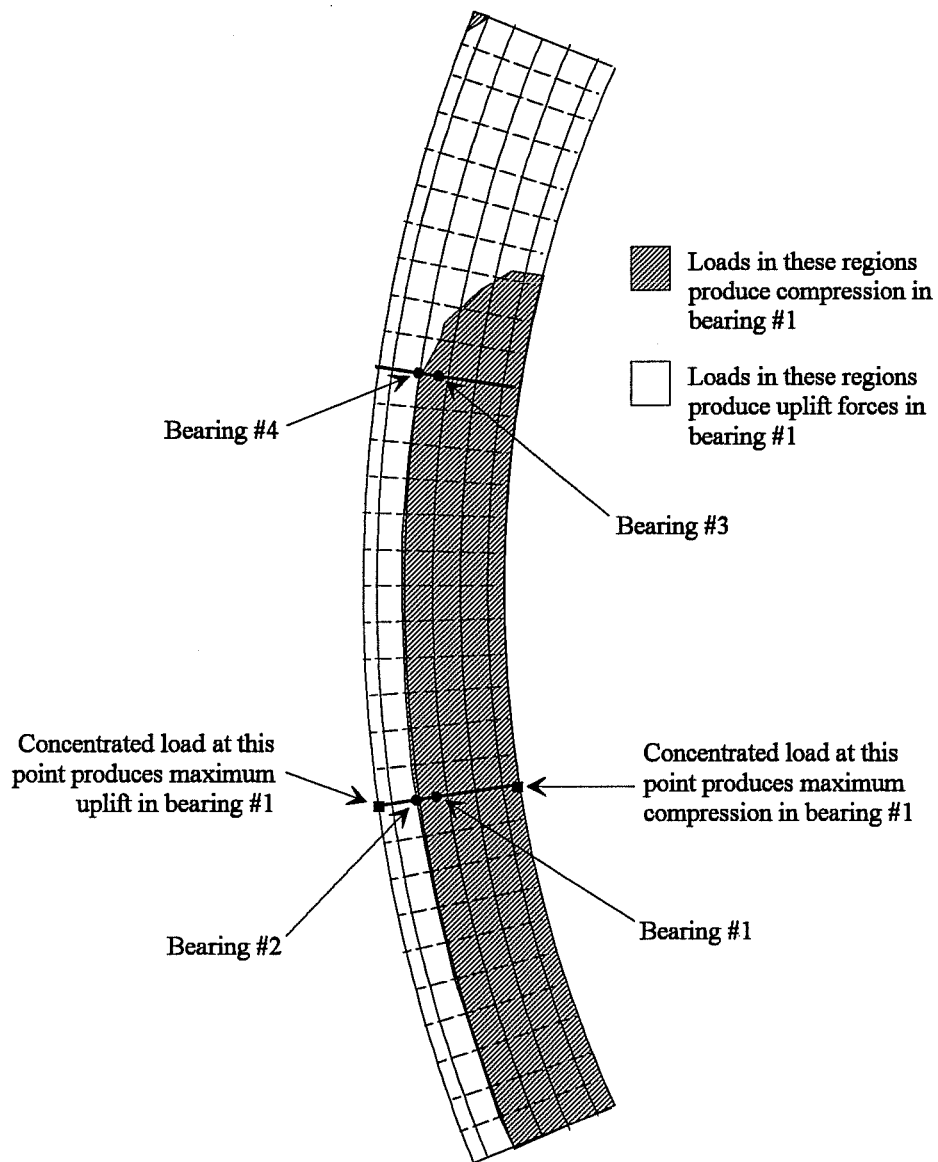


Figure 3-11: Influence surface for an interior bearing of a symmetric 2000' radius bridge with the centerline of the bearings offset 72" from the centerline of the deck

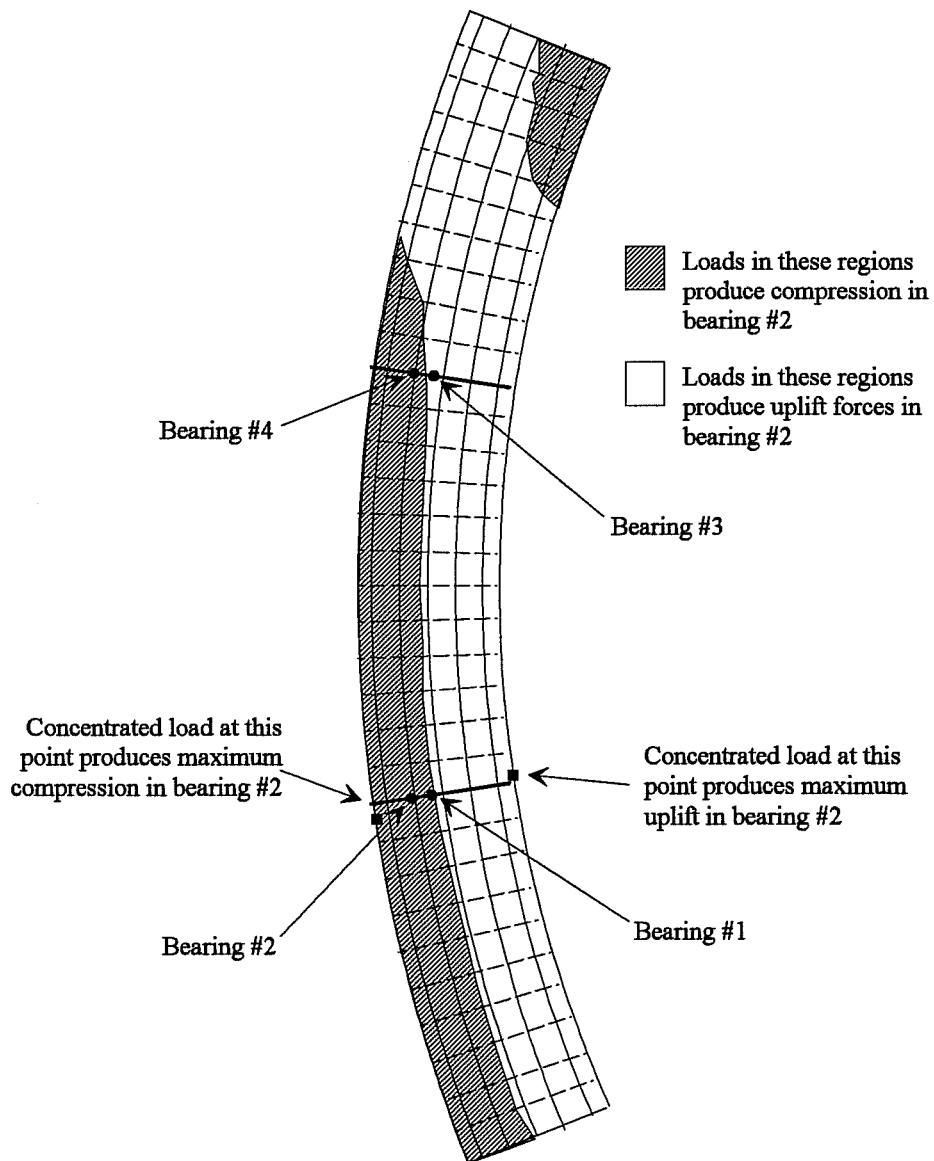


Figure 3-12: Influence surface for an exterior bearing of a symmetric 2000' radius bridge with the centerline of the bearings offset 72" from the centerline of the deck

Figures 3-13 through 3-16 show the simplified influence surfaces for the reactions in the bearings. Figure 3-17 and 3-18 show the influence surfaces for the rotations in the bearings.

Typical results of Analysis

The influence surfaces previously described were applied to an existing TxDOT bridge. The bridge is a seven girder 548 foot long plate girder bridge. The bridge has three spans of 160 feet, 208 feet, and 180 feet in length. The bridge has a radius of curvature of 1910 feet. The range of bearing forces was calculated for the bearings at the support between the 208 foot and 180 foot spans. The maximum upward force produced by the live load never exceeded the downward force produced by the dead load, so uplift never occurred. The range of downward forces in the bearings is shown in Table 3-1.

Table 3-1: Range of bearing forces

	Minimum downward force	Maximum downward force
Interior bearing	557 kips	1342 kips
Exterior bearing	689 kips	1496 kips

The rotations at the bearings are shown in Table 3-2. Rotations are considered positive when the deck rotates downward toward the middle span and negative when the deck rotates downward toward the end span.

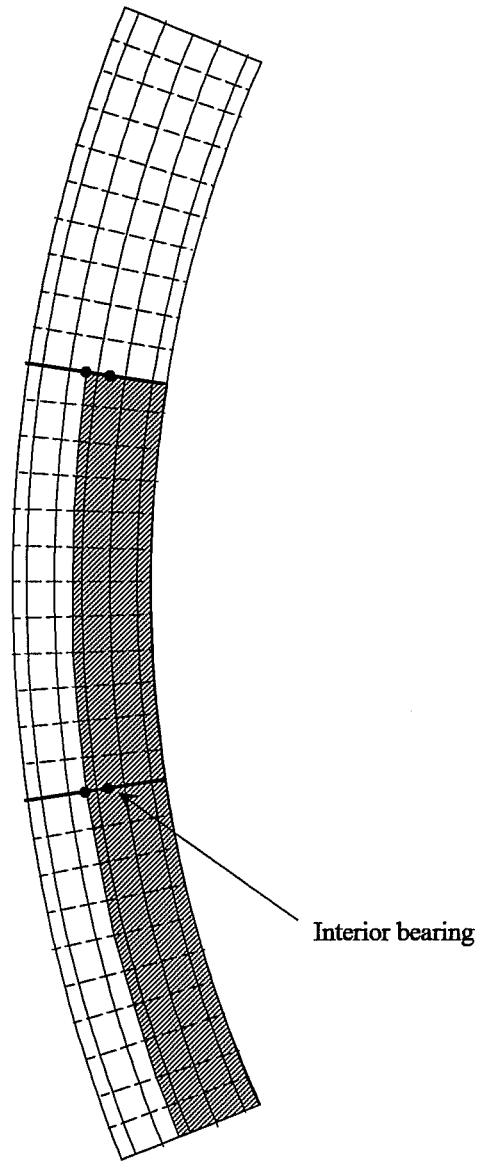


Figure 3-13: Loading pattern to produce maximum vertical downforce in interior bearing

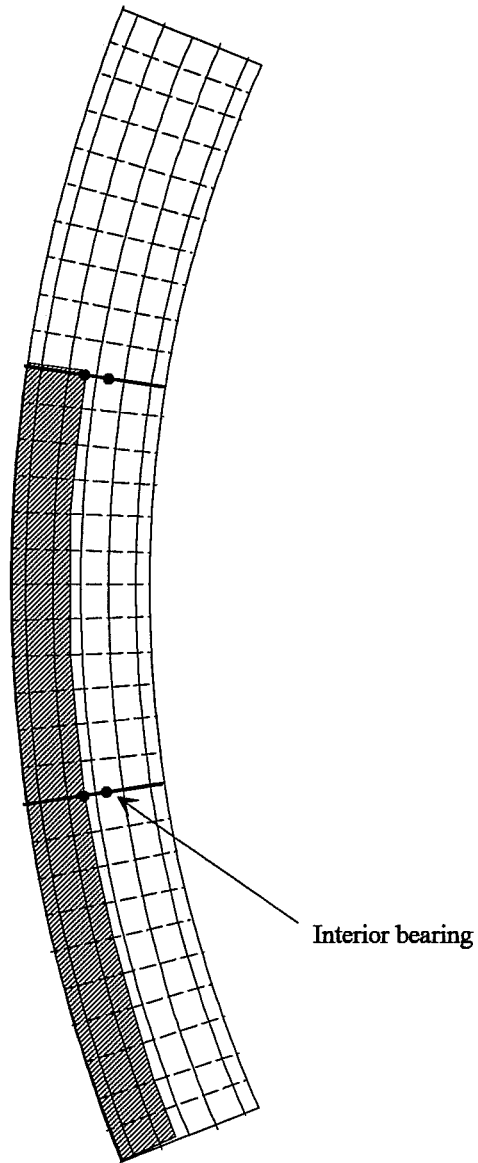


Figure 3-14: Loading pattern to produce maximum vertical uplift in interior bearing

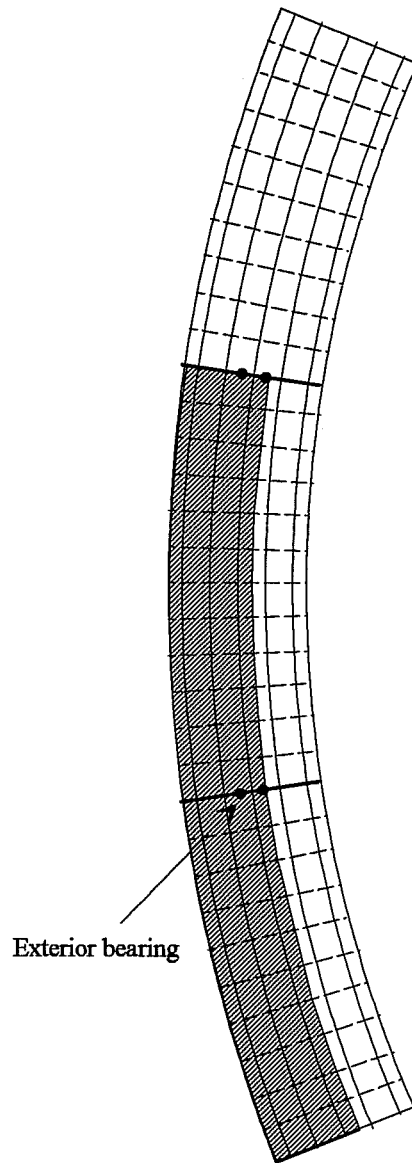


Figure 3-15: Loading pattern to produce maximum vertical downforce in exterior bearing

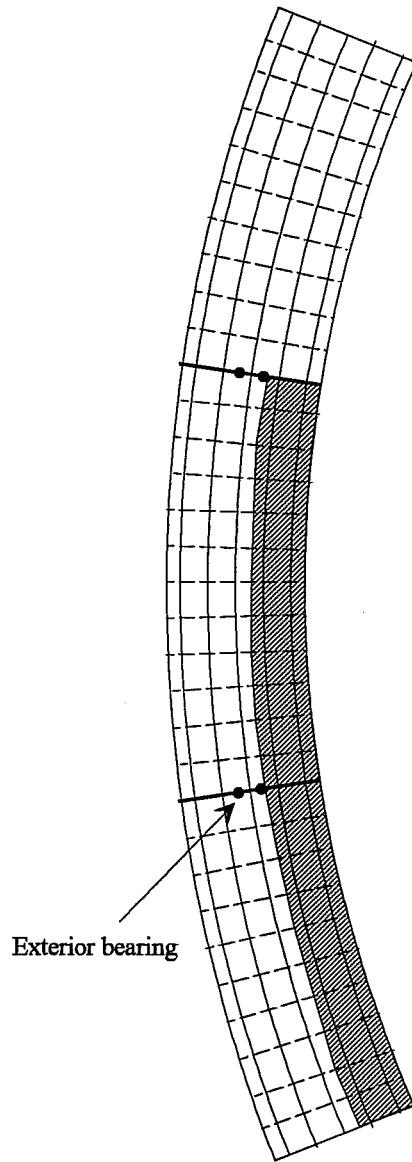


Figure 3-16: Loading pattern to produce maximum vertical uplift in exterior bearing

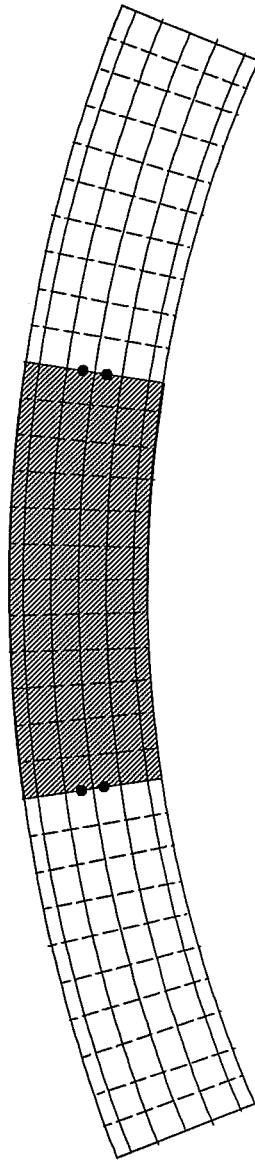


Figure 3-17: Loading pattern to produce maximum rotation such that deck rotates downward toward center span

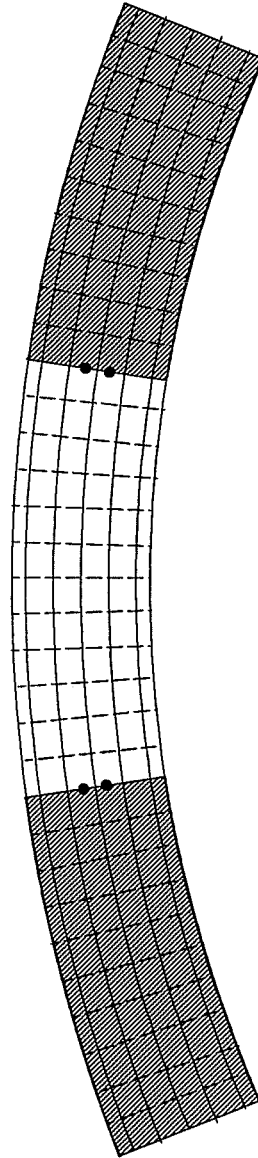


Figure 3-18: Loading pattern to produce maximum rotation such that deck rotates downward toward end span

Table 3-2: Range of bearing rotations

	Minimum rotation	Maximum rotation
Interior bearing	-0.000366 radians	0.000935 radians
Exterior bearing	-0.000375 radians	0.000939 radians

CHAPTER 4

EVALUATION OF THE V-LOAD METHOD

Introduction

In design practice curved steel bridges are often analyzed using a simplified analysis technique known as the V-load method, rather than finite element methods. The bridge systems under consideration in this study, however, violate one of the basic assumptions of the V-load method. The V-load method, as described in Appendix C, assumes that all girders are directly supported by bearings at the pier locations. For the bridges under consideration here, interior supports consist of steel bent caps connected to narrow piers, where the piers may be placed either at the deck's center or eccentrically. The girders not directly above the piers rest on flexible supports, namely the bent caps. Although attempts are made in the design of these bridges to approximate the support conditions assumed in the V-load method by providing very stiff bent caps, these caps will necessarily allow some flexibility. This chapter will examine the extent to which this flexibility causes the behavior of the bridge to deviate from the behavior predicted by the V-load method, and will compare V-load analysis results with more exact finite element results.

Assumptions and the potential consequences of their violation

The curved bridges considered in this study obey most of the assumptions of the V-load method. The bridges are open-framed with K-braces at the ends of the bridges and X-braces frequently spaced along the lengths of the bridges. The girders are plate girders with the top flanges connected by shear studs to the slab in the positive moment regions of the girder. All girders at a cross-section have roughly equivalent flexural stiffness and are equally spaced across the cross-section.

The bridges considered herein, however, do not satisfy the implicit assumption that all girders are vertically supported directly on piers at the support locations. Instead, a single narrow pier supports the center of the bridge cross-section leaving the ends of the cross-section free to sag. If the cross-section sags at the ends, the cross-frames will resist the sag by applying upward vertical shear forces on the end girders and equilibrating downward vertical shear forces on the middle girders. These vertical shear forces will overlay the V-loads, effectively producing a different distribution of vertical shear loads from that assumed by the V-load method. The vertical shear forces would be distributed as if, rather than assuming uniform, rigid-body rotations of the cross-frames, the cross-frames were considered to undergo differential rotations. These differential rotations violate the assumptions used to calculate the C coefficients and violate the assumption of a linear distribution of the V-loads across the cross-section.

The bridges are designed with some thought given to this violation of the V-load method assumption, by providing stiff bent caps at the single-pier supports. However, it is unclear how much stiffness is required of the bent caps in order to satisfy the assumptions of the V-load method.

Method of evaluation

Evaluation of the V-load results requires the use of a more sophisticated analysis technique – one which can incorporate the effects of the support conditions. By using the finite element method, all aspects of the bridge, namely the slab, girders, diaphragms, bent caps and piers, can be incorporated into the analysis, thus providing a more accurate determination of the distribution of loads to the girders and to the bent caps. Thus, V-load method analysis results will be compared to finite element method analysis results for a variety of bridge design parameters.

Evaluation of girder moments

As mentioned before, if each girder is not individually supported directly on the pier, the shear forces on the girders as calculated by the V-load method may have incorrect magnitudes and these V-loads may not be distributed linearly among the girders. If the V-loads applied to the girders are incorrect, then the moments in the girders as calculated by the V-load method will be incorrect. Thus, it is necessary to verify that the moments in the girders as calculated by the V-load method – which considers each girder to be individually supported – do not differ greatly from the moments as calculated by the finite element method – which considers the actual support conditions.

While the V-load method returns the moments in the girders directly, the finite element method returns only the stresses at the nodes of each element. In order to compare the results from the two methods, the moments from the finite element analysis could be calculated from the stresses, or alternatively, the stresses from the V-load analysis could be calculated from the moments. Because it was simpler to calculate the latter, the results are presented in terms of the stresses – in particular, the axial stresses at the centroids of the bottom

flanges.

Both a V-load analysis and a finite element analysis were performed on the same seven girder 548 foot long plate girder bridge designed by TxDOT that was used for analysis in the section "Typical results of analysis" in Chapter 3. A plan view of the bridge indicating the support locations and girder numbers appears in Figure 4-1. Figures 4-2 through 4-8 show the bottom flange axial stresses in each of the seven girders when the bridge is subjected to dead load. The V-load results tend to be conservative.

Although this analysis is for dead load only, the critical live load case produces similar results. For girder moments the critical live load case consists of live load on all girders, since this maximizes the moments in each girder when each is treated as a straight girder and also maximizes the V-loads which are based on the sum of all of the girder moments at the cross-frame locations. Thus, the dead load and live load case both consist of a uniformly distributed load across the width of the deck, and thus the comparisons between the V-load and finite element analyses for each load case will be similar. When, live loads are not distributed across the full width of the deck, the differences between the V-load and finite element results increase. However, such load cases will not be critical for the design of the girders.

Evaluation of bent cap bearing reactions

Although the moments in the girders as determined by the V-load method match adequately with the moments as determined by the finite element method, the downward forces each girder applies to the bent caps do not necessarily correlate with the girder reactions as determined by the V-load method. The stiffness of the support which the bent cap provides to each girder differs. The middle girders enjoy stiffer vertical support since the bent cap itself

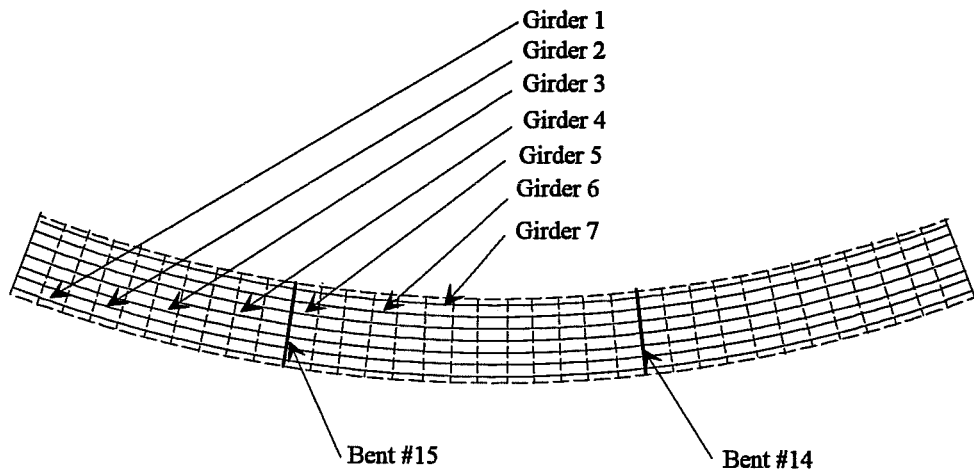


Figure 4-1: Plan view of 548 foot long bridge

Figure 4-2: Dead load bottom flange stresses in girder 7

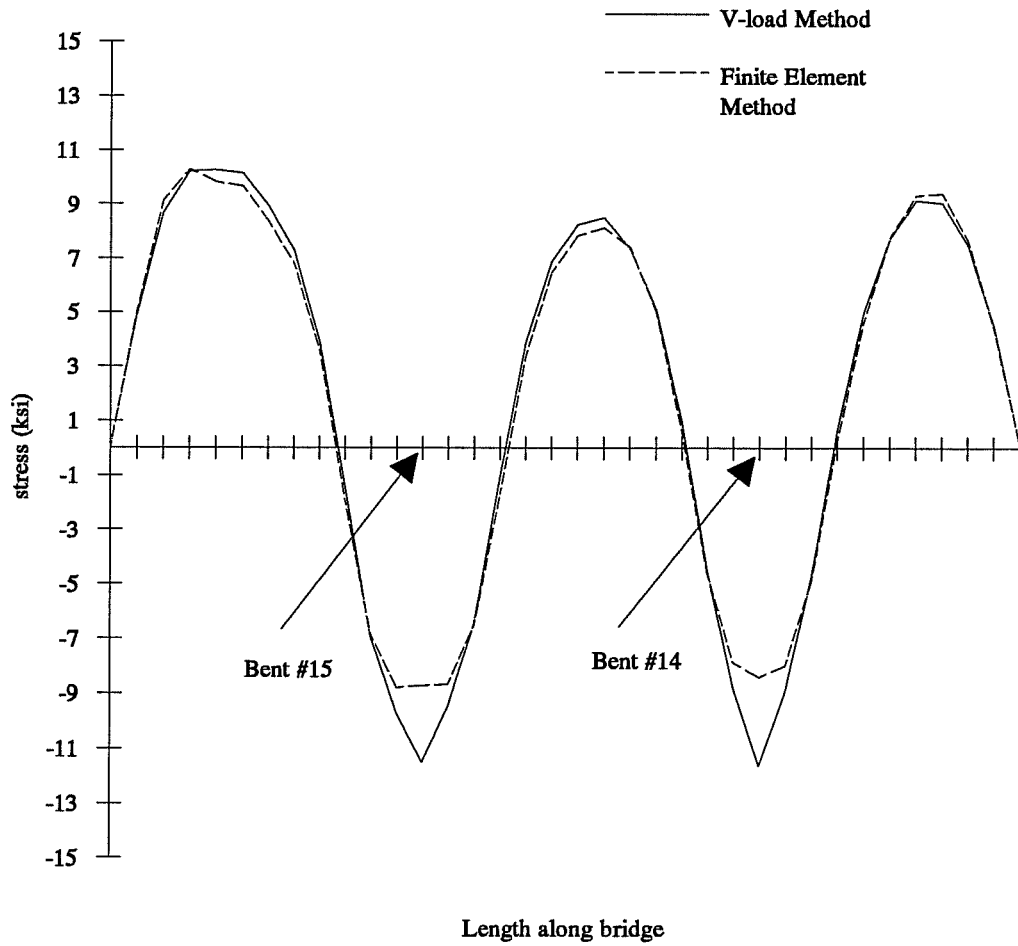


Figure 4-3: Dead load bottom flange stresses in girder 6

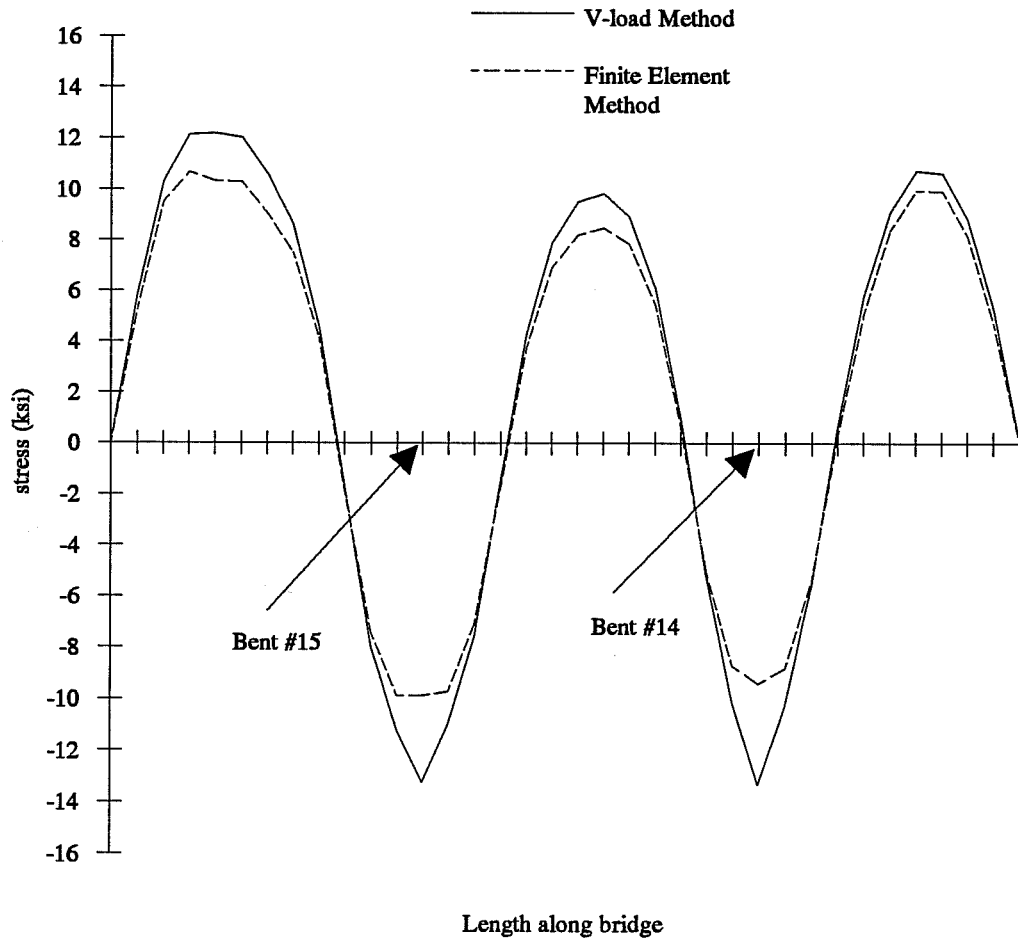


Figure 4-4: Dead load bottom flange stresses in girder 5

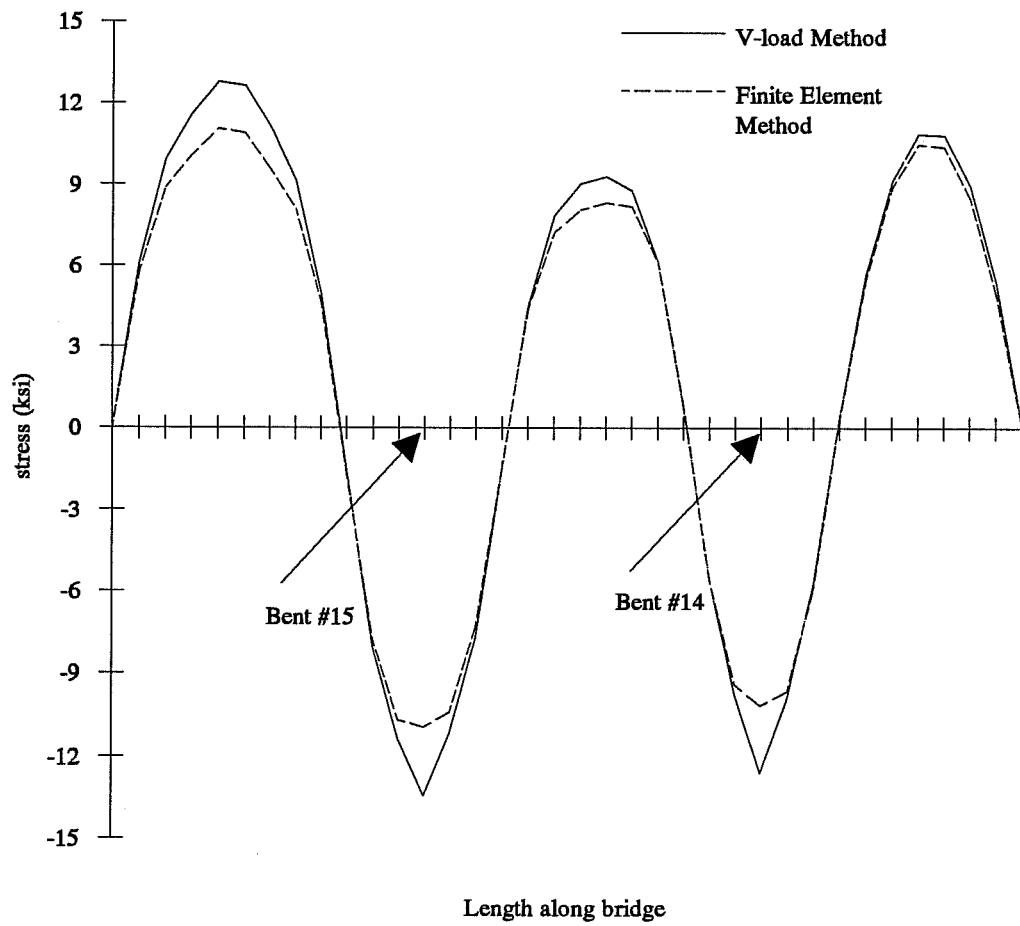


Figure 4-5: Dead load bottom flange stresses in girder 4

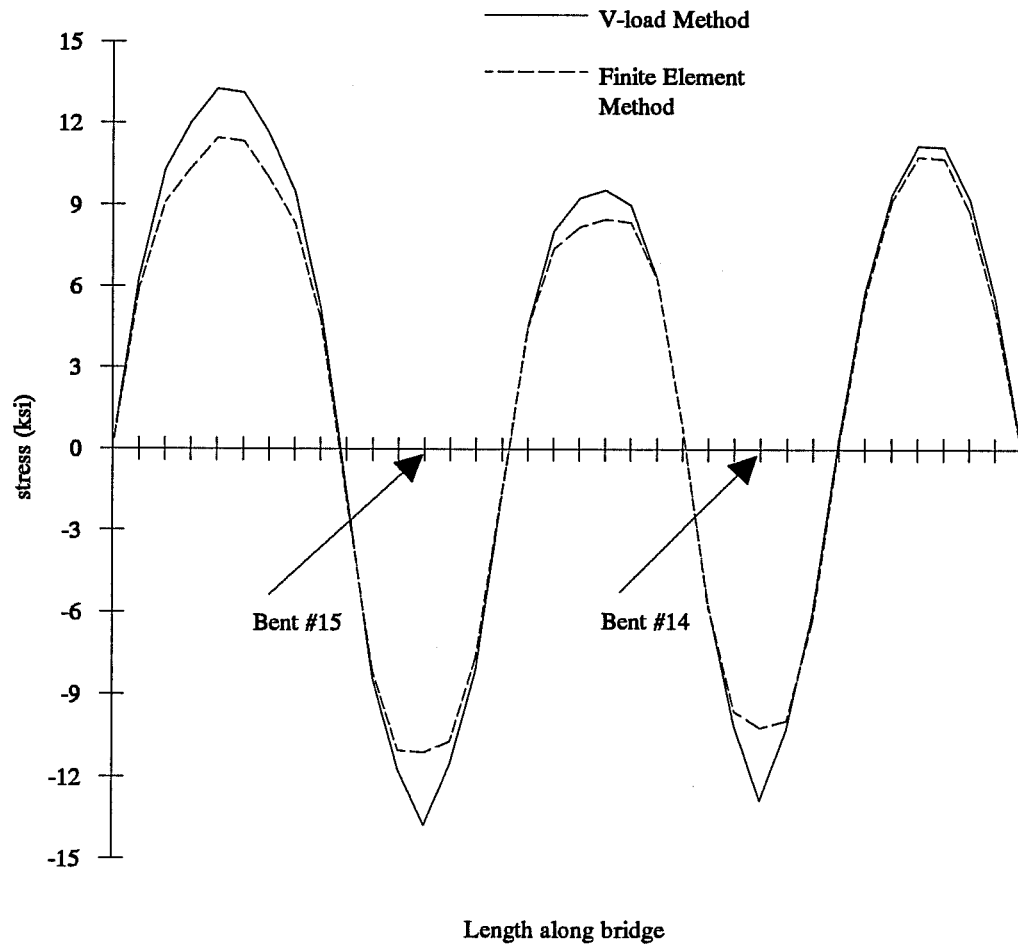


Figure 4-6: Dead load bottom flange stresses in girder 3

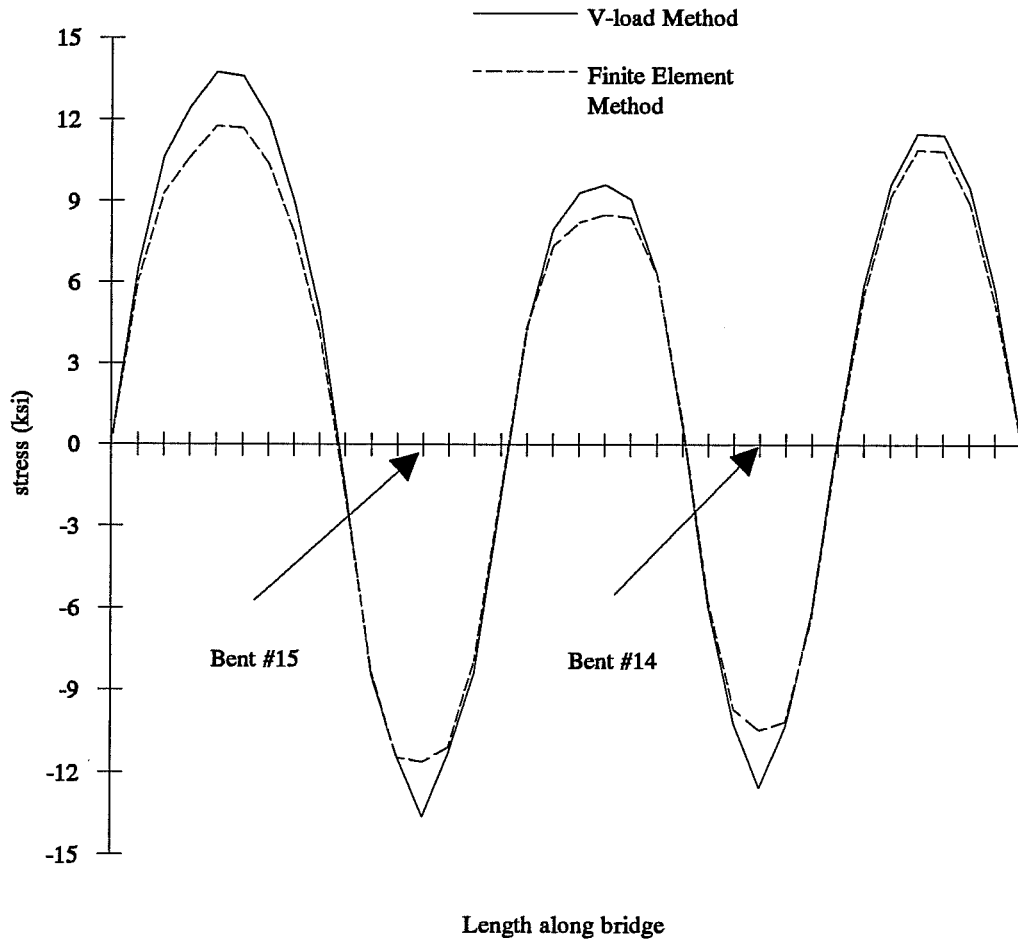


Figure 4-7: Dead load bottom flange stresses in girder 2

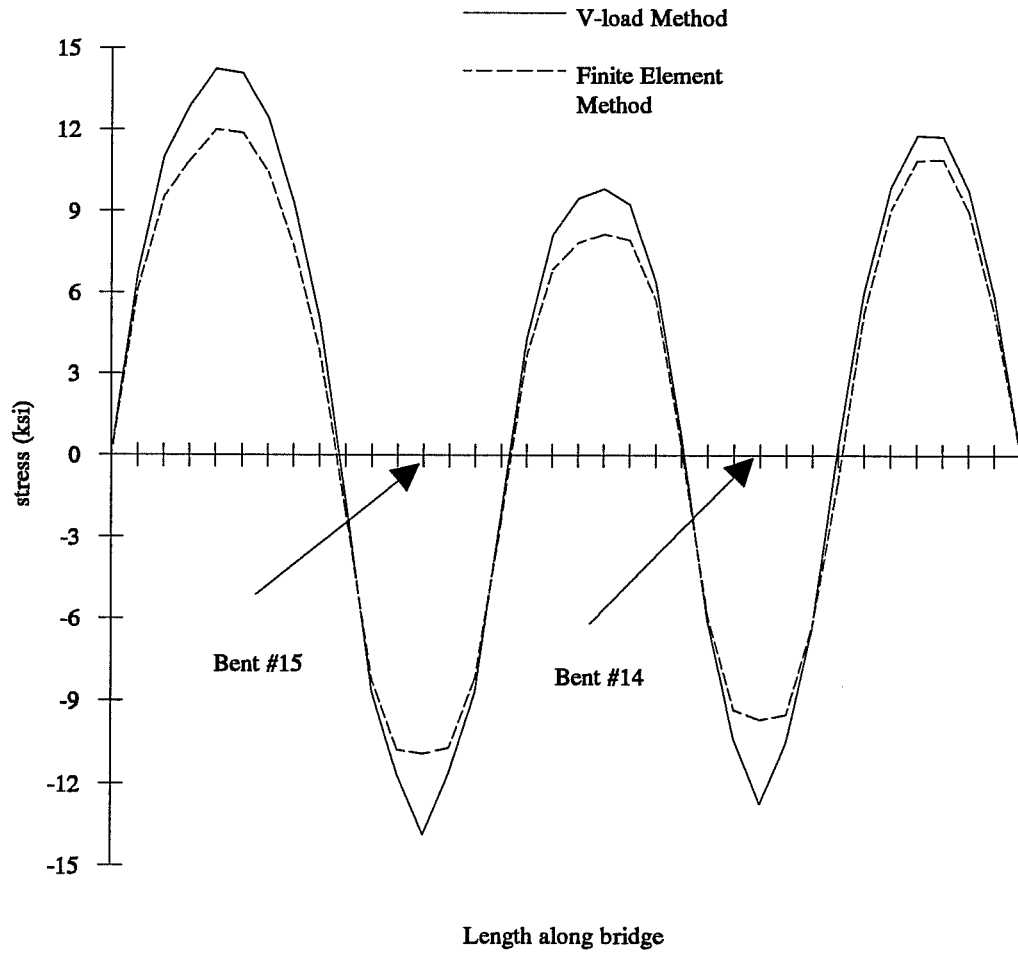
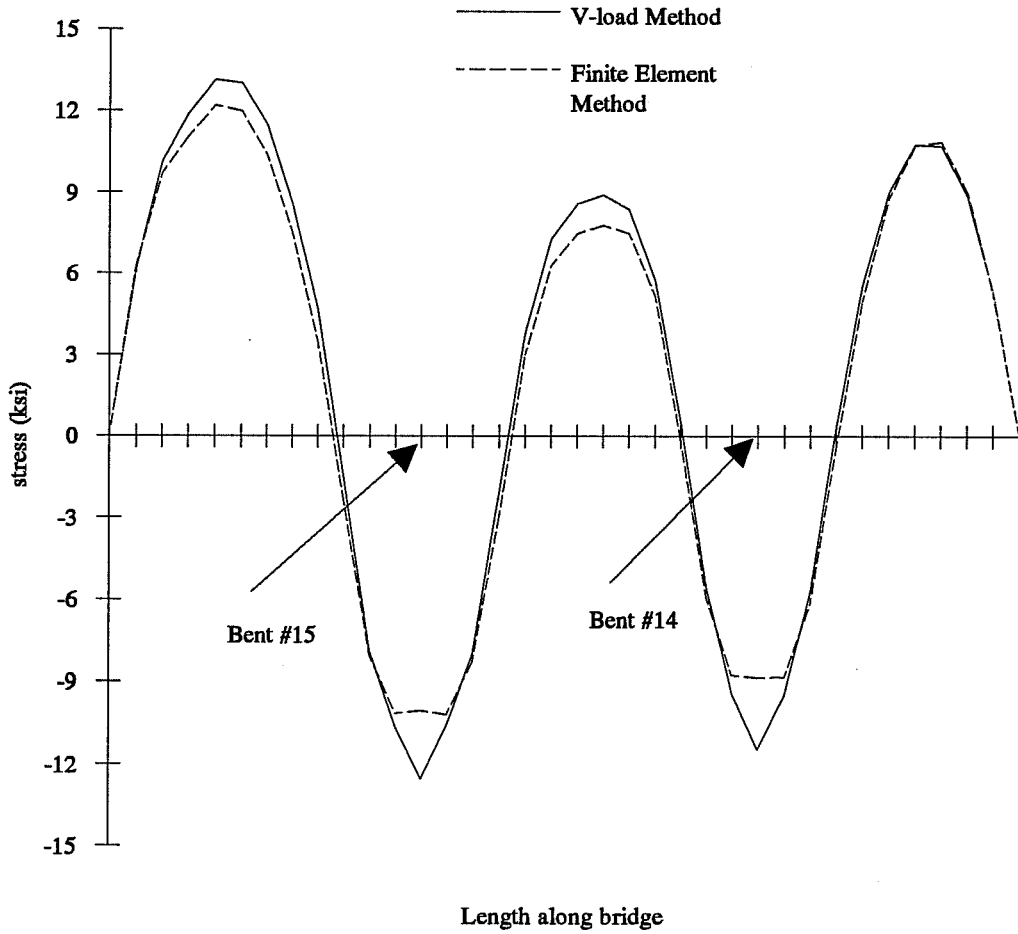


Figure 4-8: Dead load bottom flange stresses in girder 1



is directly supported by the pier in the middle of the deck cross-section. More flexible support is provided to the end girders, however, since the ends of the bent cap can deflect. The tendency for differential vertical movement of the girders at the bent cap is resisted by the cross-frames in the vicinity of the bent cap, as shown later in Figure 5-9. When the end girders try to deflect vertically with the bent cap ends, the cross-frames between the girders transfer some of the vertical load from the end girders to the middle girders. If this transfer of vertical forces is confined mostly to the cross-frames adjacent to the bent caps, the moments in the girders will not be significantly affected by the transfer. Thus, although the V-load method adequately predicts the moments in the girders, the V-load method may not adequately predict the distribution of reaction forces between each of the girders and the bent cap.

The redistribution of forces acting on the bent cap will not affect the total vertical force transferred through the bearings from the bent caps to the piers. The redistribution, however, will affect the transverse moments transferred to the piers, and therefore will affect the vertical forces developed at the bearings. The relationship between the total vertical force at the pier, the transverse moment at the pier, and the forces developed in the bearings is shown in Figure 4-9.

A sample five girder, three span bridge was modeled using both the V-load method and the finite element method. Initially the three spans were set at 150 feet, 180 feet, and 150 feet and the radius of curvature was set at 2000 feet. The interior bents were set on bearings spaced at 72 inches, where the centerline of the pier corresponded to the centerline of the deck. Table 4-1 shows a comparison of the total vertical force and the total moment about a longitudinal axis transferred to one of the interior piers when the bridge is subjected to dead load. A positive moment indicates that the upward force of

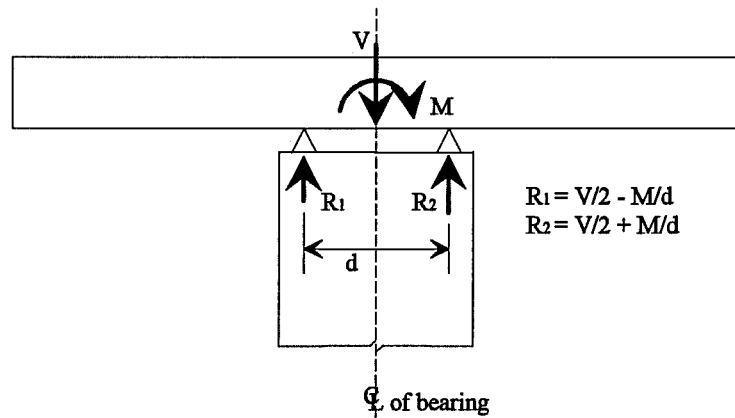


Figure 4-9: Relationship of vertical force and transverse moment at the pier to the vertical bearing forces

the couple acts on the interior bearing and the downward force of the couple acts on the exterior bearing. Table 4-1 also shows vertical forces developed at the bearings. A positive force acts downward, producing compression in the bearing.

Table 4-1: Comparison of V-load and finite element results for sample bridge under dead load

	V-load method	Finite element method
Vertical force	1028 kips	1028 kips
Moment	-30.9 kip-feet	138.6 kip-feet
Force at interior bearing	519 kips	491 kips
Force at exterior bearing	509 kips	537 kips

The total vertical force transferred to the pier is the same for both methods, but the moments differ greatly in both direction and magnitude. Note, however, that in this case the large error in transverse moment has little impact on the predicted bearing forces, since the transverse moment under dead load is relatively small. Similar results can be shown for uniform live load.

When live load is applied to only the innermost or outermost traffic lanes, the transverse moment will be greater. Table 4-2 shows the bearing force data for the same bridge with a single lane load in the innermost lane. The V-load method overpredicts the transverse moments by almost 15 percent in this case. As a result the V-load method produces a conservative estimate of the compression in the interior bearing and a conservative estimate of the uplift, or in this case minimum compression, in the exterior bearing. On the other hand, when the outermost lane is loaded, the V-load method produces an unconservative estimate of the compression in the exterior bearing and an unconservative estimate of the minimum compression in the interior bearing, as

shown in Table 4-3.

Table 4-2: Comparison of V-load and finite element results for sample bridge under dead load and with live load in the innermost traffic lane

	V-load method	Finite element method
Vertical force	1137 kips	1136 kips
Moment	-1467 kip-feet	-1284 kip-feet
Force at interior bearing	813 kips	782 kips
Force at exterior bearing	324 kips	354 kips

Table 4-3: Comparison of V-load and finite element results for sample bridge under dead load and with live load in the outermost traffic lane

	V-load method	Finite element method
Vertical force	1138 kips	1138 kips
Moment	1404 kip-feet	1602 kip-feet
Force at interior bearing	335 kips	302 kips
Force at exterior bearing	803 kips	836 kips

These two live load cases produce the critical uplift, or minimum compression, forces in the exterior and interior bearings, respectively. For this bridge, however, uplift is never actually reached – the bearings are always subjected to at least 300 kips of compression. Nevertheless, the bearings would be designed assuming that some uplift were possible. Consequently, the unconservative errors in the V-load method do not affect the design of the bearing to resist uplift forces when the V-load method predicts that there will always be substantial compressive forces in the bearings. When the bearing spacing is reduced to 24 inches, both the V-load method and the finite element method predict uplift in the bearings, as

shown in Tables 4-4 and 4-5. The V-load method conservatively predicts the maximum uplift forces in both the interior and the exterior bearings.

Thus, if uplift is not present, the unconservative estimates of the minimum bearing compression by the V-load method do not affect the design, while if uplift is present, the V-load method is conservative in estimating the uplift forces. Consequently, the V-load method appears adequate for determining uplift forces.

Table 4-4: Comparison of V-load and finite element results for sample bridge with a 24 inch bearing spacing under dead load and with live load in the innermost traffic lane

	V-load method	Finite element method
Vertical force	1137 kips	1134 kips
Moment	-1467 kip-feet	-1250 kip-feet
Force at interior bearing	1302 kips	1192 kips
Force at exterior bearing	-165 kips	-58 kips

Table 4-5: Comparison of V-load and finite element results for sample bridge with a 24 inch bearing spacing under dead load and with live load in the outermost traffic lane

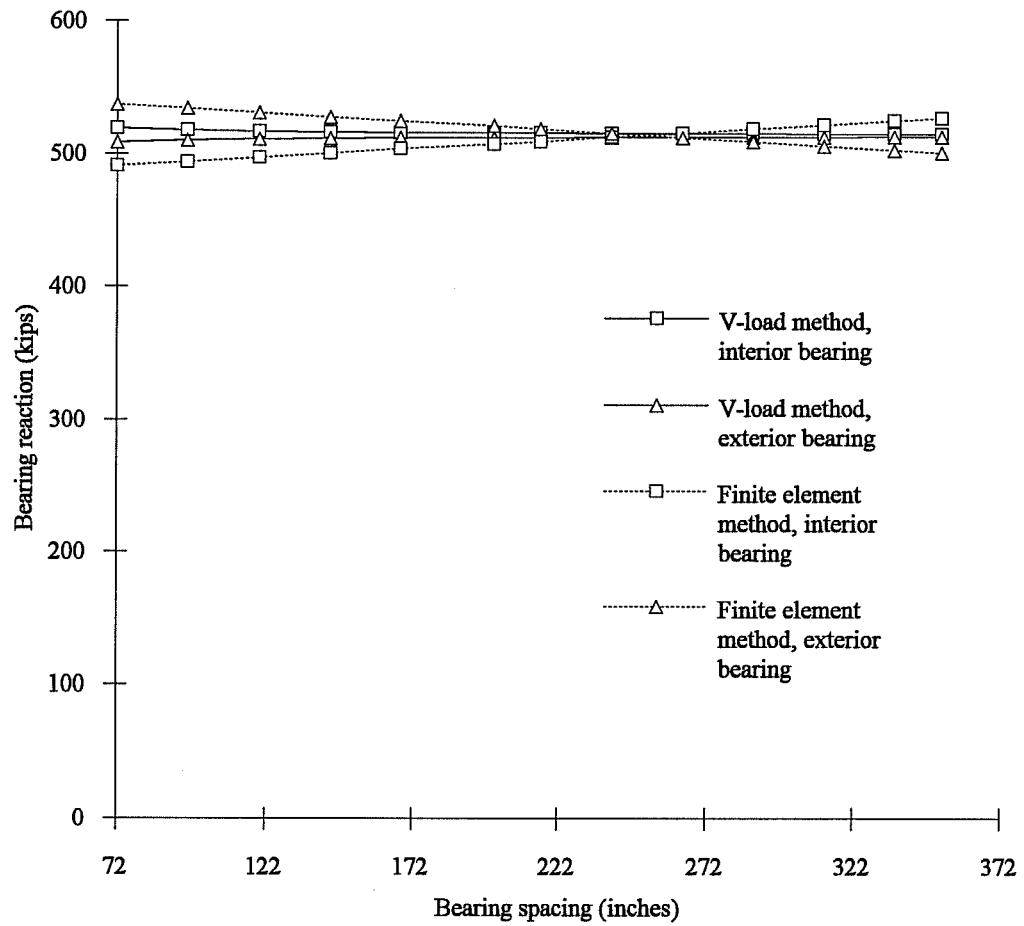
	V-load method	Finite element method
Vertical force	1138 kips	1141 kips
Moment	1404 kip-feet	1365 kip-feet
Force at interior bearing	-133 kips	-112 kips
Force at exterior bearing	1271 kips	1253 kips

To maximize compression in the interior or exterior bearing, live load should be placed in the two innermost or two outermost lanes, respectively.

Although the results are not tabulated, the V-load method conservatively estimates the maximum interior bearing reaction and unconservatively estimates the maximum exterior bearing reaction. For the maximum compressive reaction, the errors are about three to four percent, which is likely to be an acceptable error. In general, the V-load method is conservative in estimating bearing reactions when live load is in the innermost lanes and is unconservative in estimating bearing reactions when live load is in the outermost lanes when there is no uplift, and is conservative when there is uplift.

For the first sample bridge, the bearings were closely spaced at only six feet. Consequently, the support stiffness provided to the end girders is significantly less than the support stiffness provided to the middle girder, leading to a substantial redistribution of vertical reactions at the bent cap. A wider bearing spacing could potentially reduce the effects of the redistribution of girder forces on the bent caps as the support stiffness provided by the bent cap to each girder becomes more uniform. On the other hand, if the bearing spacing were increased to the full width of the bridge such that the end girders were directly above the bearings, the middle girders would have more flexible supports. The middle girders would then redistribute load to the end girders leading to the same problems that arise from narrow supports. Figure 4-10 bears out these arguments. The figure shows how the bearing reactions vary with bearing spacing for the sample bridge described above. The analysis is for dead load only. The finite element method predicts greater variation in the bearing reactions than the V-load method. For the narrowest bearing spacing of 72 inches, the exterior bearing reaction from the V-load method is about five percent unconservative compared to the finite element method. At a bearing spacing of about 22 feet, the bearing reactions are identical for the two methods. That the bearing reactions are identical does not indicate that no

Figure 4-10: Bearing reactions under varying bearing spacing



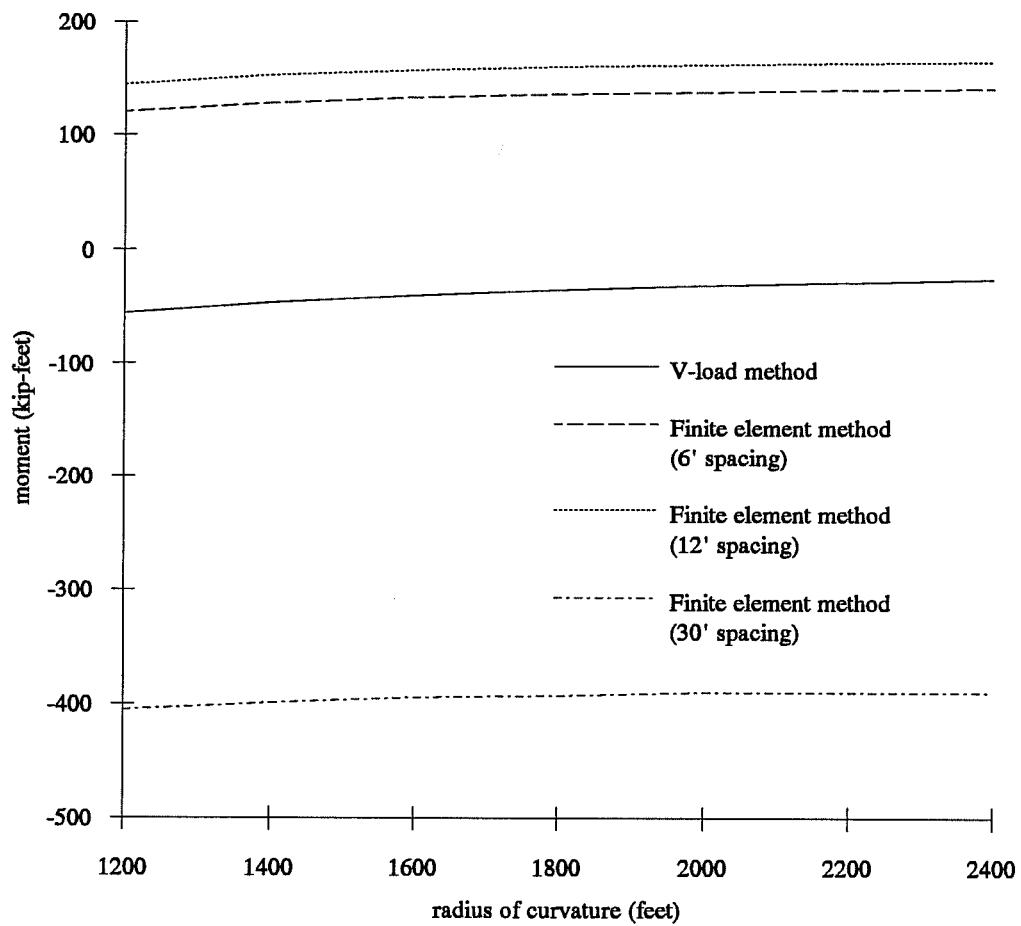
redistribution of girder forces is occurring but rather that the redistribution is such that the resulting total moment of the downward forces from the girders after redistribution equals the total moment before redistribution. At the widest bearing spacing of 30 feet, the interior bearing reaction predicted by the V-load method is only two percent unconservative. Thus, the V-load method does not accurately account for the redistribution of forces applied to the bent cap when a narrow pier supports the bent cap, but the effect is not very significant.

Besides the bearing spacing, other parameters which may affect the redistribution of girder forces include the radius of curvature and the ratios of span lengths. These parameters do not affect the support stiffness provided to each girder. Instead, these parameters affect the ratios of the girder bending stiffness, which in turn affects the extent to which the girders will shed vertical forces to or accept vertical forces from other girders. Considering variation of the radius of curvature, for small radii of curvature the girders on the inside of the curve are significantly shorter than the girders on the outside. The inside girders are therefore stiffer than the outside girders. As the radius of curvature increases, the differences in lengths, and therefore the differences in stiffness, of the girders decrease. Likewise, considering variation of the ratios of the span lengths, the girders on short spans will be stiffer than the girders on long spans.

Figure 4-11 shows that varying the radius of curvature does not lead to any additional redistribution of forces. The shape of the pier moment curves for the finite element analyses are essentially the same as that for the V-load analysis. The only discrepancy between the finite element analyses and the V-load analysis appears to be related to the bearing spacing.

For a three span bridge, at least two parameters must be varied to determine the effects of variation of the span length ratios. For the analyses of the sample bridges under varying span ratios, the total length of the bridge was

Figure 4-11: Pier moments under varying radius of curvature



kept constant at 480 feet – the same length as for the sample bridges used for determining the effects of varying the bearing spacing and the radius of curvature. Also like the previous sample bridges, the width of the bridge will remain constant at five girders spaced at eight feet with bearings spaced at 72 inches. The first parameter to be varied is the length of the end span opposite the pier at which moments are being calculated. The second parameter to be varied is the length of the end span adjacent to the bearing at which moments are being calculated. Since the total length of the bridge is kept constant, the length of the center span equals 480 feet minus the lengths of the two end spans. The lengths of the two end spans are each varied from 90 feet to 210 feet in increments of 30 feet. Figure 4-12 shows a plan view of the sample bridge and indicates how the two variables for the end span lengths are varied.

Figures 4-13 through 4-17 show the results of the analysis for dead load. In all cases, when the end span adjacent to the bearing is short, the V-load results differ significantly from the finite element results. In a like manner, when the end span opposite the bearing is short, the results differ more greatly over a wider range of lengths of the adjacent span. Although the largest errors occur for bridges with very unlikely span lengths, errors are also present for bridges with more reasonable span lengths. For example, the V-load method predicts a reaction in the exterior bearing which is about 15 percent unconservative for a bridge with span lengths of 150 feet, 210 feet, and 120 feet. Overall, results seem to correlate best when both end spans are fairly long. Again, however, good correlation does not indicate that the V-load method is redistributing forces in a manner similar to the finite element method. Instead, the forces from the V-load analysis happen to produce the same bearing reactions as the finite element method.

Thus, the V-load method can produce somewhat inaccurate, and

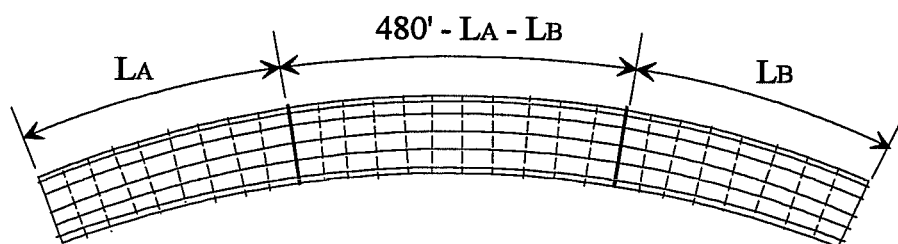


Figure 4-12: Relationship of variable span lengths

Figure 4-13: Bearing reactions under varying span ratios
(LB = length of far end span = 90 feet)

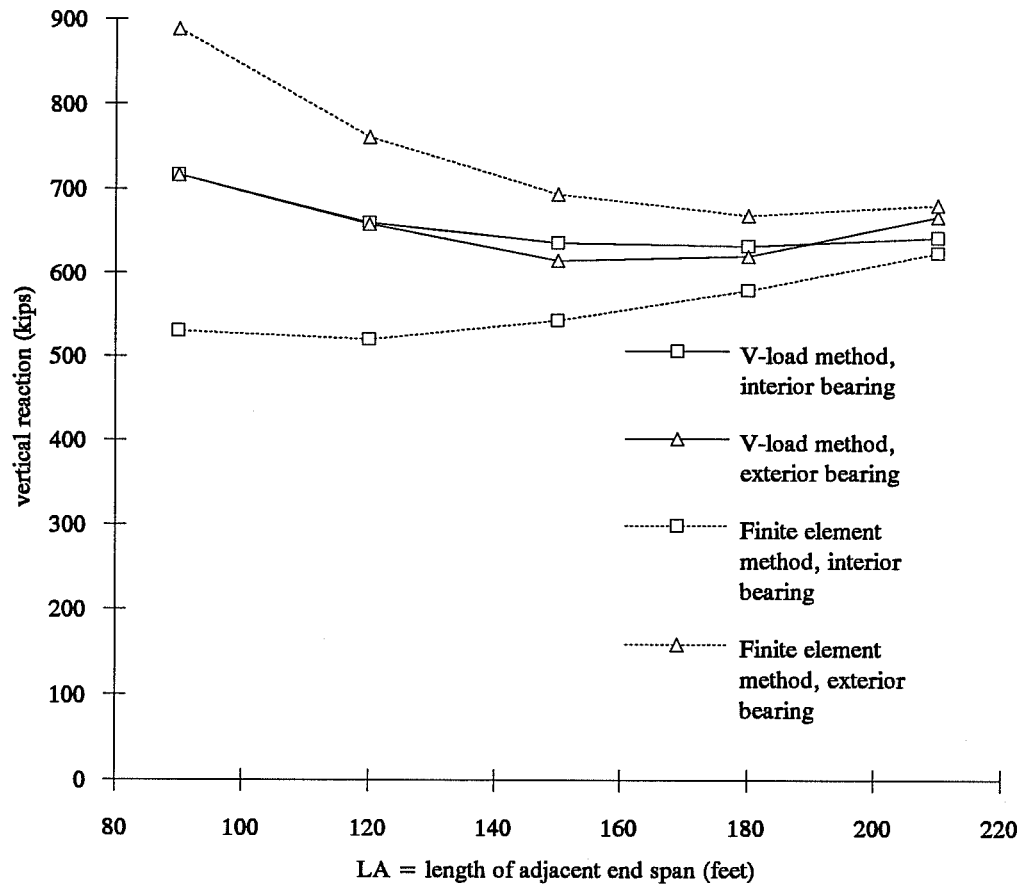


Figure 4-14: Bearing reactions under varying span ratios
(LB = length of far end span = 120 feet)

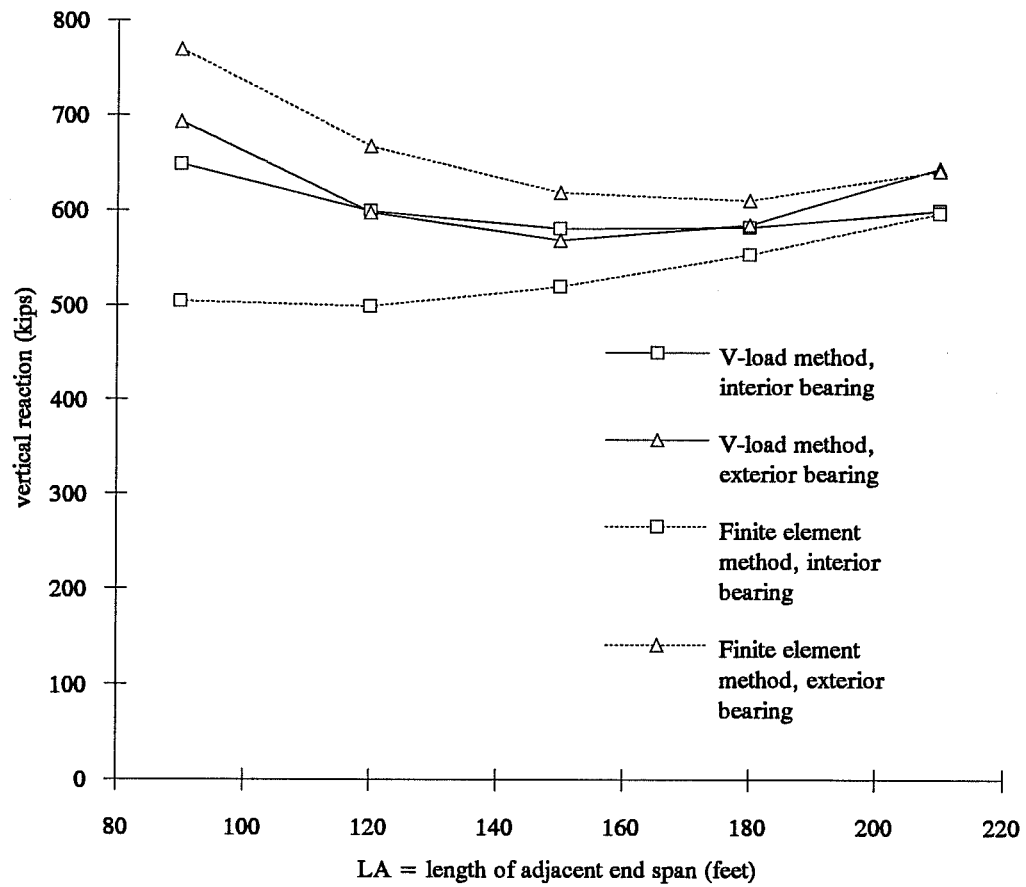


Figure 4-15: Bearing reactions under varying span ratios
(LB = length of far end span = 150 feet)

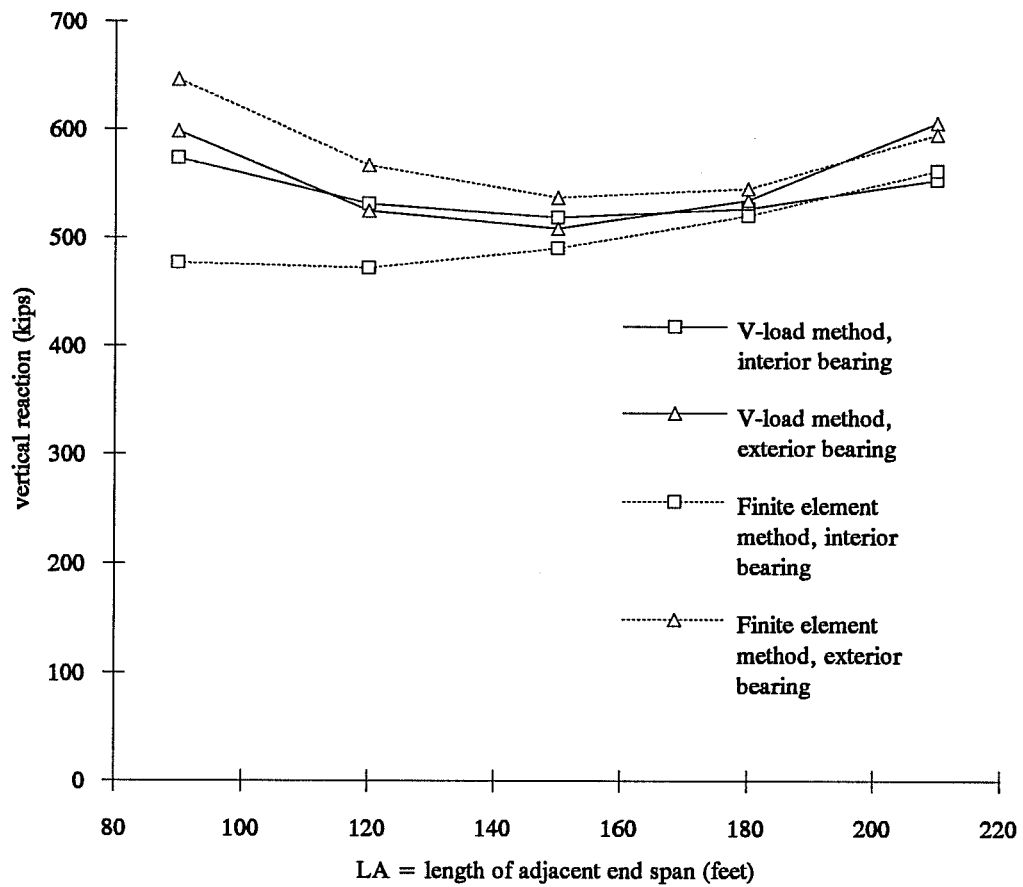


Figure 4-16: Bearing reactions under varying span ratio
(LB = length of far end span = 180 feet)

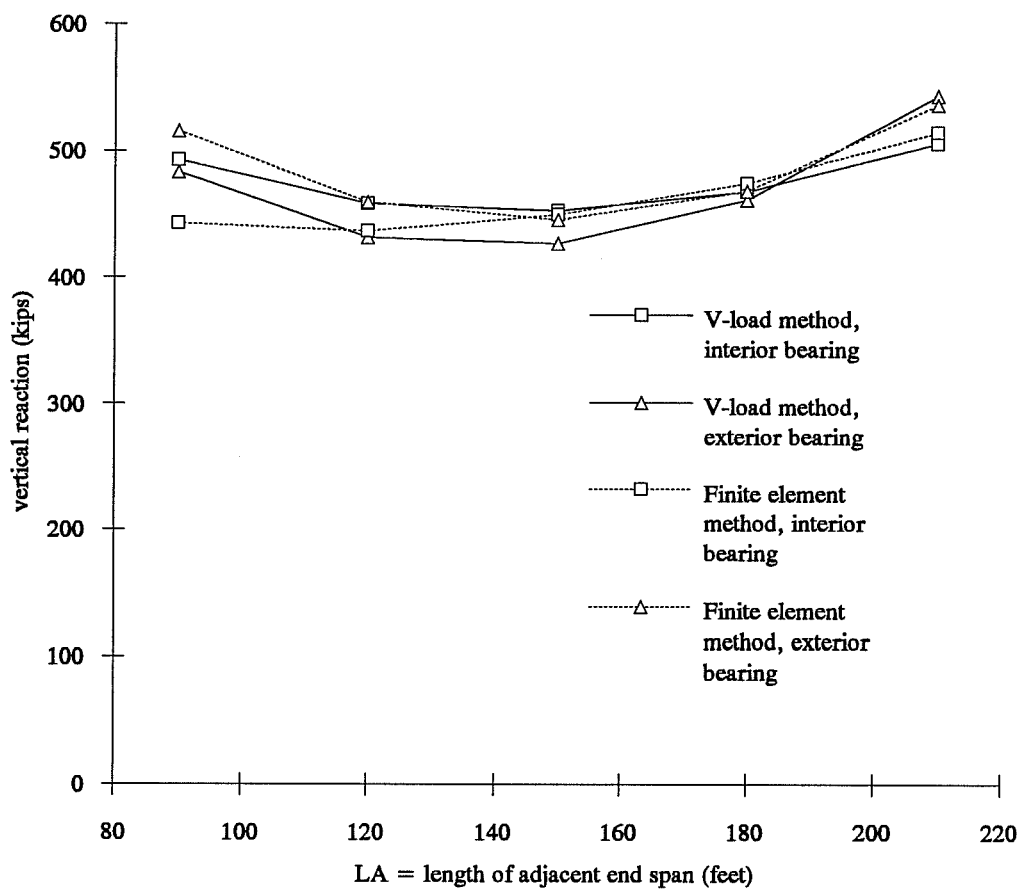
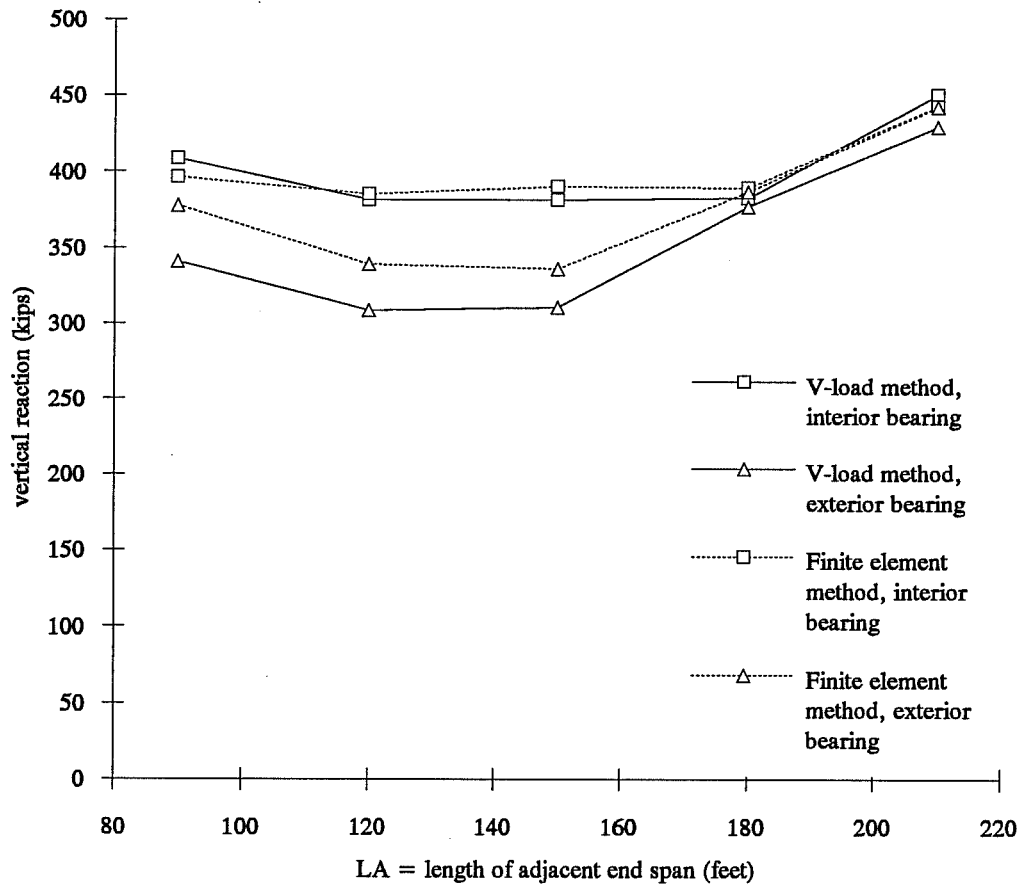


Figure 4-17: Bearing reactions under varying span ratios
(LB = length of far end span = 210 feet)



unconservative, bearing reactions when the end spans are particularly short relative to the length of the entire bridge. It is unlikely, however, that such short span lengths would be used in an actual bridge.

Effects of off-center piers

As discussed above, the V-load method sometimes produces inaccurate estimates of transverse moments at the pier for bridges where the centerline of the pier coincides with the centerline of the deck. When the deck is cantilevered from the pier, however, the results improve. In a centered system, the redistribution of vertical girder forces leads to significant changes in transverse moment since the initial forces before redistribution are fairly well balanced and do not lead to significant moments themselves. On the other hand, in a cantilevered system, as shown in Figure 4-18, there is already a large transverse moment on the bent cap before any redistribution of girder forces occurs. Consequently, changes in transverse moment due to bent cap flexibility are considerably less significant. To validate this argument, an analysis was made of the same five girder bridge used for evaluating the bent cap bearing reactions of the centered system. The bridge has a radius of curvature of 2000 feet, span lengths of 150 feet, 180 feet, and 150 feet, and a bearing spacing of 72 inches. Figure 4-19 shows the transverse moments at a pier as the pier is moved from the center of the deck to 12 feet outside the center of the deck. This figure indicates an insignificant difference between V-load and finite element results. Figures 4-20 through 4-23 further show that as the cantilever arm increases, the differences between the V-load method and the finite element method under the variation of span lengths tend to become insignificant. Thus, for a cantilevered deck, the V-load method produces consistently conservative results relative to the finite element method.

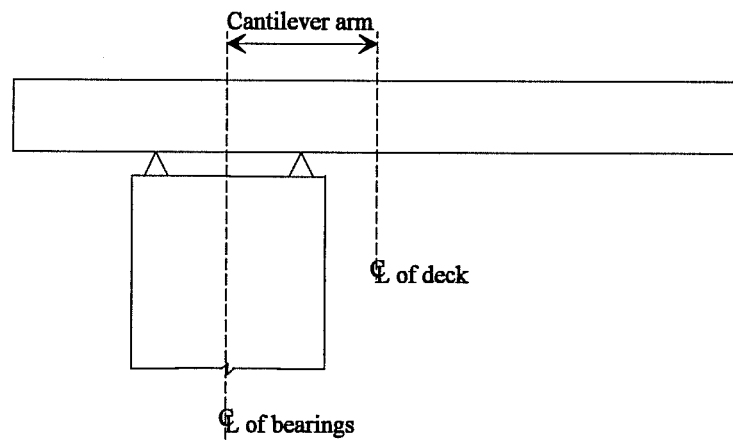


Figure 4-18: Cantilever arm in off-center systems

Figure 4-19: Pier moments under varying cantilever arm

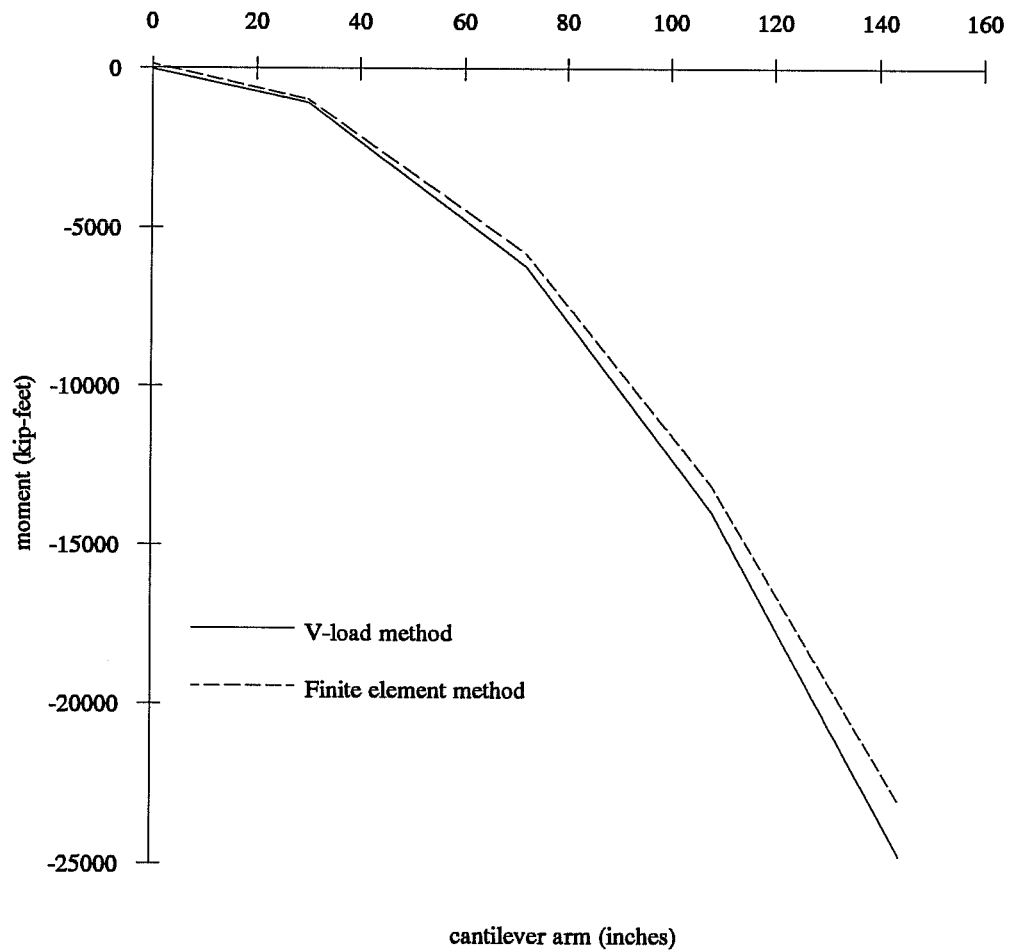


Figure 4-20: Pier moments under varying span lengths
(30 inch cantilever arm, LB = length of far end span = 150 feet)

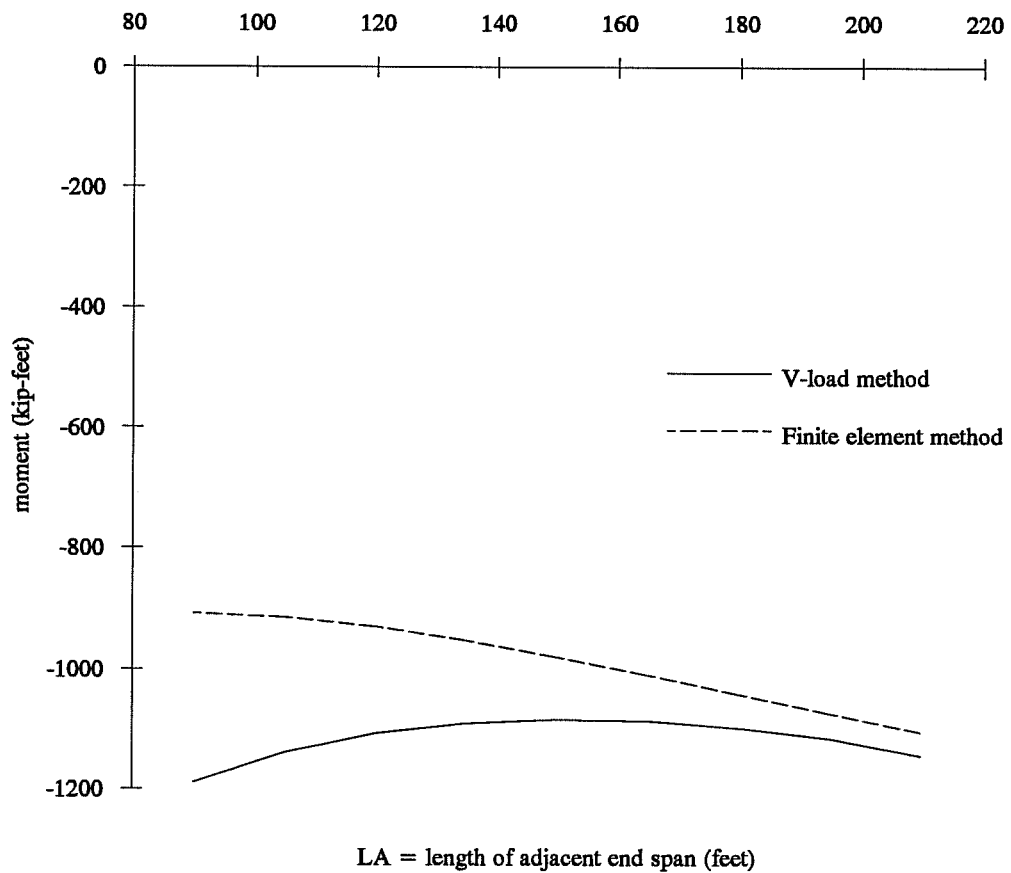


Figure 4-21: Pier moments under varying span length
(72 inch cantilever arm, LB = length of far end span = 150
feet)

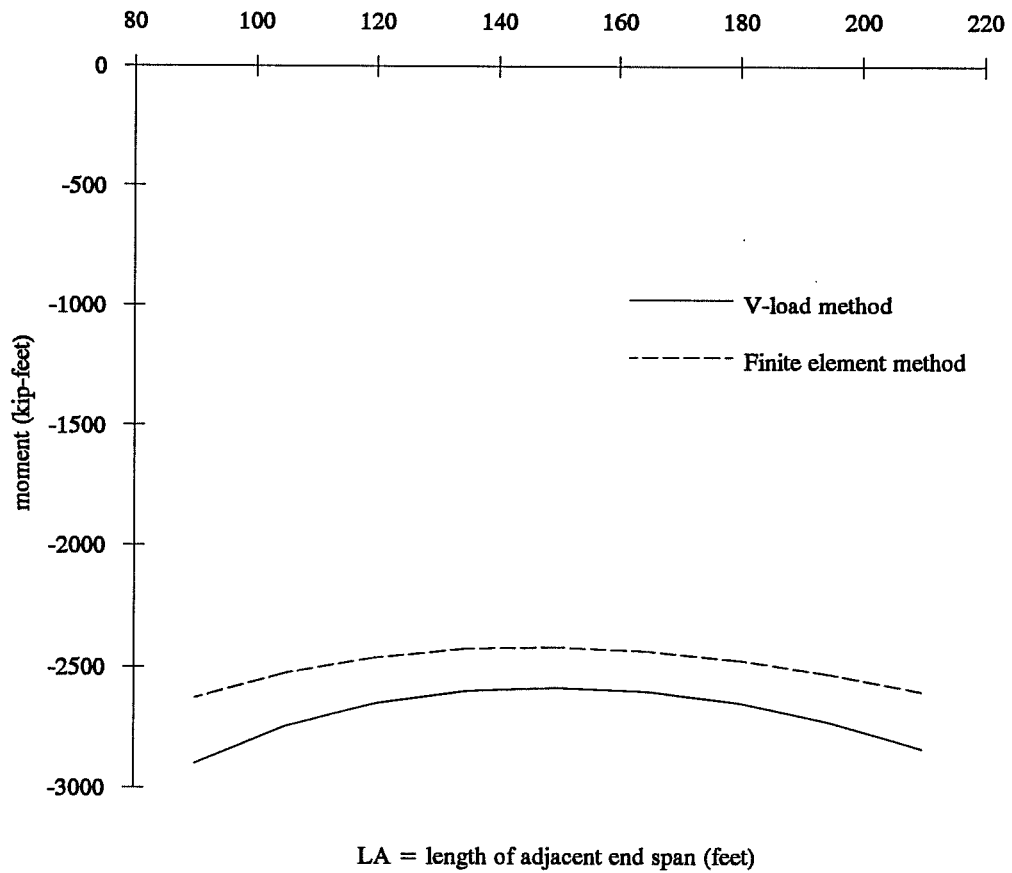


Figure 4-22: Pier moments under varying span length
(108 inch cantilever arm, LB = length of far end span =
150 feet)

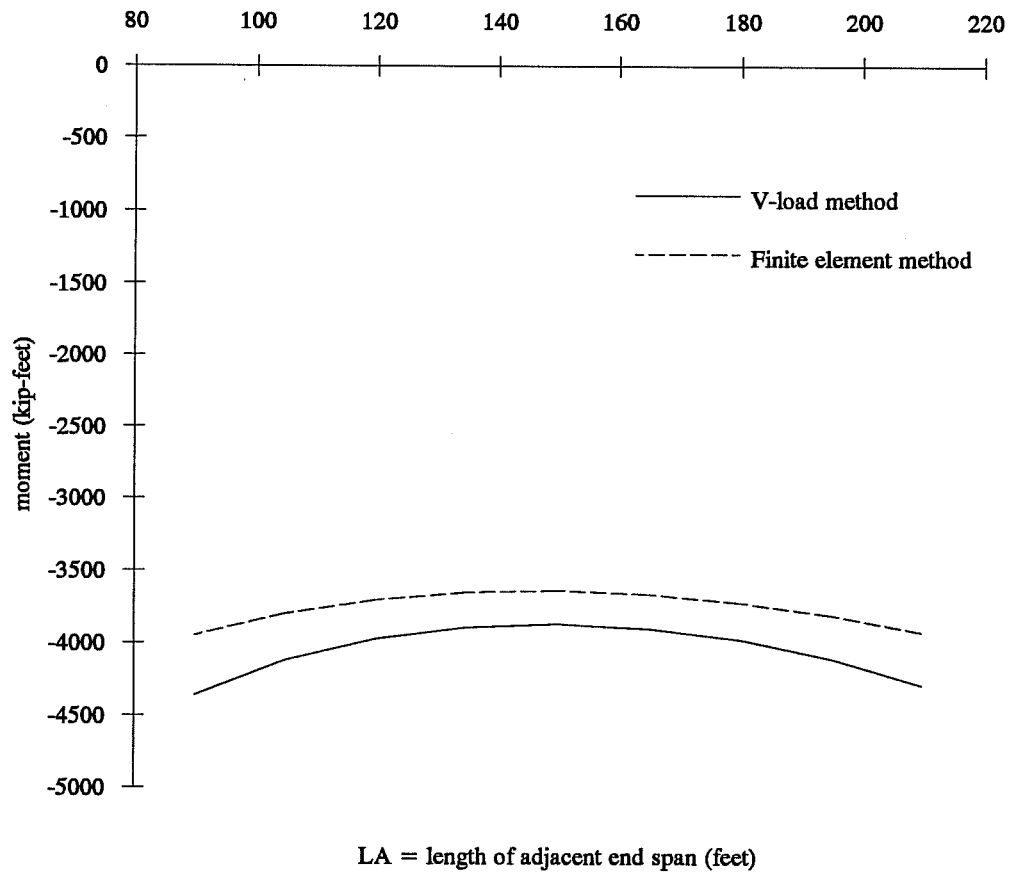
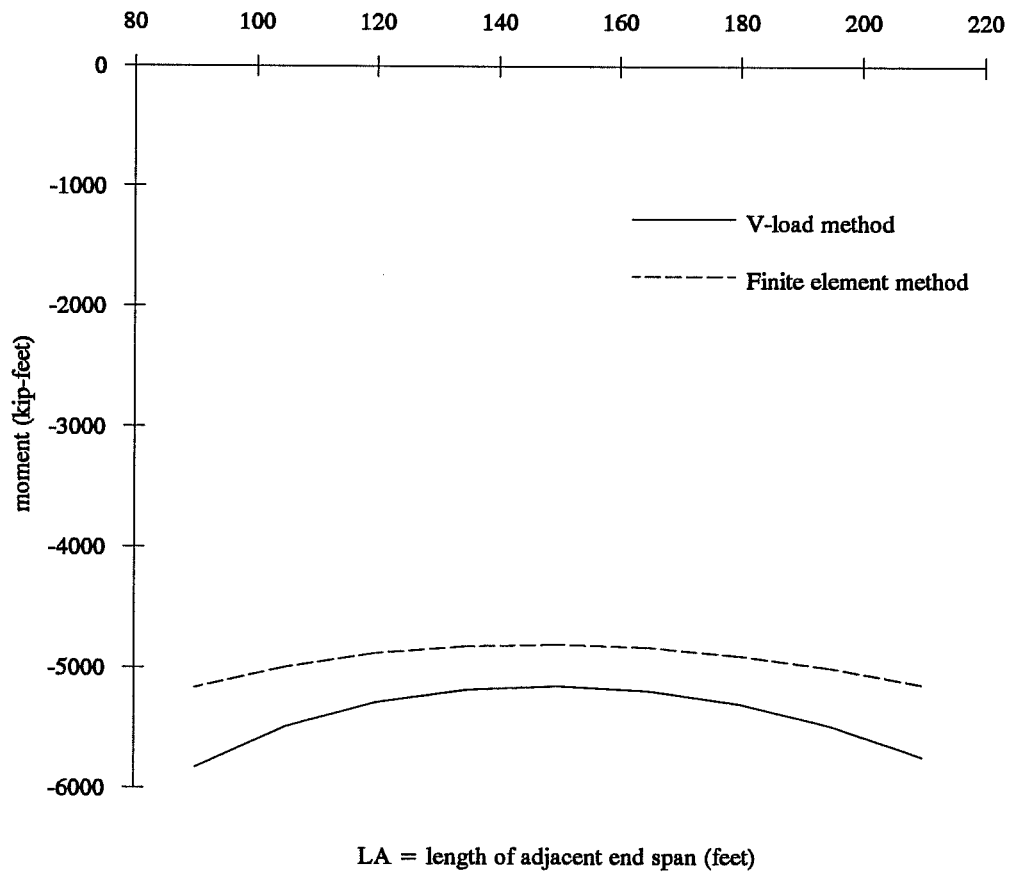


Figure 4-23: Pier moments under varying span length
(144 inch cantilever arm, LB = length of far end span =
150 feet)



Design Recommendations

The V-load method produces reasonably accurate girder moments for bridges supported on narrow piers. The vertical forces exerted by the girders on the bent caps, however, are not distributed properly by the V-load method. In some cases this results in somewhat unconservative estimates of the bearing reactions.

Unconservative estimates of the bearing reactions can arise when the live load is not placed in all of the lanes. When live load is placed in the interior lanes, the V-load method conservatively predicts bearing reactions, but when the live load is placed in the exterior lanes, the V-load method unconservatively predicts the bearing reactions. The unconservative errors in the maximum compressive force in the bearings will typically be only three or four percent, while unconservative errors in the maximum uplift – or more typically, the minimum compression – force can be more than ten percent. If the V-load method predicts that there will always be substantial compression in the bearings, the error in the minimum compression forces will not affect the design since the bearings are usually designed to withstand some amount of uplift even when none is expected. If the V-load method predicts uplift, however, the V-load method's error will be conservative.

The V-load method's results are not significantly unconservative when the end spans are fairly long relative to the length of the bridge. For such bridges, bearing designs based on V-load analyses should be adequate albeit slightly unconservative. For bridges with short end spans and long center spans, estimates of the bearing reactions can be more than 15 percent unconservative. For these cases designers should consider using a finite element analysis that properly models the support conditions.

For off-center pier supports, the V-load method produces results which

are fairly consistent with the finite element method results, so the V-load method should be adequate for bearing designs of bridge with off-center piers.

CHAPTER 5

EVALUATION OF CROSS- FRAME FORCES

AASHTO specifications for cross-frames

The American Association of State Highway and Transportation Officials (AASHTO) specifies requirements for the design of the cross-frames for horizontally curved bridges in two documents. The basic specifications for the cross-frames of steel I-girder bridges, curved or straight, are given in the *Standard Specifications for Highway Bridges* [1]. Additional requirements for the cross-frames of curved bridges are provided in the *Guide Specifications for Horizontally Curved Highway Bridges* [2].

Basic specifications for the design of the cross-frames appear in Articles 10.20 and 10.21 of the *Standard Specifications*. Article 10.20.1 states the following general requirements:

- Plate girder spans shall be provided with cross frames at each support and with intermediate cross frames placed in all bays and spaced at intervals not to exceed 25 feet.
- Cross frames shall be made as deep as practicable.

- Intermediate cross frames shall preferably be of the cross type or vee type.
- Cross frames on horizontally curved steel girder bridges shall be designed as main members with adequate provisions for the transfer of lateral forces from the girder flanges.
- Cross frames shall be designed for horizontal wind forces as described in Article 10.21.2.

Article 10.21.2 specifies that “a horizontal wind force of 50 pounds per square foot shall be applied to the area of the superstructure exposed in elevation,” where half of the force is applied in the plane of each flange. Article 10.20.2.2 specifies that the maximum horizontal force, F_D in pounds, in the transverse cross frames due to this wind load is obtained from:

$$F_D = 1.14 W S_d \quad (5-1)$$

where W is the wind loading along the exterior flange in pounds per foot and S_d is the cross-frame spacing in feet. From Article 10.21.2, W equals the wind pressure of 50 pounds per square foot times the depth of the superstructure exposed in elevation in feet divided by two to distribute the force to the two flanges. No explanation is given for the 1.14 factor.

Specifications for the design of the diaphragms and cross-frames of horizontally curved bridges in particular are given in Articles 1.4 and 1.8 of the *Guide Specifications for Horizontally Curved Highway Bridges*. Article 1.4 describes the design theory for curved bridges:

- The moments, shears, and other forces required to proportion the individual members, shall be based on a rational analysis of the entire structure which takes into account the complete distribution of loads to the various members.
- Intermediate transverse cross frames must be provided between the longitudinal members for the purpose of distributing the internal torsion at any cross section to the individual members.
- Analysis shall be based on any rational method which takes into account the normal stresses developed in the curved longitudinal members due to nonuniform torsion (lateral flange bending).

This section effectively precludes the use of the simple methods of distributing loads found in the *Standard Specifications*. For those methods, it is assumed that the torsion in the girders is a negligible secondary effect so that only the bending of the girders is considered as a primary structural action. For a horizontally curved girder, torsion is a significant effect and providing restraint against this torsion is necessary for stability. Because this torsional restraint is provided through interaction of the girders, the structure must be analyzed as a system. AASHTO recommends some methods which analyze the bridge as a system including the V-load method and several programs employing the finite element method.

Article 1.8 of the *Guide Specifications for Horizontally Curved Highway Bridges* states the particular requirements for diaphragms, cross frames, and

lateral bracing. The article begins by adopting the general provisions of Article 10.20 of the *Standard Specifications*. Article 1.8 makes the following additions to Article 10.20:

- Cross frames shall be provided at each support and at intermediate intervals between supports with spacing as determined by design considerations.
- Each line of cross frames shall extend in a single plane across the width of the bridge with cross frames included between all longitudinal girders.
- Cross frames shall be full depth members designed as main structural elements to distribute torsional forces to the longitudinal girders.
- The cross frames shall be framed in such a way to transfer the horizontal and vertical forces to the flanges and webs as necessary.
- Cross frame connection plates attached to the girder web shall be connected to flange(s) as well in a manner that will prevent distortion of the web at each end of the connection plate.

Current TXDOT designs for cross-frames

A description of the standard intermediate cross-frame details appears earlier in the description of the bridge systems. Figure 5-1 presents the bracing details again. In accordance with the AASHTO requirements, each line of intermediate cross type cross-frames extends in single plane across the width of

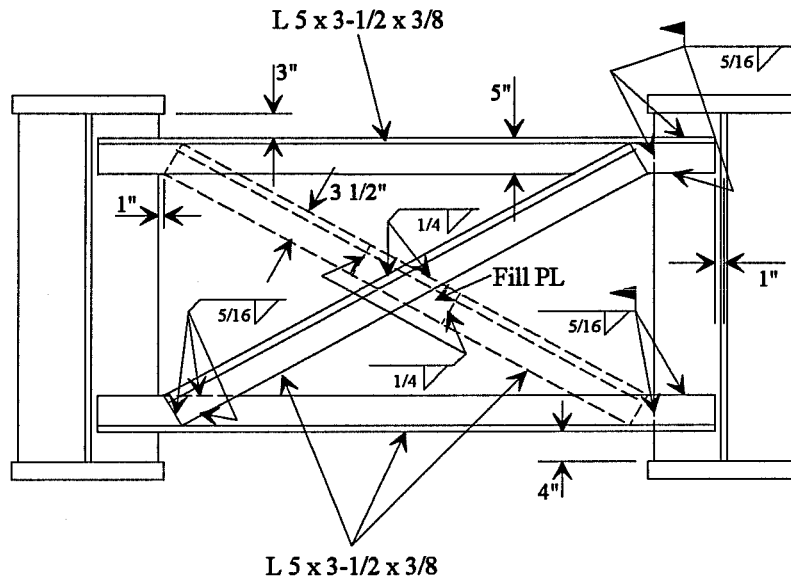


Figure 5-1: Standard X-brace detail

the bridge with cross-frames included between all longitudinal girder. The lines of cross-frames are provided at intervals of less than 25 feet. The cross-frame members transfer the horizontal and vertical forces to the girders via web connection plates. These web connection plates are welded to the webs of the girders and milled to bear on the bottom flanges of the girders and fit tightly against the top flanges so as to preclude web distortion. The cross-frames are made as deep as possible given that the cross-frame members must be placed a few inches inside of the girder flanges to allow for welding of the cross-frame members to the web connection plates.

Anticipated forces in cross-frames

The cross-frames must redistribute lateral wind forces between the girders and must redistribute forces to resist the internal torsion resulting from the curvature of the girders. AASHTO specifies a simple equation for the maximum horizontal force in a cross-frame due to wind load. The results from the AASHTO equation will be compared to the results of a finite element analysis of a bridge subjected to wind load. The Texas Department of Transportation determines the forces necessary to resist the internal torsion of the curved bridge by the V-load method. The cross-frame forces from the V-load method for a bridge will be compared to the forces determined by a finite element analysis.

Horizontal cross-frame forces due to wind loading

Because this cross-frame detail is intended for use as a standard detail for all bridges conforming to the layout specified previously in the description of bridge systems in Chapter 2, the frame must be designed to transfer the worst-case wind load expected in any of these bridges. From the equation for the maximum horizontal force in a cross-frame due to wind load, the worst-case

horizontal force results when the cross-frame spacing and the depth of the superstructure exposed in elevation are at their maximum values. The maximum cross-frame spacing is 25 feet. The maximum depth of the superstructure results when the webs of the girders are deepest and when the width and superelevation of the slab are at a maximum. For this analysis the maximum girder depth was assumed to be 66 inches, the maximum slab width was taken as 60 feet, and the maximum superelevation was assumed to be 6 percent. Including the thicknesses of the slab and the girder flanges, the maximum depth of the superstructure is about 10 feet. Although no barriers were shown in the bridge designs used for this study, such barriers should be included in the calculation of the depth of the superstructure. In the following calculations, the height of the barriers is ignored. Including the barrier height in the calculations would increase all of the results by the same ratio, so ignoring the barriers will not affect the comparison. Thus, given a superstructure depth of 10 feet, the maximum wind load on each flange is

$$W = 50 \text{ psf} \times 10 \text{ ft} / 2 = 250 \text{ lbs/ft} \quad (5-2)$$

Thus, the maximum horizontal force in a cross-frame is

$$F_D = 1.14 \times 250 \text{ lbs/ft} \times 25 \text{ ft} = 7125 \text{ lbs} = 7.1 \text{ kips} \quad (5-3)$$

This horizontal force is then distributed among the four members in each cross-frame.

Another simple way to estimate the horizontal force in a cross-frame is to assume that the cross-frames distribute the wind pressure on the exposed girder evenly among all of the girders. It is further assumed that the concrete slab does not help distribute the wind load to the girders. Each line of cross-frames, then, would be responsible for distributing a total force F_T equal to the wind pressure times the depth of the superstructure exposed in elevation times a tributary length

of span equal to the cross-frame spacing. For the worst-case bridge described above,

$$F_T = 50 \text{ psf} \times 10 \text{ ft} \times 25 \text{ ft} = 12.5 \text{ kips} \quad (5-4)$$

Since there are seven girders, each girder would resist one-seventh of this force. The maximum horizontal force in a cross-frame will appear in the cross-frame adjacent to the girder exposed to the wind, since the girder exposed to the wind is subjected to the total force F_T but resists only one-seventh of this force, leaving six-sevenths of the force to be transmitted by the cross-frame. From this argument the maximum horizontal force in a diaphragm would be,

$$F_D = 6/7 \times 12.5 \text{ kips} = 10.7 \text{ kips} \quad (5-5)$$

A finite element analysis of this worst-case bridge bears out this result. When the slab is excluded from the model, the maximum horizontal force seen in a cross-frame is 10.99 kips in a cross-frame adjacent to an exposed girder. The distribution of forces in the line of cross-frames also compares well to the forces expected from an equal distribution of forces to the girders as shown in Table 5-1. In the table cross-frame 1 corresponds to the cross-frame adjacent to the exposed girder.

Table 5-1: Distribution of cross-frame forces due to wind load

Cross-frame	Forces distributed evenly among the girders	Finite element analysis
1	10.7 kips	11.0 kips
2	8.9 kips	9.2 kips
3	7.1 kips	7.4 kips
4	5.4 kips	5.6 kips
5	3.6 kips	3.8 kips
6	1.8 kips	1.9 kips

When the slab is included in the model, the slab attracts some of the horizontal forces away from the cross-frames. With the slab the maximum horizontal force in the cross-frames comes close to the load given by AASHTO, specifically 7.7 kips predicted by the finite element analysis of the bridge with a slab compared to 7.1 kips predicted by the AASHTO equation. From this comparison, it is seen that the AASHTO specifications for cross-frame forces due to wind loads provide reasonably close approximations to the forces predicted by more complicated methods when the slab is considered to help resist the wind load.

Of course, the maximum wind force to which a bridge is subjected is not known with much certainty. Consequently, the small differences in the results from the different analysis methods are not significant.

Cross-frame forces due to resistance of internal torsion

Besides resisting the horizontal forces from the wind load, the cross-frames must resist the internal torsion resulting from the curvature of the girders. AASHTO specifies that the bridge must be analyzed as a system to determine the forces in the cross-frames. To this end the Texas Department of Transportation

analyzes the bridges using the V-load method.

As described in the discussion of the V-load method, when a curved I-girder is subjected to a vertical load, the girder resists the load by developing axial stresses primarily in the flanges, much like a straight I-girder. Unlike a straight girder, however, the axial stresses are not collinear along the length of the curved girder. Thus, at any cross-sectional slice of the girder there is a tangential component of the axial stress and a normal component. The tangential component of the stress is associated with the conventional bending of the girder while the normal component is associated with lateral flange bending. The primary purpose of the cross-frames in a curved bridge is to resist this lateral flange bending. The cross-frames accomplish this by redistributing the forces which would lead to lateral flange bending as vertical forces on the girders in such a way that the internal torsion of the cross-section is balanced.

In the development of the V-load method equations as given in Appendix C, it is first assumed that the vertical load produces moments in the girder as if the girder were straight. The moments from the analysis of the straight girder are used to find the magnitudes of the normal forces which, unrestrained, would lead to lateral flange bending. Given a moment in the girder at the cross-frame of M , a cross-frame spacing of d , a girder depth of h , and a radius of curvature for the girder of R , the lateral flange force is calculated as,

$$H = M d / h R \quad (5-6)$$

where this lateral flange force H is directed away from the center of curvature in the compression flange and toward the center of curvature in the tension flange. The torsion resulting from the application of these forces must be balanced by the torsion resulting from the vertical reactions at the girders such that,

$$h \Sigma H_i = \Sigma V_j x_j \quad (5-7)$$

where H_i is the lateral force in a flange of girder i , V_j is the vertical reaction from girder j , and x_j is the distance of girder j from the centroid of the bridge cross-section. The V-load method assumes that the bridge rotates as a rigid body such that the vertical reactions are proportional to the distance from the centroid of the cross-section.

From this discussion it can be seen that the horizontal and vertical forces in the cross-frames will be maximized when:

- The moments in the girders are maximized.
- The spacing of the cross-frames is maximized.
- The depths of the girders are minimized.
- The radius of curvature of the bridge is minimized.
- The distances from the centroid of the bridge cross-section to the girders are minimized

To maximize the girder moments, the span lengths and loads should be maximized. Thus full dead and live load should be used on a span of about 200 feet. The maximum allowable cross-frame spacing according to AASHTO is 25 feet. The minimum girder depth used for these bridges is about 48 inches, the minimum radius of curvature is about 900 feet. The minimum distances from the centroid to the girders occurs when the girder-to-girder spacing and the number of girders are minimized, so the girder-to-girder spacing should be about 7.5 feet and four girders should be used.

A bridge based on these dimensions was analyzed using the V-load method. The line of cross-frames at the cross-section where the moments in the girders were greatest naturally had the highest lateral flange forces. The lateral

flange forces for this line of cross-frames is shown in Figure 5-2. Balancing these lateral forces are vertical forces from the girders as shown in Figure 5-3. These external forces on the cross-frame lead to internal forces in the cross-frame members as shown in Figure 5-4, where half of the vertical reaction from each girder is assumed to act on the top connection between the girder and cross-frame and the other half is assumed to act on the bottom connection.

These results were compared to the results from a finite element analysis, as shown in Figure 5-5. For the initial finite element analysis all of the girders were directly supported on individual pin supports at the bent cap locations and the slab was considered to have no stiffness. This was done to make the results of the two types of analysis directly comparable, since the V-load method makes these same assumptions about the girder supports and slab stiffness. Later finite element analyses will be conducted with the slab stiffness included and the girders will be supported by the bent caps.

A comparison of the V-load results and the finite element results shows that the forces in the diagonal members are higher in the V-load analysis than in the finite element analysis. This indicates that the vertical reactions from the girders as computed by the V-load method are conservative. This can be attributed partly to the V-load assumption that the moment along the tributary length of the girder has a constant value equal to the moment at the cross-section containing the line of cross-frames. In this case, the moment at the cross-section containing the line of cross-frames was at a maximum and decreased on either side of this cross-section, so that the true lateral flange force would be less.

A comparison of the results also shows that whereas the forces in the horizontal members from the V-load analysis are almost symmetric about the vertical centerline of the cross-section, the forces from the finite element analysis are weighted toward the outside of the cross-section. The near symmetry in the

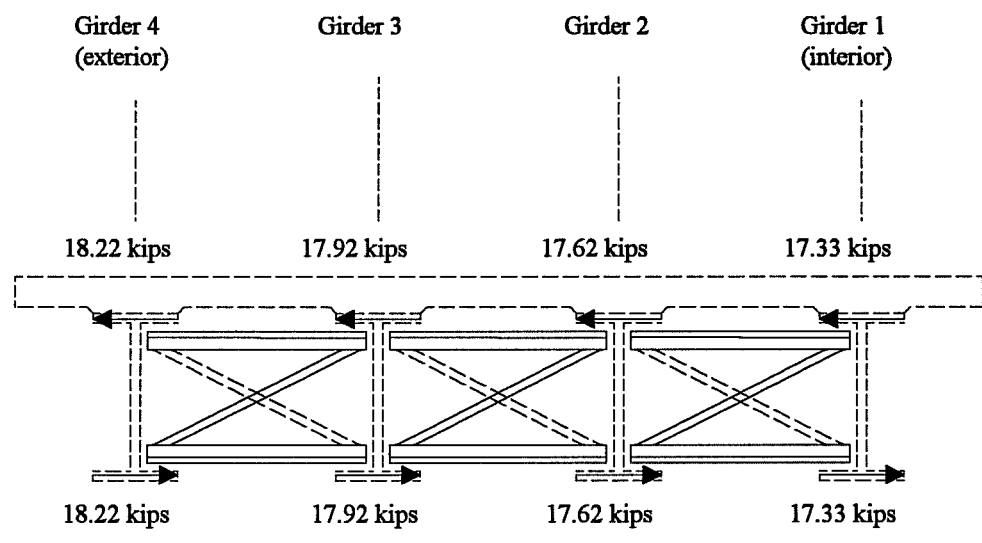


Figure 5-2: Lateral flange forces acting on the cross-frames according to the V-load method

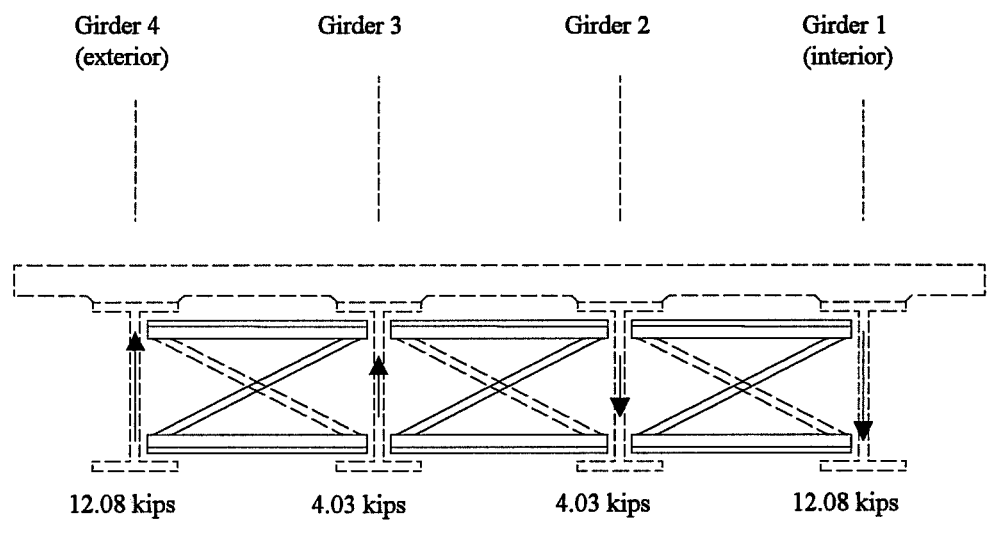


Figure 5-3: Vertical reactions of the girders on the cross-frames according to the V-load method

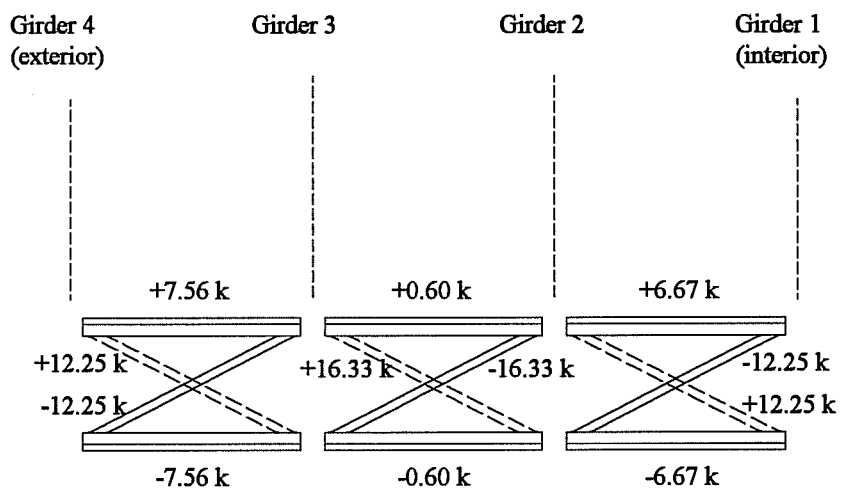


Figure 5-4: Forces in cross-frame members according to the V-load method

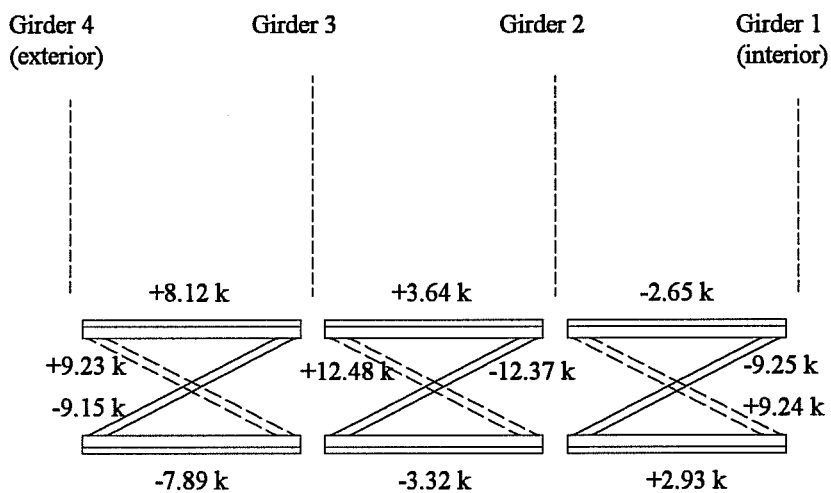


Figure 5-5: Forces in cross-frame members according to the finite element analysis not including the effects of bent cap flexibility

V-load case results from having nearly identical moments in all four girders leading to nearly identical lateral flange forces in all girders. The finite element analysis indicates that the lateral flange forces are much greater in the exterior girder than in the interior girder. This can be partly attributed to the fact that the V-load method makes only a first-order calculation of the lateral flange forces.

The V-load method calculates the lateral flange forces only once based on the moments in straight girders under just the dead and live loads. When the girders are analyzed again to produce final moment diagrams for the curved girders by adding the initial dead and live loads to the vertical shear forces needed to balance the internal torsion, the distribution of moments among the girders changes such that moments in the interior girders decrease while moments in the exterior girders increase. For this particular bridge for example, the moment in girder 1 decreases by about 25 percent and the moment in girder 4 increases by about 30 percent. If the lateral flange forces were recalculated based on these new moment diagrams, the lateral flange forces will be much higher in girder 4 than in girder 1, thus correlating better with the finite element analysis.

It should be noted that these second-order effects impact only the distribution of lateral flange forces and not the distribution or magnitude of the vertical shear forces. The magnitudes of the vertical shear forces are based on the sum of the moments across the cross-section, so the decreases in moments in the interior girders cancel the increases in moments in the exterior girders. The distribution of the vertical shear forces is fixed such that the vertical shear force in a girder is proportional to the distance of the girder from the centroid of the deck's cross-section. Thus, using the V-load method for determining the girder moments gives adequate results without considering second-order effects, while

using the method for determining the cross-frame forces requires consideration of the second-order effects.

As mentioned before, these results have ignored the stiffness of the concrete slab. When the slab is added to the model, some of the lateral flange forces will be distributed to the slab rather than the cross-frame members. Figure 5-6 shows the distribution of cross-frame member forces when the slab is included. The forces have changed substantially from when the stiffness of the slab was excluded from the analysis. The first reason for the difference is that the distribution of stresses in the girders has changed since the girders now act compositely with the slab, thus altering the distribution of lateral flange and slab forces. The second reason for the difference is that the lateral flange and slab forces are now partly distributed by the slab thereby reducing the horizontal forces in the cross-frames. The third reason for the difference is that the slab has torsional stiffness which allows the slab to resist some of the internal torsion, thereby reducing the vertical shear forces on the girders. The overall effect of including the slab, then, is to alter the distribution and decrease the overall magnitudes of the cross-frame forces, so the V-load method still produces conservative estimates of the cross-frame forces in resisting the internal torsion.

Additional cross-frame forces due to flexibility of the bent caps

Heretofore the finite element models have included individual vertically rigid pin supports under each girder at the bent cap locations. The real bridges, however, do not have vertically rigid pin supports at each girder, but rather, the girders are supported by the bent caps. Although the bent caps are very stiff, the girders at the ends of the bent cap inevitably sag slightly at the bent cap cross-sections. This sag puts additional forces on adjacent cross-frames as the cross-frames attempt to straighten the cross-section. The forces will be such that the

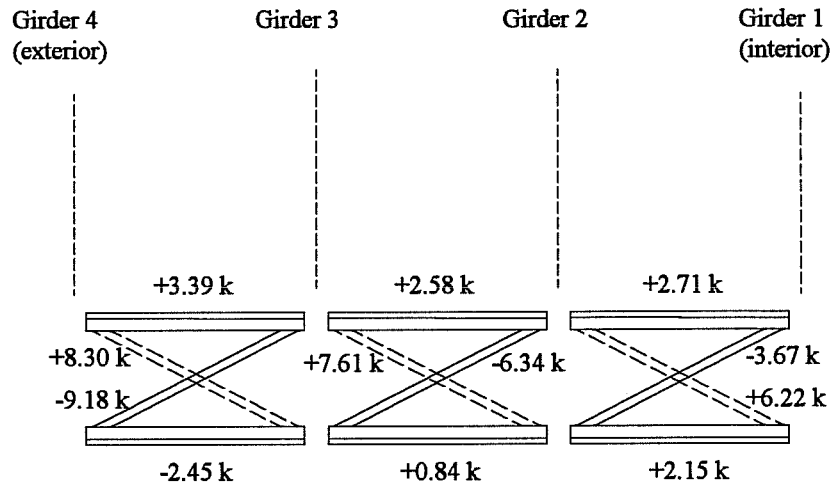


Figure 5-6: Forces in cross-frame members according to the finite element analysis considering the stiffness of the slab

slab, which will now be considered in the finite element model, will be in tension in the transverse direction while the bottom chords will be in compression. When the individual pin supports are replaced with bent caps with 72 inch wide bearing supports, the forces in the cross-frames adjacent to the bent caps are as shown in Figure 5-7. These forces include not only the effects of bending of the cross-frames due to the bent cap flexibility but also include the effects of torsion in the bridge. The maximum forces – relative to the capacities of the members which are presented later – have not changed significantly from the earlier analyses indicating that, for this particular bridge, the cross-frame bending effects do not overwhelm the torsional effects. On the other hand, the bent caps in this model are not the most flexible bent caps used in these bridges.

Because the worst-case forces in the cross-frames occur when the bent caps have the greatest flexibility, the model was changed to a wider, seven girder bridge with a very flexible bent cap. The resulting worst-case cross-frame member forces are shown in Figure 5-8. The maximum compressive forces in the bottom chords are about 52 kips, much higher than the maximum compressive force due to torsional effects of 7.6 kips as predicted by the V-load method alone. Admittedly, the bent caps used in this model are probably much more flexible than ones likely to be seen in real bridges. The particular bent caps in this model allow the ends to sag about 0.75 inches, whereas more typical bent caps allow sags of only about 0.3 inches. Even when the bent caps are made stiffer so that the ends sag only 0.3 inches, however, the maximum compressive forces in the bottom chords are still around 27 kips. Thus, the forces which result from the flexibility of the bent caps will be significant in the design of the cross-frame members. It should be noted that only the cross-frames immediately adjacent to the bent cap are significantly affected by bent cap flexibility.

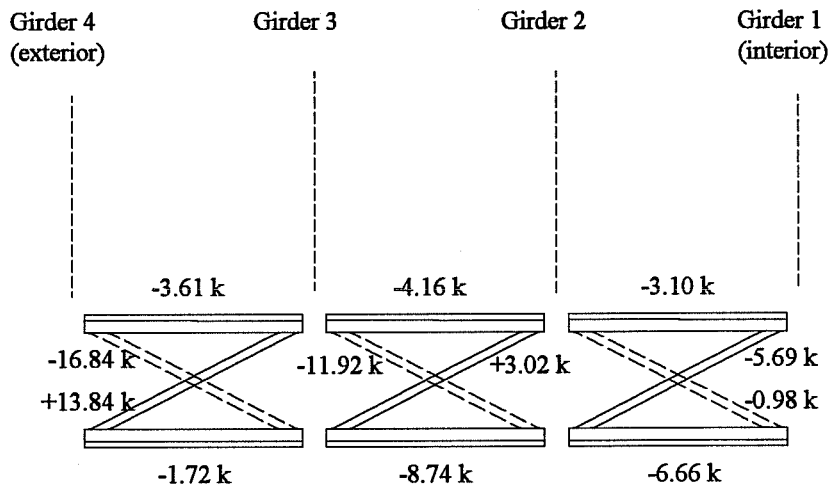


Figure 5-7: Forces in cross-frame members according to the finite element analysis considering the flexibility of the bent caps

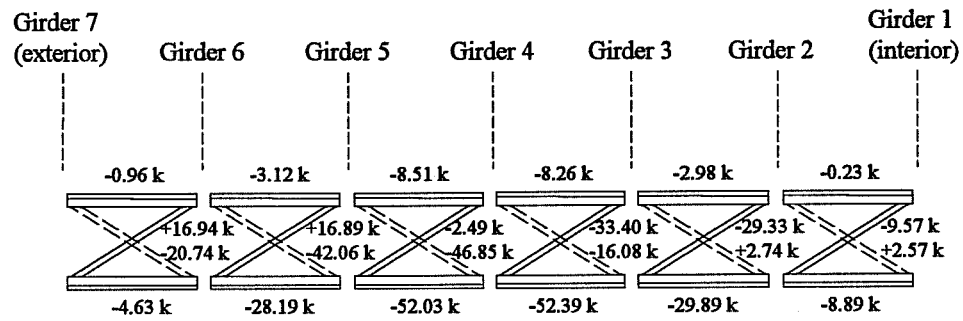


Figure 5-8: Forces in cross-frame members according to the finite element analysis considering the flexibility of the bent caps

Conclusions on forces

The AASHTO approximation of the maximum horizontal force in the cross-frames due to wind load and the V-load method approximations of the cross-frame member forces due to internal torsion appear adequate for bridges where all girders are individually supported at the interior support locations. When the girders are supported by bent caps at the interior support locations, the flexibility of the bent cap will lead to cross-frame forces significantly larger than those predicted by the V-load method.

Allowable forces in TxDOT cross-frame members

In this section allowable loads on the members of the standard cross-frame, as shown in Figure 5-1, will be estimated. Because the AASHTO specifications are not as thorough in the treatment of axially loaded angles as the American Institute of Steel Construction (AISC) *Allowable Stress Design* specifications [3], allowable forces in the cross-frame members will be determined by the AISC specification.

For a tension member, the allowable force is 91 kips, controlled by fracture of the effective net area at the connection. For a horizontal compression member with an unbraced length of up to 96 inches and an assumed k-factor of 1.0, the allowable force is 28 kips, based on flexural-torsional buckling. For a diagonal compression member with an unbraced length of up to 113 inches and an assumed k-factor of 1.0, the allowable force is 20 kips, based on flexural-torsional buckling. These allowable forces are based on A588 steel.

Design recommendations for cross-frames

The cross-frames must be designed to distribute wind forces to the girders and to redistribute forces resulting from torsion in the curved bridge. The

maximum horizontal cross-frame forces due to wind load are predicted reasonably well by the AASHTO equation for these forces, except when the slab has not developed adequate stiffness to help the cross-frames distribute the wind forces to the girders. The forces in the cross-frame members which are required to distribute forces arising from the internal torsion of the bridge are predicted conservatively by the V-load method. The current TxDOT cross-frame designs are conservative for the distribution of the wind load and of the forces arising from the torsion in the bridge. In the cross-frames adjacent to the bent caps, however, the flexibility of the bent caps result in cross-frame forces well in excess of the forces predicted by the AASHTO equation and the V-load analysis. For these cross-frames additional design criteria should be considered in the design of the cross-frames.

Member forces from wind load and internal torsion

The AASHTO equation for wind load estimates the maximum horizontal force in a cross-frame for a worst-case bridge as 7 kips, although during construction when the slab has not developed enough stiffness to help distribute the wind forces, a finite element analysis estimates a maximum horizontal force of 11 kips. During construction, however, no live load is applied to the bridge, so the forces arising from the resistance of the internal torsion will not be at the maximum levels. Furthermore, when the bridge is in operation, full live load and wind load need not be considered simultaneously. Only 30 percent of the wind load need be applied with full live load.

The V-load method conservatively predicts maximum tensile and compressive forces in the cross-frame diagonals of 16 kips. The V-load method also adequately predicts maximum tensile and compressive forces in the cross-frame horizontals of 8 kips. Finite element analyses show the horizontal forces

to reach as high as 8 kips in both tension and compression.

For the current TxDOT designs the member forces from wind and the resistance of internal torsion fall within the allowable forces, which allow 91 kips in the tension members, 29 kips for the horizontals in compression, and 20 kips for the diagonals in compression.

Member forces from flexibility of the bent caps

In addition to distributing wind forces and the forces arising from internal torsion of the bridge, the cross-frames adjacent to the bent caps must resist the sagging of the girders at the ends of the cross-section of the bridge which results when the flexible bent caps are supported only at the center of the bridge's cross-section. A simple technique for estimating the cross-frame forces can be developed which bases the forces in the cross-frames on the displacements at the ends of the bent cap. Because the bent caps experience a great deal of shear deflection and because the bent caps have nonuniform cross-sections, estimates of the end deflections may prove difficult. Nevertheless, presenting the simple technique may help illustrate the necessary conditions which guarantee an adequate design for the cross-frames.

Estimation of the cross-frame forces resulting from the sagging of the ends of the bent caps can be achieved by treating the line of cross-frames as a frame or truss, the ends of which displace downward relative to the center by the same amount as the ends of the bent cap, as shown in Figure 5-9. The slabs and other cross-frames, however, will help to straighten the cross-section of the bridge, so the assumption that the ends of the line of cross-frames adjacent to the bent caps must deflect the same amount as the ends of the bent caps is conservative. Nonetheless, if both ends of the bent cap, and therefore both ends of the line of cross-frames adjacent to that bent cap, displace the same amount Δ , then by

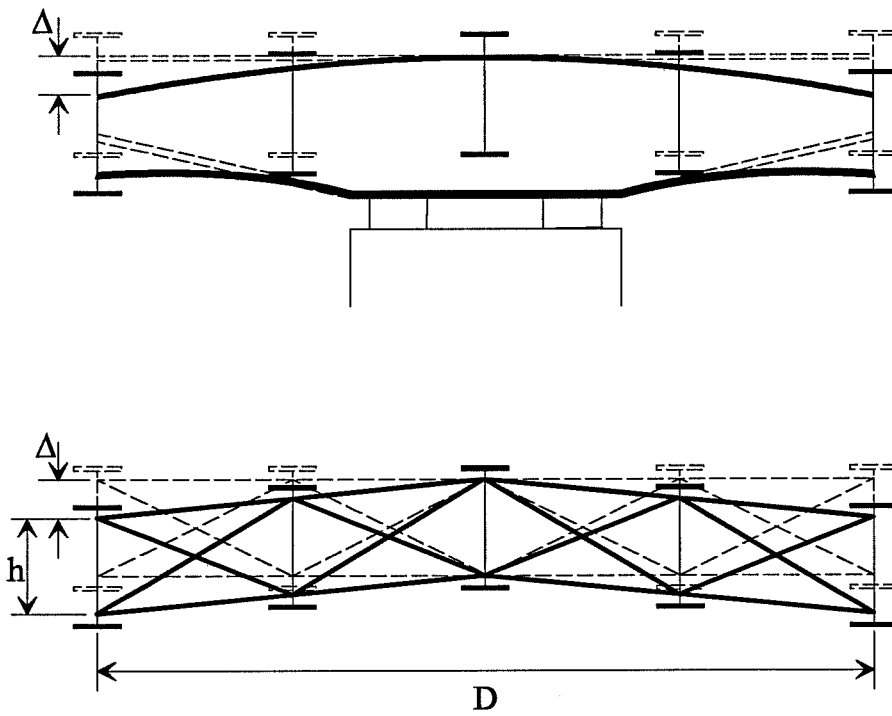


Figure 5-9: Similar deflections of the bent caps and adjacent line of cross-frames

symmetry, the line of cross-frames can be divided in half, so that each half of the line of cross-frames acts like a cantilevered frame with an end displacement equal to the end displacement of the bent cap. A plane frame or truss analysis program can be used to determine the cross-frame forces under the applied end displacement.

The only practical way to ensure that the maximum forces in the cross-frames are below the allowable forces is to control the bent cap deflections. It is either useless or impossible to modify the cross-sectional area of the cross-frame members, the depth of the cross-frames, or the width of the bridge in order to control cross-frame forces. Increasing the cross-sectional area of the cross-frame members would increase their capacity, but because most of the forces in the cross-frames near the bent caps result from an imposed displacement, member forces would increase in a roughly proportionate manner. Increasing member size will help reduce the imposed displacement slightly, but the gains from increasing member size are modest. For example, doubling the member size would still result in an increase in the member forces of 70 to 80 percent. Likewise, reducing the cross-sectional area of the cross-frame members would decrease the forces in the members but at the same time would decrease their capacity by roughly the same degree. Reducing the depth of the cross-frames is not allowed under AASHTO, which requires that the cross-frames be made as deep as practicable. The width of the bridge cross-section, of course, is predetermined by the number of traffic lanes and cannot be altered simply to reduce forces in the cross-frames. Thus, the only cross-frame parameter which can be altered to reduce the cross-frame forces is the bent cap deflections.

As mentioned before, however, calculating the bent cap deflections can be difficult. If the deflections can be calculated, a plane frame or truss analysis program should be used to determine the cross-frame forces. Otherwise, the

designer should at least be aware that it is necessary to limit bent cap deflections in order to guarantee that the forces in the cross-frames are below the allowable limits. Furthermore, the designer should be aware that these deflection limits can be quite small. For example, given that the maximum allowable compressive force in a horizontal member given the current TxDOT cross-frame design is 29 kips, the deflection limit for a narrow bridge with a bent cap 24 feet across, bearings spaced at 72 inches, and with cross-frames 59 inches deep (corresponding to a web depth of 66 inches) is only 0.12 inches, while the deflection limit for a wide bridge with a bent cap 48 feet across and with cross-frames 59 inches deep is only 0.41 inches.

Conclusions on design recommendations

Current TxDOT cross-frame designs appear adequate for the distribution of forces due to wind load and forces resulting from the internal torsion of the bridge. To ensure that these designs are also adequate in resisting the sag of the ends of the bridge cross-section near the bent caps, additional analyses of the cross-frames may be required, or deflection limits may need to be placed on the bent caps.

CHAPTER 6

SUMMARY AND CONCLUSIONS

Introduction

This thesis has pursued four goals. The first goal was to determine reaction forces and deflections at the bearings using the finite element method. Achieving the first goal required the pursuit of the second goal of determining loading patterns which produced maximum bearing forces and deflections. The third goal was to verify the adequacy of the V-load method for determining both the behavior of the longitudinal girders and the behavior of the bent cap and bearings. The fourth goal was to investigate the forces developed in the cross-frames.

Bearing reactions and deflections

The loading patterns that produce the maximum bearing reactions and rotations are presented in Chapter 3. The loading patterns are summarized in Figures 6-1 and 6-2. Although these patterns are shown for a bridge with the centerline of the bearings coincident with the centerline of the deck, the patterns also apply when the bearings are offset from the center of the deck. When the bearings are offset, the edges of the loaded areas move with the bearings.

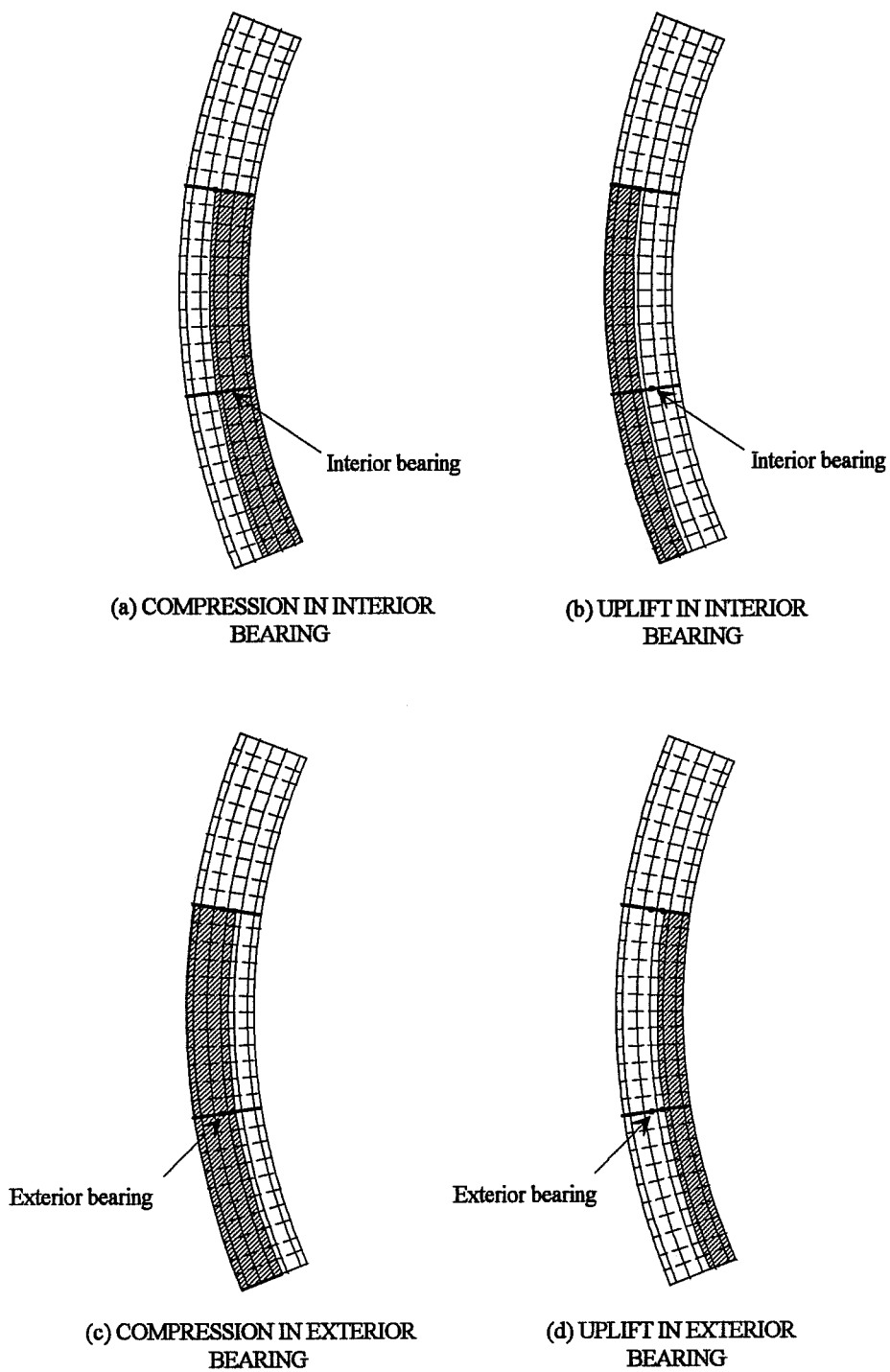
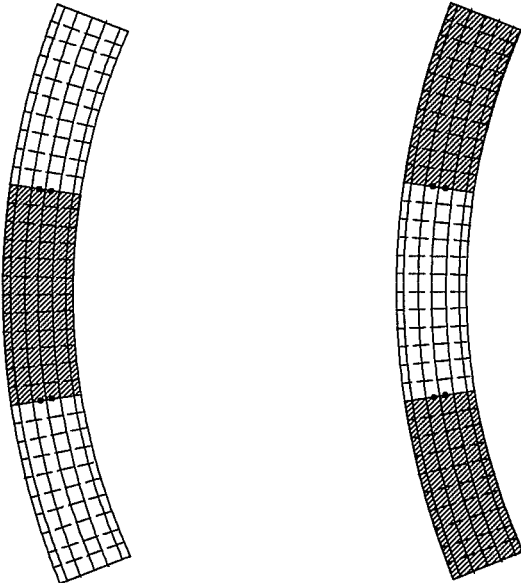


Figure 6-1: Loading patterns to produce maximum vertical reactions in bearings



(a) DECK ROTATES DOWNWARD
TOWARD CENTER SPAN

(b) DECK ROTATES DOWNWARD
TOWARD END SPANS

Figure 6-2: Loading patterns to produce maximum rotation in bearings

Evaluation of the V-load method

Chapter 4 presents a comparison between the V-load method and the finite element method in determining the girder moments and the bearing reactions. The V-load method predicts reasonably accurate girder moments for bridges supported on narrow piers. The vertical forces exerted by the girders on the bent caps, however, are not distributed properly by the V-load method. In some cases this results in somewhat unconservative estimates of the bearing reactions.

Unconservative estimates of the bearing reactions can arise when the live load is not placed in all of the lanes. When live load is placed in the interior lanes, the V-load method conservatively predicts bearing reactions, but when the live load is placed in the exterior lanes, the V-load method unconservatively predicts the bearing reactions. The unconservative errors in the maximum compressive force in the bearings will typically be only three or four percent, while unconservative errors in the maximum uplift – or more typically, the minimum compression – force can be more than ten percent. If the V-load method predicts that there will always be substantial compression in the bearings, the error in the minimum compression forces will not affect the design since the bearings are designed to withstand some amount of uplift even when none is expected. If the V-load method predicts uplift, however, the V-load method's error will be conservative.

The V-load method's results are not significantly unconservative when the end spans are fairly long relative to the length of the bridge. For example, typical bridges with span ratios of 1.0 – 1.2 – 1.0 unconservatively estimate the vertical reaction in the exterior bearing by about five percent. For such bridges, bearing designs based on V-load analyses should be adequate albeit slightly unconservative. For bridges with short end spans and long center spans,

estimates of the bearing reactions can be more than 15 percent unconservative. For these cases designers should consider using a finite element analysis that properly models the support conditions.

For off-center pier supports, the V-load method produces results which are fairly consistent with the finite element method results, so the V-load method should be adequate for bearing designs of bridge with off-center piers.

Cross-frame forces

Chapter 5 presents analyses of the cross-frame forces in distributing wind load, distributing forces to resist the internal torsion of the deck, and distributing forces to resist the sag at the ends of the bent caps. The maximum horizontal cross-frame forces due to wind load are predicted reasonably well by the AASHTO equation for these forces. The forces in the cross-frame members which are required to distribute forces arising from the internal torsion of the bridge are predicted conservatively by the V-load method. The current TxDOT cross-frame designs are conservative for the distribution of the wind load and of the forces arising from the torsion in the bridge. In the cross-frames adjacent to the bent caps, however, the flexibility of the bent caps result in cross-frame forces well in excess of the maximum forces predicted by the AASHTO equation and the V-load analysis. For these cross-frames additional design criteria should be considered in the design of the cross-frames, such as imposing deflection limits on the ends of the bent caps.

APPENDIX A

DESCRIPTION OF THE FINITE ELEMENT MODELS

Introduction

The bridges were modeled using the ANSYS [4] finite element analysis program by Swanson Analysis Systems, Inc. ANSYS is a commercially available general-purpose finite element program. ANSYS can consider nonlinearities in both materials and geometry. In this study, however, only first-order elastic analyses were performed.

For the multigirder, multispan steel bridges in this study, four types of components were used: longitudinal plate girders, X- and K-brace cross-frames, steel bent caps, and concrete slabs. The following paragraphs describe how each component was modeled in ANSYS and, where appropriate, how support conditions were applied. In Appendix B, a simple bridge system is modeled using ANSYS. Analysis results are compared to closed form solutions to provide some verification of the modeling techniques.

Longitudinal steel girders

The longitudinal plate girders were modeled using 4-node shell elements for the webs and 2-node beam elements for the flanges, with each of these elements extending from one cross-frame to the next, as shown in Figure A-1.

Using only one set of elements between cross-frames is a bare minimum

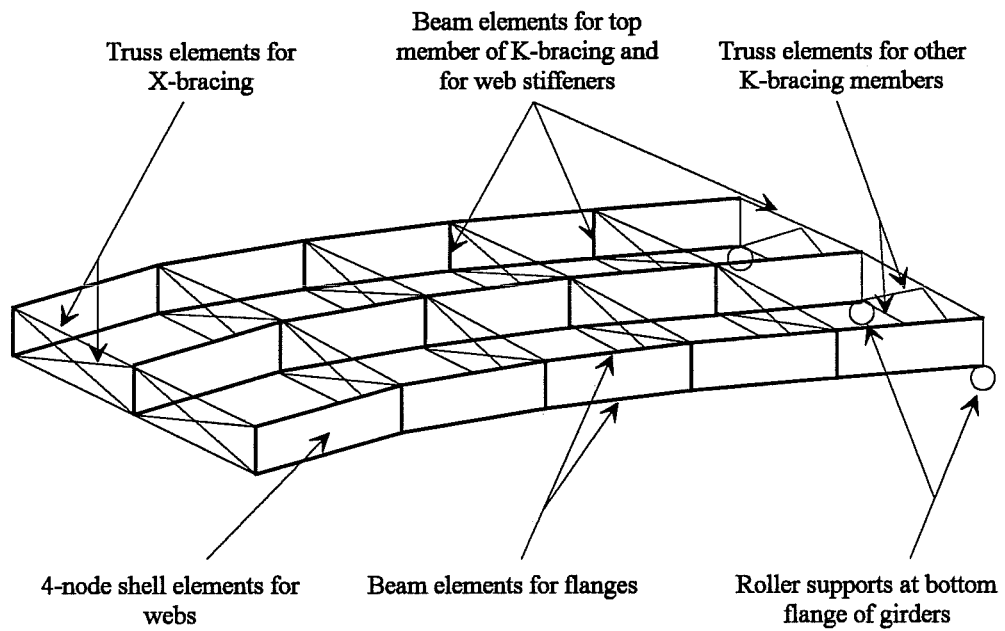


Figure A-1: Elements used to model the steel subframe

to provide the necessary connectivity between the bridge members. A finer mesh could have been used, but analyses showed that accuracy improved very little with mesh refinement while computer time and memory increased greatly with mesh refinement. Analyses were performed on a model with one set of elements between cross-frames and on a model with three sets of elements between cross-frames. The deformations and stresses given by the models differed by about only one percent, where the model with only one set of elements between the cross-frames tended to be stiffer than the model with three sets of elements between the cross-frames. Although models with finer element meshes tend to be more accurate, by tripling the number of elements, the accuracy improved by only about one percent while the computer run time and memory requirements tripled. Thus, such model improvements are not very practical and were not included in the models.

Another problem arising from using a coarse mesh is that element properties, namely web and flange thicknesses, cannot change between cross-frames. Where designs call for a change in plate thickness between cross-frames, the model simply uses a single thickness – the thickness of whichever plate occupies the greater length of the distance between the cross-frames. Because the cross-frames are typically spaced about 15 feet apart, the splice between the two different plates will always be within 7.5 feet of the correct location. This discrepancy in splice location is small relative to the total length of the bridge, so the discrepancy does not produce an appreciable error. For example, when the location of a splice in one model was moved about 15 feet and where the increase in plate thickness at the splice was 25 percent, the reactions at the bearings near the splice changed only 0.5 percent while the reactions in the bearings further from the splice changed even less. Thus, using a single plate thickness between the cross-frames seems adequate for modeling

the girders.

The element types used to model the girders were chosen to provide both accuracy and simplicity. Because the girders act primarily as bending members, the bending stresses will concentrate in the flange elements as axial stresses. The web elements, then, must primarily model the transfer of shear. This can be accomplished by modeling the webs with only a single shell element over the web depth, where web depth is considered to be the distance between the centroids of the top and bottom flanges. Such simple web elements are possible since the web elements will be close to square – web element aspect ratios of length to depth of less than three to one – and since shell elements model in plane shear very accurately. Furthermore, shell elements model out of plane bending very well and can include the effects of web distortion. Had shell elements also been used for the flanges, the elements would have been long, thin and badly-formed, producing inaccurate results, particularly for the lateral bending of the flanges associated with torsion in plate girders. Furthermore, using shell elements for the flanges would require additional nodes not already provided by the webs, which would increase the size of the computer model and increase the time required to run the model. Lastly, it is unclear how to connect the flange tips to the slab since the slab will load the entire width of the flange vertically but will load only the middle of the slab in shear. Instead, beam elements, which produce results equivalent to engineering beam theory for any length of element regardless of the nominal aspect ratio of the plate being modeled, were chosen since they can fairly accurately model the axial flange forces due to girder bending and lateral bending moments due to torsion of the girder. These beam elements were located vertically at the middepths of the flanges so that the axial forces in the flanges due to bending, which would be centered very close to the centroids of the flanges, would coincide with the

centroids of the beam elements. At the two ends of the bridge where the longitudinal girders rest on supports, the bottom end nodes of the girders are fixed against translation in the vertical and transverse directions. The nodes are free to rotate and to translate in the longitudinal direction. Thus, the supports act as rollers which roll in the longitudinal direction.

Steel cross-bracing

The X-braces are modeled using truss elements for the brace members and beam elements for the web stiffeners. Truss elements consider only axial stiffness, and disregard bending and torsional stiffness. The elements are connected to the top and bottom flanges of the girders, as shown in Figure A-1. The K-braces are modeled using beam elements for the top cross members and truss elements for the other members. Again, all brace elements are considered to connect at the top and bottom flanges of the girders, as shown in Figure A-1.

Concrete Slab

The concrete slab is modeled as a homogeneous elastic plate with no consideration given to reinforcement or cracking. Cracking is ignored because under service level loads tensile stresses in the concrete over the negative moment region rarely exceeds the ultimate tensile stress of the concrete. The slab consists of shell elements, where each element extends laterally from one girder to the next and longitudinally from one cross-frame to the next, as shown in Figure A-2. The shells are modeled at the middepth of the slab. This means there will be a gap between the shell elements of the slab and the beam elements of the top flanges of the girders of half the slab thickness plus half the top flange thickness. To connect the slab to the girders across this gap, short, extremely stiff beam elements, “shear studs,” if you will, were provided to

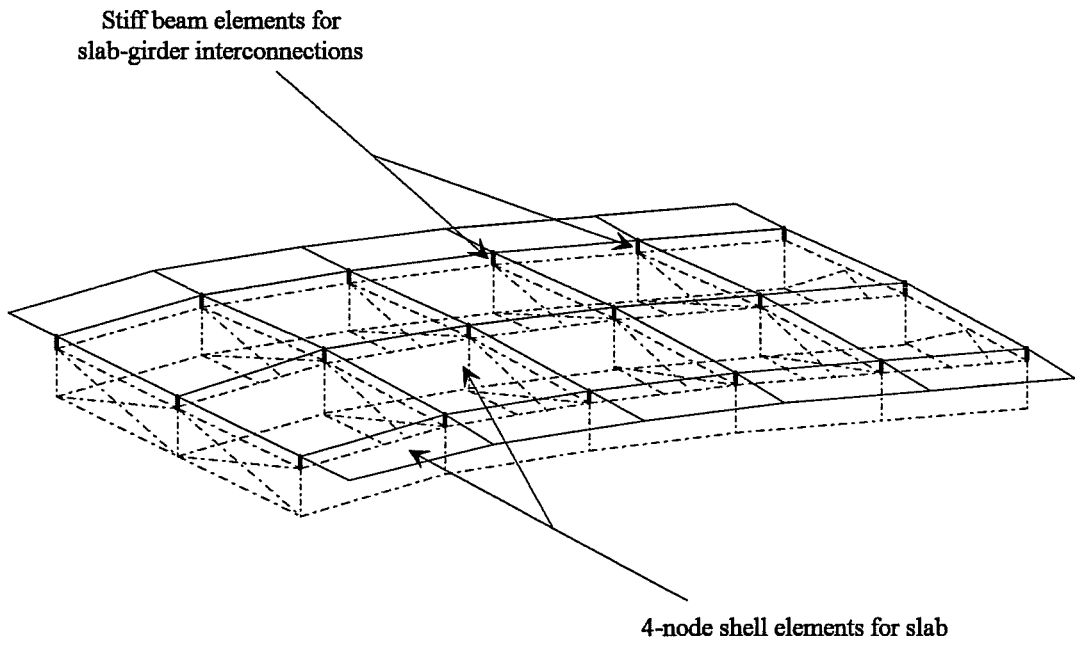


Figure A-2: Elements used to model the slab

ensure that plane sections remain plane for the girder-slab system. The slab in the negative moment regions of an actual bridge is typically not composite with the girders. Thus the “shear studs” in the negative moment region of the model provide more stiffness than would be present in the actual bridge. When the “shear studs” were replaced with elements which allowed the slab to move relative to the girders, however, the change in bearing reactions was less than two percent. Because the errors caused by using “shear studs” in the negative moment region were negligible, the “shear studs” were used over the full length of the bridge, thereby keeping the model generation simpler.

Steel bent caps

The steel bent caps are modeled like the girders, with shell elements for the webs and beam elements for the flanges, as shown in Figure A-3. To provide adequate connectivity between the bent caps and the girders, the bent caps are given the same depth as the girders – which is generally not quite true for the bent caps of the real bridges, where the central portion of the bent cap is somewhat deeper than the girders – and the bent caps are located at the same height as the girders – which is generally not true of real bridges, where the bent caps are usually placed about half a foot lower than the girders to allow splicing the top flanges of the girders together to make the girders continuous.

Where no supports lie between two adjacent girders, the bent cap elements extend from girder to girder. Where the bent caps are supported between girders, however, additional sets of nodes are provided at the support locations, as shown in Figure A-3. Rather than a single set of elements extending from girder to girder, then, one set of bent cap elements extends from one girder to the support and a second set of elements extends from the support to the second girder.

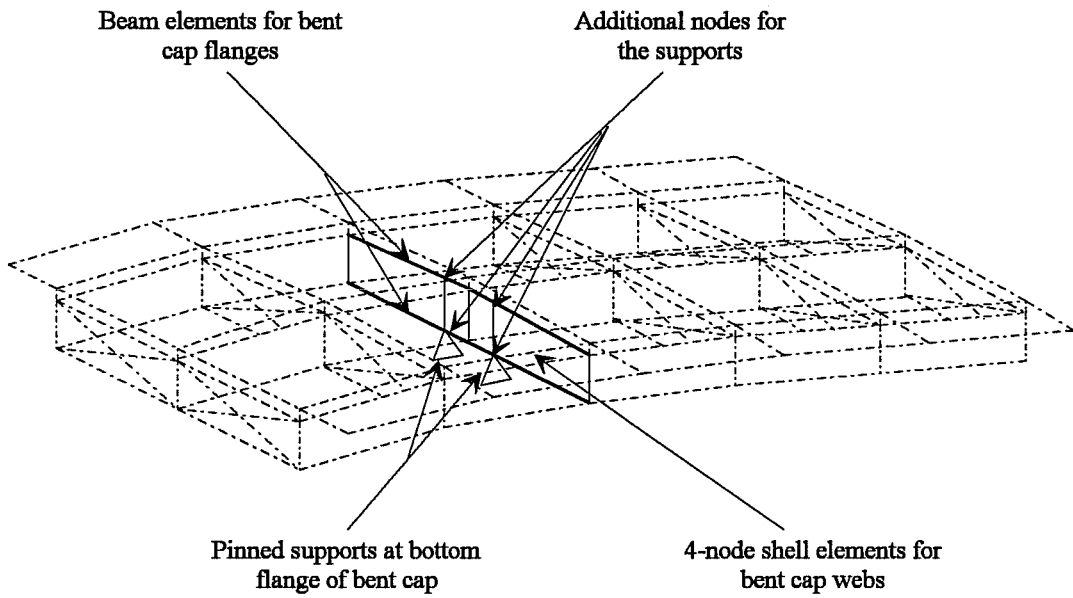


Figure A-3: Elements used to model the bent caps

Typical ANSYS input file

The ANSYS models are generated by the PREP7 preprocessor. PREP7 is a general purpose preprocessor for developing structural, thermal, magnetic field, electric field, fluid and coupled-field models. PREP7 allows for comments, by means of the /com command, to improve readability of the input files. To further improve readability and to simplify the coding, PREP7 also allows for the definition of variables. For the bridge models, variables are used extensively so that the geometry and member sizes from the bridge are all defined before the nodal and element generation process. The first data needed for the model are the number of girders, number of spans and the radius of curvature at the centerline of the deck.

```
/com,*** Enter basic girder, span and curvature data ***
/com,***     ngr = number of girders ***
/com,***     nspn = number of spans ***
/com,***     radc = centerline radius of curvature (inches) ***
ngr=5
nspn=3
radc=24000
```

PREP7 also allows for the use of arrays. The number of diaphragm bays and the diaphragm-to-diaphragm spacing for each span are defined in arrays so variable names can be consistent for bridges with different numbers of spans.

```
/com,*** Dimension arrays for span data ***
*dim,ndf,,nspn
*dim,dfsp,,nspn
*dim,dfsp,,nspn
/com,*** Enter span data ***
/com,***     ndf = diaphragm bays per span ***
/com,***     dfsp = median diaphragm spacing per span (inches) ***
ndf(1)=10,12,10
dfsp(1)=180,180,180

/com,*** Calculate some useful diaphragm data ***
/com,***     ndft = total number of diaphragm bays ***
/com,***     dfsp = diaphragm spacing per span in degrees ***
ndft=0
*do,i,1,nspn
    ndft=ndft+ndf(i)
*enddo
```

```
*do, i, 1, nspn
  dfsp(i)=dfsp(i)/radc*180/3.14159
*enddo
```

For the most part the various cross-sections of the bridge are identical, so most of the cross-sectional properties can be entered into a simple table. Although some of these properties are obvious, others need explanation. The slab overhang is the width of slab, measured from the edge of the slab to the centerline of the girder, which is cantilevered over the edges of the exterior girders. The same overhang is provided on both the inside and outside edge of the bridge. The soffit is the distance from midheight of the slab to the midheight of the top flange of the girder. The bent cap support separation is the distance between the centerlines of the two bearings. The bent cap support cantilever is the distance from the centerline of the deck to the centerline of the concrete pier, where a positive distance results when the centerline of the pier is further than the centerline of the bridge from the center of curvature of the bridge.

```
/com,*** Enter cross-section dimensions ***
/com,***   sovr = slab overhang (inches) ***
/com,***   sgtg = girder-to-girder spacing (inches) ***
/com,***   sth = slab thickness (inches) ***
/com,***   soff = soffit (inches) ***
/com,***   wd = web depth (inches) ***
/com,***   fw = flange width (inches) ***
/com,***   bcsp = bent cap support separation (inches) ***
/com,***   bcct = bent cap support cantilever (inches) ***
sovr=36
sgtg=96
sth=8
soff=5.5
wd=69
fw=20
bcsp=72
bcct=0
```

To simplify nodal generation, the following constants are defined.

```
/com,*** Calculate some useful node numbering constants ***
/com,***   nxs = number of nodes per cross-section ***
```

```

/com,***   ndn = number of deck nodes w/o k-brace and bent cap nodes ***
/com,***   nkbn = number of k-brace nodes ***
/com,***   nbcn = number of bent cap nodes ***
nxs=3*ngr+2
ndn=nxs*(ndft+1)
nkbn=2*(ngr-1)
nbcn=(nspn-1)*4

```

The only variable section properties are the plate thicknesses. It is necessary to specify the different plate thickness and to specify where each plate thickness is to be applied. The thicknesses are grouped into arrays as either flange or web thicknesses. The locations at which each plate thickness is applied are also specified in arrays. The location arrays are dimensioned so that a each cell in the array corresponds to a length of girder between two adjacent cross-frames.

```

/com,*** Enter number of plate thicknesses ***
/com,***   nfth = number of different flange thicknesses ***
/com,***   nwth = number of different web thicknesses ***
nfth=3
nwth=2

/com,*** Dimension array for plate data ***
*dim,fth,,nfth
*dim,tflange,,ndft,ngr
*dim,bflange,,ndft,ngr
*dim,wth,,nwth
*dim,web,,ndft,ngr

/com,*** Specify flange and web plate thicknesses ***
/com,***   fth = flange thicknesses (inches) ***
/com,***   wth = web thicknesses (inches) ***
fth(1)=1.25,1.75,2.5
wth(1)=0.5,0.625

/com,*** Flange and web thicknesses to girders by bay and girder ***
/com,***   tflange = top flange thickness number by bay and girder ***
/com,***   bflange = bottom flange thickness number by bay and girder ***
/com,***   web = web thickness number by bay and girder ***
tflange(1,1)=1,1,1,1,1,1,1,1
tflange(9,1)=2,3,3,2,1,1,1,1
tflange(17,1)=1,1,1,1,2,3,3,2
tflange(25,1)=1,1,1,1,1,1,1,1
tflange(1,2)=1,1,1,1,1,1,1,1
tflange(9,2)=2,3,3,2,1,1,1,1
tflange(17,2)=1,1,1,1,2,3,3,2
tflange(25,2)=1,1,1,1,1,1,1,1
tflange(1,3)=1,1,1,1,1,1,1,1
tflange(9,3)=2,3,3,2,1,1,1,1
tflange(17,3)=1,1,1,1,2,3,3,2
tflange(25,3)=1,1,1,1,1,1,1,1

```

```

tflange(1,4)=1,1,1,1,1,1,1,1
tflange(9,4)=2,3,3,2,1,1,1,1
tflange(17,4)=1,1,1,1,2,3,3,2
tflange(25,4)=1,1,1,1,1,1,1,1
tflange(1,5)=1,1,1,1,1,1,1,1
tflange(9,5)=2,3,3,2,1,1,1,1
tflange(17,5)=1,1,1,1,2,3,3,2
tflange(25,5)=1,1,1,1,1,1,1,1
bflange(1,1)=1,1,1,1,1,1,1,1
bflange(9,1)=2,3,3,2,1,1,1,1
bflange(17,1)=1,1,1,1,2,3,3,2
bflange(25,1)=1,1,1,1,1,1,1,1
bflange(1,2)=1,1,1,1,1,1,1,1
bflange(9,2)=2,3,3,2,1,1,1,1
bflange(17,2)=1,1,1,1,2,3,3,2
bflange(25,2)=1,1,1,1,1,1,1,1
bflange(1,3)=1,1,1,1,1,1,1,1
bflange(9,3)=2,3,3,2,1,1,1,1
bflange(17,3)=1,1,1,1,2,3,3,2
bflange(25,3)=1,1,1,1,1,1,1,1
bflange(1,4)=1,1,1,1,1,1,1,1
bflange(9,4)=2,3,3,2,1,1,1,1
bflange(17,4)=1,1,1,1,2,3,3,2
bflange(25,4)=1,1,1,1,1,1,1,1
bflange(1,5)=1,1,1,1,1,1,1,1
bflange(9,5)=2,3,3,2,1,1,1,1
bflange(17,5)=1,1,1,1,2,3,3,2
bflange(25,5)=1,1,1,1,1,1,1,1
web(1,1)=1,1,1,1,1,1,1,2
web(9,1)=2,2,2,2,2,1,1,1
web(17,1)=1,1,1,2,2,2,2,2
web(25,1)=2,1,1,1,1,1,1,1
web(1,2)=1,1,1,1,1,1,1,2
web(9,2)=2,2,2,2,2,1,1,1
web(17,2)=1,1,1,2,2,2,2,2
web(25,2)=2,1,1,1,1,1,1,1
web(1,3)=1,1,1,1,1,1,1,2
web(9,3)=2,2,2,2,2,1,1,1
web(17,3)=1,1,1,2,2,2,2,2
web(25,3)=2,1,1,1,1,1,1,1
web(1,4)=1,1,1,1,1,1,1,2
web(9,4)=2,2,2,2,2,1,1,1
web(17,4)=1,1,1,2,2,2,2,2
web(25,4)=2,1,1,1,1,1,1,1
web(1,5)=1,1,1,1,1,1,1,2
web(9,5)=2,2,2,2,2,1,1,1
web(17,5)=1,1,1,2,2,2,2,2
web(25,5)=2,1,1,1,1,1,1,1

```

Additional plate thicknesses are specified for the bent caps and for the web stiffeners of the longitudinal girders.

```

/com,*** Specify plate sizes for bent caps ***
/com,*** bcfw = bent cap flange width ***

```

```

/com,***      bctf = bent cap top flange thickness ***
/com,***      bcbf = bent cap bottom flange thickness ***
/com,***      bcwt = bent cap web thickness ***
bcfw=20
bctf=2
bcbf=3
bcwt=1

/com,*** Specify plate sizes for girder web stiffeners ***
/com,***      gsw = girder web stiffener width (inches) ***
/com,***      gwst = girder web stiffener thickness (inches) ***
gsw=8
gwst=0.5

```

Because all the bridges to be modeled are curved about a single center of curvature, it is expedient to define the model in polar coordinates.

```

/com,*** Set polar coordinate system ***
local,11,1,0,0,0,0,-90,0
csys,11

/com,*** Set starting location for nodal generation ***
/com,***      radi = innermost radius of bridge ***
/com,***      hgti = height of center of slab at radi ***
/com,***      angi = angle theta at start of bridge ***
radi=radc-(ngr-1)/2*sgtg-sovr
hgti=0
angi=0

```

A typical cross-section of nodes is generated at the starting angle theta. The node points correspond to the endpoints and connection points of the slab, "shear studs," flanges and webs.

```

/com,*** Nodes for typical cross-section ***
n,1,radi,angi,hgti
ngen,2,1,1,,,sovr,0,0
ngen,ngr,1,2,,,sgtg,0,0
ngen,2,1,ngr+1,,,sovr,0,0
ngen,2,ngr+1,2,ngr+1,1,0,0,-soff
ngen,2,ngr,ngr+3,2*ng+2,1,0,0,-wd

```

Once the first cross-section is defined, the pattern is copied to generate new cross-sections at each cross-frame location.

```

/com,*** Repeat cross-section over length of bridge ***
sdfn=0
*do,i,1,nsfn
  ns=sdfn+1
  ne=sdfn+nxs

```

```

    ngen,ndf(i)+1,nxs,ns,ne,1,0,dfsp(i),0
    sdfn=sdfn+nxs*ndf(i)
*enddo

```

Additional nodes are added at the two end cross-frames because the k-braces require an extra connection between the diagonal members and the top cross-member. Additional nodes are also added at the bent cap cross-sections because the bent caps require an additional connection to the bearings. The additional bent cap nodes will not be sequential with the other bent cap nodes defined as part of the typical cross-section. Because the bent cap elements will later be generated in sequence from the inside to outside of the bridge, the reference numbers of the bent cap nodes are arranged into an array so that the nodes are in sequence from inside to outside.

```

/com,*** Extra k-brace nodes ***
*do,i,1,2
    ns=(i-1)*nxs*ndft+ngr+3
    ne=ns+ngr-1
    ninc=(i-1)*(ngr-1)+ndn+1-ns
    ngen,2,ninc,ns,ne,1,sgtg/2,0,0
*enddo

```

```

/com,*** Extra bent cap nodes ***
sdfn=nxs*ndf(1)
dref=sgtg*(ngr-1)/2-bcsp/2+bcct
*dim,bcnl,,ngr+2,nspn-1,2
*do,i,1,nspn-1
    nref=sdfn+ngr+3
    ninc=(i-1)*4+ndn+nkbn+1-nref
    ns=nref+ninc
    ne=ns+1
    ngen,2,ninc,nref,,dref,0,0
    ngen,2,1,ns,,bcsp,0,0
    ngen,2,2,ns,ne,1,0,0,-wd
    xbc1=dref
    xbc2=dref+bcsp
    bcnl(1,i,1)=nref
    bcnl(1,i,2)=bcnl(1,i,1)+ngr
    xgr1=0
    k=2
    *do,j,1,ngr-1
        xgr2=xgr1+sgtg
        *if,xgr1,lt,xbc1,then
            *if,xbc2,lt,xgr2,then
                bcnl(k,i,1)=ns
                bcnl(k,i,2)=ns+2

```

```

        bcnl(k+1,i,1)=ne
        bcnl(k+1,i,2)=ne+2
        bcnl(k+2,i,1)=bcnl(k-1,i,1)+1
        bcnl(k+2,i,2)=bcnl(k+2,i,1)+ngr
        k=k+3
    *elseif,xbc1,lt,xgr2
        bcnl(k,i,1)=ns
        bcnl(k,i,2)=ns+2
        bcnl(k+1,i,1)=bcnl(k-1,i,1)+1
        bcnl(k+1,i,2)=bcnl(k+1,i,1)+ngr
        k=k+2
    *else
        bcnl(k,i,1)=bcnl(k-1,i,1)+1
        bcnl(k,i,2)=bcnl(k,i,1)+ngr
        k=k+1
    *endif
*elseif,xgr1,lt,xbc2
    *if,xbc2,lt,xgr2,then
        bcnl(k,i,1)=ne
        bcnl(k,i,2)=ne+2
        bcnl(k+1,i,1)=bcnl(k-1,i,1)+1
        bcnl(k+1,i,2)=bcnl(k+1,i,1)+ngr
        k=k+2
    *else
        bcnl(k,i,1)=bcnl(k-1,i,1)+1
        bcnl(k,i,2)=bcnl(k,i,1)+ngr
        k=k+1
    *endif
*else
    bcnl(k,i,1)=bcnl(k-1,i,1)+1
    bcnl(k,i,2)=bcnl(k,i,1)+ngr
    k=k+1
*endif
xgr1=xgr2
*enddo
sdfn=sdfn+nxs*ndf(i+1)
*enddo

```

To simplify the application of support conditions later, the support nodes at the ends of the bridge and at the bent caps are grouped into components.

```

/com,*** Define end support nodes ***
ns=ndft*nxs+2*ngr+3
ne=ns+ngr-1
nsel,s,node,,ns,ne
ns=2*ngr+3
ne=ns+ngr-1
nsel,a,node,,ns,ne
cm,endsupps,node
nsel,all

/com,*** Define bent cap support nodes ***
ns=ndn+nkbn+1
ne=ns+nbcn-1

```



```

nset,s,node,,ns,ne
cm,capsups,node
nset,all

```

Three types of elements will be used in the model. Shell elements are used to model the slab, the girder webs, and the bent cap webs. Beam elements are used to model the “shear studs,” girder flanges, bent cap flanges, web stiffener plates, and the top cross-members of the k-braces. Truss elements are used for the x-braces and for the diagonal and bottom cross-members of the k-braces.

```

/com,*** 4-node shell elements ***
et,1,shell163

/com,*** 2-node beam elements ***
et,2,beam4

/com,*** 2-node truss elements ***
et,3,link8

```

Three material types are used. The slab will be given concrete properties. The girders, bent caps, and cross-frames will be given steel properties. The “shear studs,” which do not exist physically, will be given the stiffness of steel but no mass.

```

/com,*** Concrete ***
mp,ex,1,3120
mp,nuxy,1,0.2
mp,dens,1,0.000086806

/com,*** Steel ***
mp,ex,2,29000
mp,nuxy,2,0.3
mp,dens,2,0.00028356

/com,*** Massless steel ***
mp,ex,3,29000
mp,nuxy,3,0.3

```

The next step is to define the member sizes. The slab thickness is simply entered as a shell thickness. The “shear stud” properties are set to arbitrarily large values to approximate a fixed connection between the midheight of the slab and the midheights of the top flanges of the girders. The standard bracing member sizes are entered directly at this point in the input file since they will never be changed. Next,

the bent cap properties are entered, where some calculation is necessary for those components modeled with beam elements. Finally, the girder flange, web, and web stiffener properties are set.

```

/com,*** Slab thickness ***
r,1,sth

/com,*** "Shear studs" ***
r,2,1000,1000000,1000000,100,100,0
rmore,0,1000000,0,0

/com,*** X- and K-braces ***
r,3,3.05
r,4,12.4,166,47.2,9.02,12.05,0
rmore,0,1.84
r,5,2.48

/com,*** Bent cap plates ***
area=bctf*bcfw
izz=bcfw*bctf**3/12
iyy=bctf*bcfw**3/12
ixx=izz*4
r,6,area,izz,iyy,bcfw,bctf
rmore,0,ixx
area=bcbf*bcfw
izz=bcfw*bcbf**3/12
iyy=bcbf*bcfw**3/12
ixx=izz*4
r,7,area,izz,iyy,bcfw,bcbf
rmore,0,ixx
r,8,bcwt

/com,*** Girder flange plates ***
srsf=8
*do,i,1,nfth
  rset=srsf+i
  area=fth(i)*fw
  izz=fw*fth(i)**3/12
  iyy=fth(i)*fw**3/12
  ixx=izz*4
  r,rset,area,izz,iyy,fw,fth(i)
  rmore,0,ixx
*enddo

/com,*** Girder web plates ***
srsw=nfth+srsf
*do,i,1,nwth
  rset=srsw+i
  r,rset,wth(i)
*enddo

/com,*** Girder web stiffener plates ***
srss=srsw+nwth

```

```

rset=srss+1
area=gsw*gwst
izz=gsw*gwst**3/12
iyy=gwst*gsw**3/12
ixx=izz*4
r,rset,area,izz,iyy,gsw,gwst
rmore,0,ixx

```

At this point, the elements can be defined. The elements for the slab, “shear studs,” the girders, the k-braces, the x-braces, and the bent caps are defined in groups and assembled into components.

```

/com,*** Slab ***
type,1
real,1
mat,1
*do,i,1,ndft
  *do,j,1,ngr+1
    ni=(i-1)*nxs+j
    nj=ni+1
    nk=nj+nxs
    nl=ni+nxs
    e,ni,nj,nk,nl
  *enddo
*enddo
esel,s,real,,1
cm,slab,elem
esel,all

/com,*** "Shear studs" ***
type,2
real,2
mat,3
*do,i,1,ndft+1
  *do,j,1,ngr
    ni=(i-1)*nxs+j+1
    nj=ni+ngr+1
    e,ni,nj
  *enddo
*enddo
esel,s,real,,2
cm,studs,elem
esel,all

/com,*** Girders ***
mat,2
*do,i,1,ndft
  *do,j,1,ngr
    ni=(i-1)*nxs+j+ngr+2
    nj=ni+nxs
    nk=nj+ngr
    nl=ni+ngr
    type,2

```

```

        real,tflange(i,j)+srsf
        e,ni,nj
        real,bflange(i,j)+srsf
        e,nl,nk
        type,1
        real,web(i,j)+srsw
        e,ni,nj,nk,nl
    *enddo
*enddo
esel,s,real,,srsf+1,srsf+nfth
cm,flanges,elem
esel,s,real,,srsw+1,srsw+nwth
cm,webs,elem
esel,all

/com,*** K-braces ***
mat,3
*do,i,1,2
    *do,j,1,ngr-1
        ni=(i-1)*nxs*ndft+j+ngr+2
        nj=ni+1
        nk=nj+ngr
        nl=ni+ngr
        nm=(i-1)*(ngr-1)+j+ndn
        type,2
        real,4
        e,ni,nm
        e,nm,nj
        type,3
        real,3
        e,nl,nk
        real,5
        e,nl,nm
        e,nm,nk
    *enddo
*enddo
esel,s,real,,3,5
cm,kbraces,elem
esel,all

/com,*** X-braces ***
sdfn=0
*do,i,1,nspn
    *do,j,2,ndf(i)
        *do,k,1,ngr-1
            ni=sdfn+(j-1)*nxs+k+ngr+2
            nj=ni+1
            nk=nj+ngr
            nl=ni+ngr
            type,3
            real,3
            e,ni,nj
            e,nl,nk
            e,ni,nk
            e,nl,nj
            type,2

```

```

                real,srss+1
                e,ni,nl,nj
                e,nj,nk,ni
            *enddo
        *enddo
        sdfn=sdfn+nxs*ndf(i)
    *enddo
    cmsel,u,kbraces
    esel,r,real,,3
    cm,xbraces,elem
    esel,all
    esel,s,real,,srss+1
    cm,plates,elem
    esel,all

/com,*** Bent caps ***
*do,i,1,nspn-1
    *do,j,1,ngr+1
        ni=bcnl(j,i,1)
        nj=bcnl(j+1,i,1)
        nk=bcnl(j+1,i,2)
        nl=bcnl(j,i,2)
        type,2
        real,6
        e,ni,nj
        real,7
        e,nl,nk
        type,1
        real,8
        e,ni,nj,nk,nl
    *enddo
*enddo
esel,s,real,,6,8
cm,bentcaps,elem
esel,all

```

Next, a couple of bookkeeping tasks must be performed on the elements and nodes of the model. To reduce the wavefront of the model, and thus the computation time, the elements are reordered. To orient the nodes in the global polar coordinate system, the nodes must be rotated since ANSYS defines the nodes using a cartesian nodal coordinate system.

```

/com,*** Reorder elements and rotate nodes ***
waves
nrotat,all

```

Roller supports are provided at the ends of the bridge and pinned supports are provided at the bent cap bearings. Loads, such as dead load here, are applied.

The model is saved and the preprocessor is exited.

```
/com,*** Rollers at end supports ***  
cmsgel,s,endsupps  
d,all,uz,0,,,,ux  
nsgel,all  
  
/com,*** Pins at interior supports ***  
cmsgel,s,capsupps  
d,all,uz,0,,,,ux,uy  
nsgel,all  
  
/com,*** Apply self-weight ***  
acel,,1  
  
save  
finish
```

This completes the model generation process. The model is now ready to be solved using the ANSYS static solver.

APPENDIX B

VERIFICATION OF THE MODELS

Introduction

A simple, closed-form solution for the behavior of a complex structure such as the typical bridge considered in this study does not exist. Consequently, it is necessary to make simplifications in the analysis of the bridge, such as modeling the bridge with finite elements. Because of the simplifications inherent in a finite element analysis, the behavior calculated in the analysis will not be the true behavior of the bridge. If the bridge is modeled well, however, the behavior calculated in the analysis will be sufficiently close to the true behavior. Therefore, it is necessary to verify that the behavior, as calculated by the finite element analysis for the model chosen to represent the bridge, is close to the true behavior.

The first stage of the verification process is to select a test structure. Although it would be ideal to use a typical bridge for the test structure, a simple closed-form solution for such a complex structure does not exist. Consequently, there would be no way to calculate the true behavior for comparison against the behavior predicted by the finite element analysis. It is therefore necessary to choose the test structure for which a simple-closed solution exists. The test structure, however, should exhibit the important properties of the bridge which will ultimately be modeled. The second stage is to find a suitable closed-form solution against which the results of the finite element model can be compared.

The closed-form solution should incorporate both bending and torsional effects on thin-walled open cross-sections. The third stage is to generate a finite element model of the test structure. The model will be assembled from finite elements as described in Appendix A. The fourth stage is to compare the results of the finite element model with the closed-form solutions. The aspects of the model which are to be compared are deflections due to pure bending, rotations due to pure torsion, bending stresses and torsional warping stresses.

Selection of the test structure

The test structure chosen was a straight concrete slab supported on two wide-flange steel plate girders, the general cross-section of which is shown in Figure B-1. Although the dimensions of the model could be easily modified, the dimensions given in the figure were the only ones used during the verification.

Closed-form model

The second stage in verifying the suitability of the finite element method is to find a closed-form solution against which the results of the finite element model can be compared. The closed-form solution should handle bending and torsion on a thin-walled open cross-section. A method offered by Heins [5] which is based on earlier work by Kollbrunner and Basler [6] was chosen for this purpose.

For a straight elastic member, the effects of bending and torsion can be calculated separately by decomposing forces that do not act through the shear center of a cross-section into a system of forces acting through the shear center and torsional moments equal to the magnitudes of the forces times their respective distances from the shear center, as shown in Figure B-2. The forces acting through the shear center will produce bending only with no torsion. The

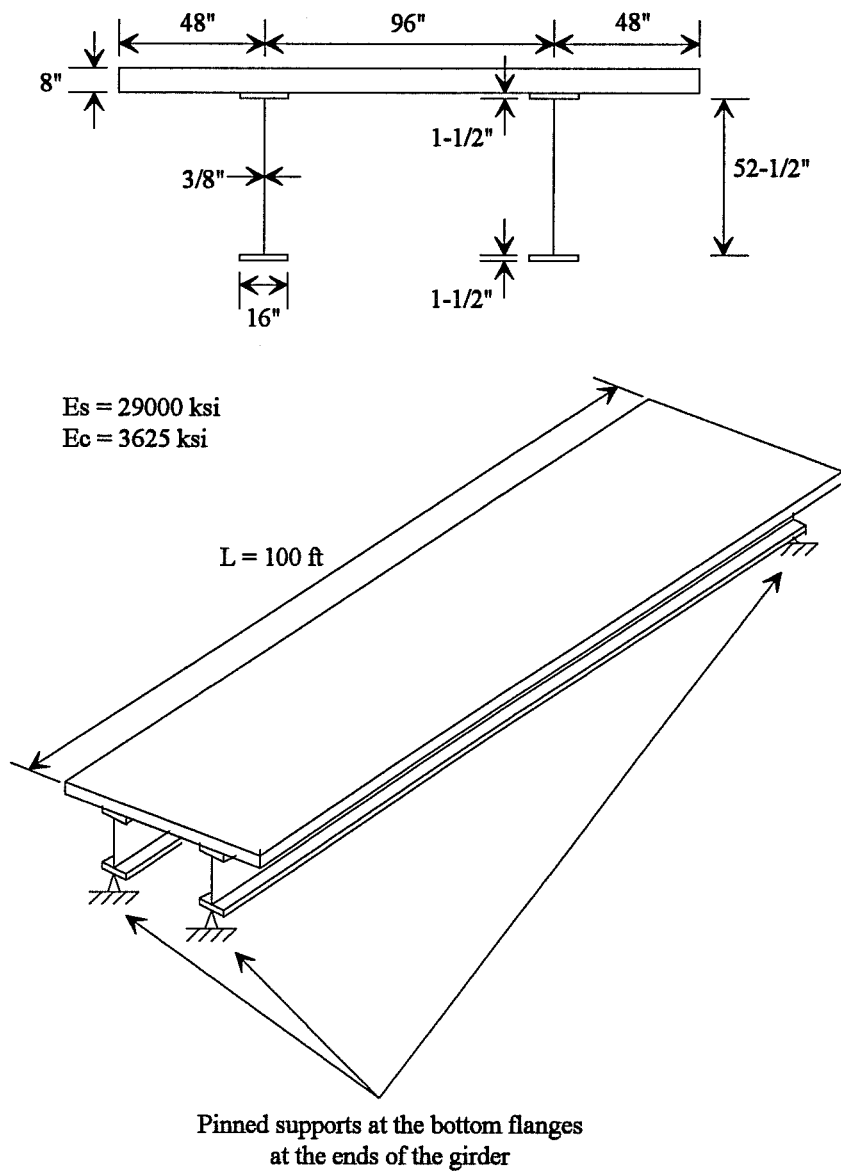


Figure B-1: Cross-sectional properties of the test structure and support conditions

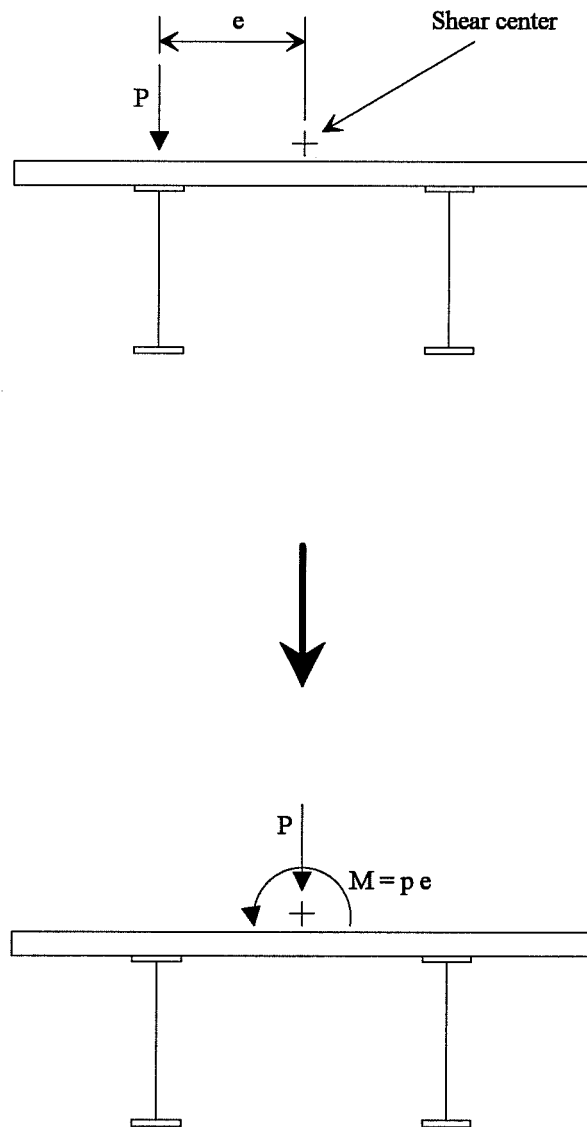


Figure B-2: Decomposition of a load into pure bending and pure torsional components

torsional moments will produce pure (St. Venant's) torsion and warping torsion only. The deformations and stresses calculated separately for bending and torsion can be combined by superposition, given that the material remains elastic and second order geometric effects are neglected.

Once the shear center is found and the forces and moments are decomposed into their components acting through the shear center, bending and torsional analyses can be conducted. The analyses first require the computation of cross-sectional constants, which are then included in the differential equations of the closed-form solutions. Next, the differential equations are solved for deflections, vertical displacements in the case of bending and twist in the case of torsion, for the given boundary conditions. Finally, stresses are calculated.

Shear center

To separate bending and torsional effects, the shear center must first be located. A coordinate system for the cross-section is chosen with the origin at the centroid of the cross-section. The x-axis extends horizontally and the y-axis extends vertically. The location for the shear center relative to the centroid is given by Heins [5] as

$$X_0 = (I_{xy} I_{wx} - I_{yy} I_{wy}) / (I_{xy}^2 - I_{xx} I_{yy}) \quad (\text{B-1})$$

$$Y_0 = (I_{xx} I_{wx} - I_{xy} I_{wy}) / (I_{xy}^2 - I_{xx} I_{yy}) \quad (\text{B-2})$$

The I_{xx} , I_{yy} and I_{xy} terms are the moments of inertia and cross-product of inertia which are typically used for bending analysis. In order to make torsional analysis analogous to bending analysis, a new coordinate w , the sectorial coordinate, must be introduced. This coordinate when included in the integrals for the moments of inertia in place of one of the x 's or y 's produces the integrals for the sectorial products of inertia, I_{wx} and I_{wy}

The w coordinate for a point on the cross-section is based on a path integral around the cross-section, namely, it is the integration of a function p around the cross-section from some arbitrary free end to the point w . An illustration of the p function is shown in Figure B-3. The p function is the distance from the centroid to a line tangent to the path, where p is positive if the path runs counterclockwise around the centroid and is negative otherwise. Because the cross-section is made up of straight horizontal and vertical plates, a single p for each entire plate can be found easily: for vertical plates with the path running from bottom to top, p equals the x -coordinate of the endpoints; for horizontal plates with the path running from left to right, p equals the negative of the y -coordinate of the endpoints. To begin the process of finding the w coordinates, one arbitrarily chosen point has its w coordinate set equal to zero, usually a free end of one of the elements. This gives an initial value for the starting point of the first element. To find the w at the ending point of the element, the p for the element is multiplied by its length and this product is added to the w of the element's starting point. This w for the ending of the first element becomes the w for the starting points of the elements which connect to it. The process continues until all endpoints have w values.

Since the cross-section is made up of plates of constant thicknesses, the integrals for the five constants can be converted into simpler algebraic expressions.

$$I_{xx} = 1/3 \Sigma (y_i^2 + y_i y_j + y_j^2) t_{ij} L_{ij} / n_{ij} \quad (\text{B-3})$$

$$I_{yy} = 1/3 \Sigma (x_i^2 + x_i x_j + x_j^2) t_{ij} L_{ij} / n_{ij} \quad (\text{B-4})$$

$$I_{xy} = 1/3 \Sigma (x_i y_i + x_j y_j) t_{ij} L_{ij} / n_{ij} + 1/6 \Sigma (x_i y_i + x_j y_j) t_{ij} L_{ij} / n_{ij} \quad (\text{B-5})$$

$$I_{wx} = 1/3 \Sigma (x_i w_i + x_j w_j) t_{ij} L_{ij} / n_{ij} + 1/6 \Sigma (x_i w_i + x_j w_j) t_{ij} L_{ij} / n_{ij} \quad (\text{B-6})$$

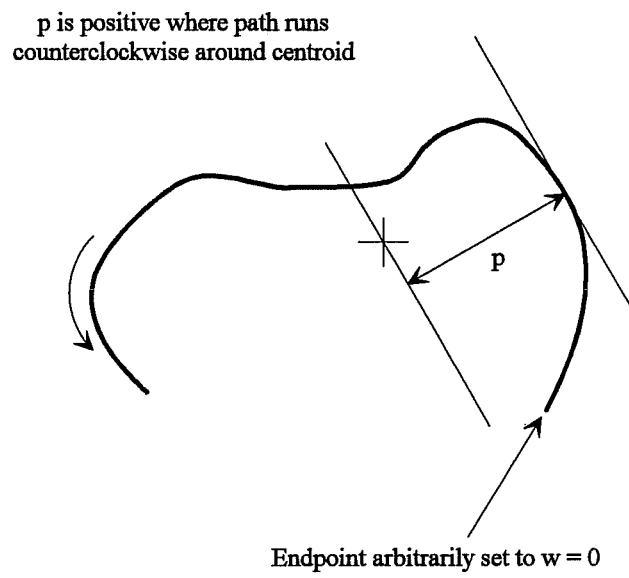


Figure B-3: Magnitude and sign of p

$$I_{wy} = 1/3 \Sigma (wy_i + wy_j) t_y L_y / n_y + 1/6 \Sigma (wy_i + wy_j) t_y L_y / n_y \quad (\text{B-7})$$

where (x_i, y_i, w_i) and (x_j, y_j, w_j) are the coordinates of the end points, t_y is the thickness, L_y is the length, and n_y is the modular ratio of each plate. The modular ratio is provided to allow the structure to be composed of two different materials. To make use of these equations, the cross-section must be divided into connecting plate elements, as shown in Figure B-4, where each node is given a reference number. Because the centerlines of the plates must connect, simplifications must be made at the connections between the tops of the girders and the slab. The web is considered to extend all the way to the center of the slab and the top flange is ignored, which is consistent with the methods of both Basler and Heins. The coordinate system originates at the centroid of the transformed cross-section. The values needed to calculate the moments of inertia can be put into a spreadsheet as shown in Table B-1. The values for the moments of inertia and the location of the shear center are shown in Table B-2.

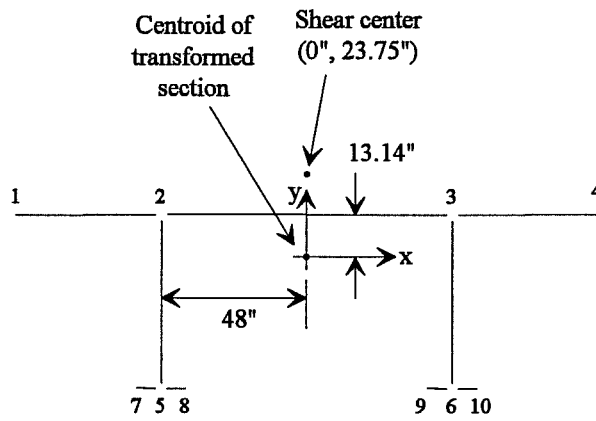


Figure B-4: Discretization of the test structure

Table B-1: Calculation of Moments of Inertia and Shear Center

Node	x	y	L_{ij}	t_{ij}	n_{ij}	P_{ij}	w_{ij}	w
1	-96	13.14						0
			48	8	8	-13.14	-631	
2	-48	13.14						-631
			96	8	8	-13.14	-1261	
3	48	13.14						-1892
			48	8	8	-13.14	-631	
4	96	13.14						-2523
2	-48	13.14						-631
			54	0.375	1	48	2592	
5	-48	-40.86						1961
3	48	13.14						-1892
			54	0.375	1	-48	-2592	
6	48	-40.86						-4484
7	-56	-40.86						1634
			8	1.5	1	40.86	327	
5	-48	-40.86						1961
			8	1.5	1	40.86	327	
8	-40	-40.86						2288
9	40	-40.86						-4811
			8	1.5	1	40.86	327	
6	48	-40.86						-4484
			8	1.5	1	40.86	327	
10	56	-40.86						-4157

Table B-2: Results of Calculations

$$\begin{aligned}
 I_{xx} &= 131000 \text{ in}^4 \\
 I_{yy} &= 795000 \text{ in}^4 \\
 I_{xy} &= 0 \text{ in}^4 \\
 \\
 I_{wx} &= -18900000 \text{ in}^4 \\
 I_{wy} &= -341 \text{ in}^4 \\
 \\
 X_o &= 0 \text{ in} \\
 Y_o &= 23.75 \text{ in}
 \end{aligned}$$

Torsional constants

Now that the shear center is located, forces can be decomposed into their bending and torsional parts and the torsional constants J and I_{ww} which are St. Venant's constant and the warping constant, respectively, can be calculated. St. Venant's constant for a cross-section composed of thin rectangular elements is given as

$$J = 1/3 \Sigma L_{ij} t_{ij}^3 / n_{ij} \quad (\text{B-8})$$

The warping constant I_{ww} is calculated in a manner similar to that of the other moments of inertia, namely

$$I_{ww} = 1/3 \Sigma (W_i^2 + W_i W_j + W_j^2) t_{ij} L_{ij} / n_{ij} \quad (\text{B-9})$$

where the W terms are normalized sectorial coordinates. To find the normalized sectorial coordinates, first the unnormalized sectorial coordinates must be found again, but this time relative to the shear center rather than the centroid. To distinguish the new p and w about the shear center from those about the centroid, those about the shear center will be designated p_o and w_o . To normalize the w_o 's to form the W 's,

$$W_{ni} = \Sigma [(w_{oi} + w_{oj}) t_{ij} L_{ij} / n_{ij}] / \Sigma 2 (t_{ij} L_{ij} / n_{ij}) - w_{oi} \quad (\text{B-10})$$

The computations are set up in a spreadsheet as shown in Table B-3 and the

results of these computations are shown in Table B-4.

Table B-3: Finite Difference Calculation of Torsional Constants

Node	p_o	L_{ij}	t_{ij}	n_{ij}	w_o	w_n
1					0.0	1019
	10.61	48	8	8		
2					509	509
	10.61	96	8	8		
3					1528	-509
	10.61	48	8	8		
4					2037	-1019
2					509	509
	48	54	0.375	1		
5					3101	-2083
3					1528	-509
	-48	54	0.375	1		
6					-1064	2083
7					2584	-1566
	64.61	8	1.5	1		
5					3101	-2083
	64.61	8	1.5	1		
8					3618	-2600
9					-1581	2600
	64.61	8	1.5	1		
6					-1064	2083
	64.61	8	1.5	1		
10					-547	1566

Table B-4: Results of Torsional Constants Calculations

$$J = 4134 \text{ in}^4$$

$$I_{ww} = 327000000 \text{ in}^4$$

Bending analysis

As noted earlier bending and torsional analyses are conducted separately, and the results are then combined by superposition. Bending analysis is conducted by using standard engineering beam analysis. The results of this analysis are the bending deflections, as well as the normal and shear stresses due to bending.

Torsional analysis

The torsional analysis includes the effects of both pure torsion and warping torsion. Under pure torsion, also known as St. Venant's torsion, no restraint to cross-sectional warping is assumed. The cross-section resists the torsional moment by developing pure torsional shear stresses. The second effect of torsion is warping torsion. Under warping torsion, restraint of cross-sectional warping is present. As a result of warping restraint, warping shear stresses and warping normal stresses will develop to resist the torsional moment, and torsional stiffness will increase. The pure torsional shear stresses, warping shear stresses and warping normal stresses combine to resist the applied torsional moment. Torsional rotations of the cross-section, ϕ , are computed by solving the differential equation of torsion, given by Equation B-11, and applying appropriate torsional boundary conditions. Torsional shear and normal stresses can then be computed.

$$M = GJ \phi' - EI_{ww} \phi'''. \quad (\text{B-11})$$

For a typical bridge, the boundary conditions would consist of end supports which allow the girders to rotate freely in bending and to warp without restraint and a distributed torque. For such support conditions and for a uniform torque, the differential equation can be solved to give

$$\phi(x) = ma^2/GJ [L^2/2a^2(x/L - x^2/L^2) - \tanh(L/2a) \sinh(x/a) + \cosh(x/a) - 1] \quad (\text{B-12})$$

where m is the uniform torque, L is the length and

$$a^2 = EI_{ww} / GJ \quad (\text{B-13})$$

The normal warping stress at point n is given by

$$\sigma = EW_n \phi'' \quad (\text{B-14})$$

W_n has been tabulated for only the few points in the structure where plates have free ends or connect to other plates, so stresses can only be calculated at selected locations on the cross-section.

Comparison of results

The finite element model was subjected first to a uniform vertical load of 1 kip/foot to produce a pure bending response. A comparison of the vertical deflections predicted by the closed-form beam theory and the finite element model for the bending case is shown in Figure B-5. The finite element model follows the shape of the closed-form solution very well. The predicted bending stresses at the middepths of the bottom flanges are shown in Figure B-6. Again, correlation between the finite element model and the closed-form solution are very good.

The finite element model was next subjected to a uniform axial torque of 1 kip-foot/foot. A comparison of the rotations predicted by the closed-form method and the finite element model for the torsion case is shown in Figure B-7. The finite element model again correlates well with theory. A comparison of the warping normal stresses at the centroid of one of the bottom flanges is shown in Figure B-8. Again, correlation is excellent. In the finite element model, however, warping normal stresses at the ends do not equal zero because the finite element model places the supports at the bottom flanges of the girders

Figure B-5: Bending Deflections Due to Uniform Load

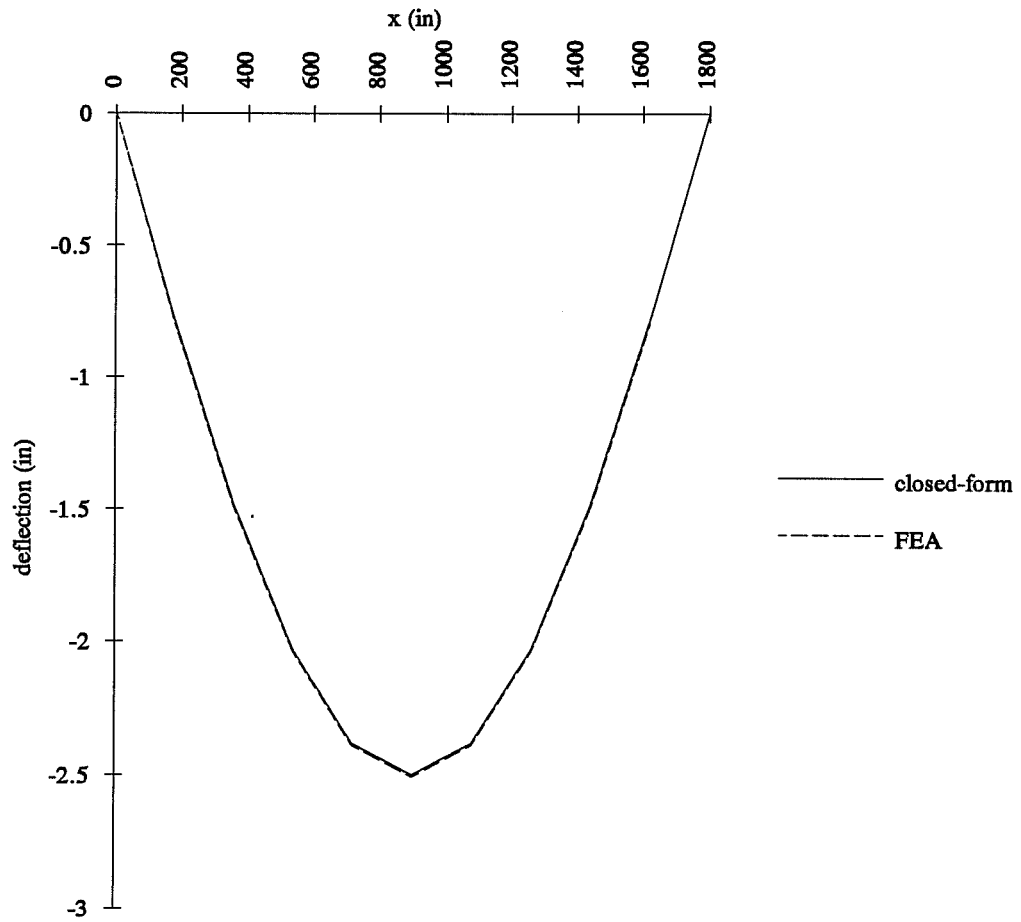


Figure B-6: Bottom Flange Bending Stresses Due to Uniform Load

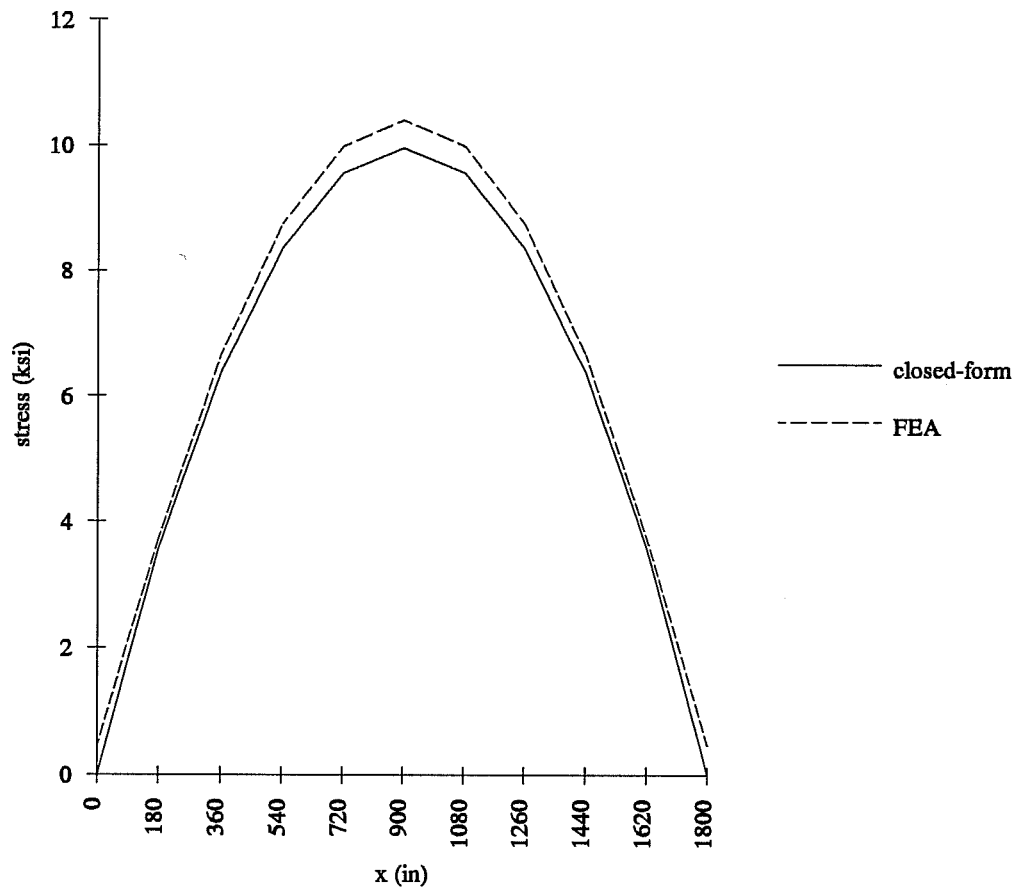


Figure B-7: Deck Rotations Due to Uniform Torque

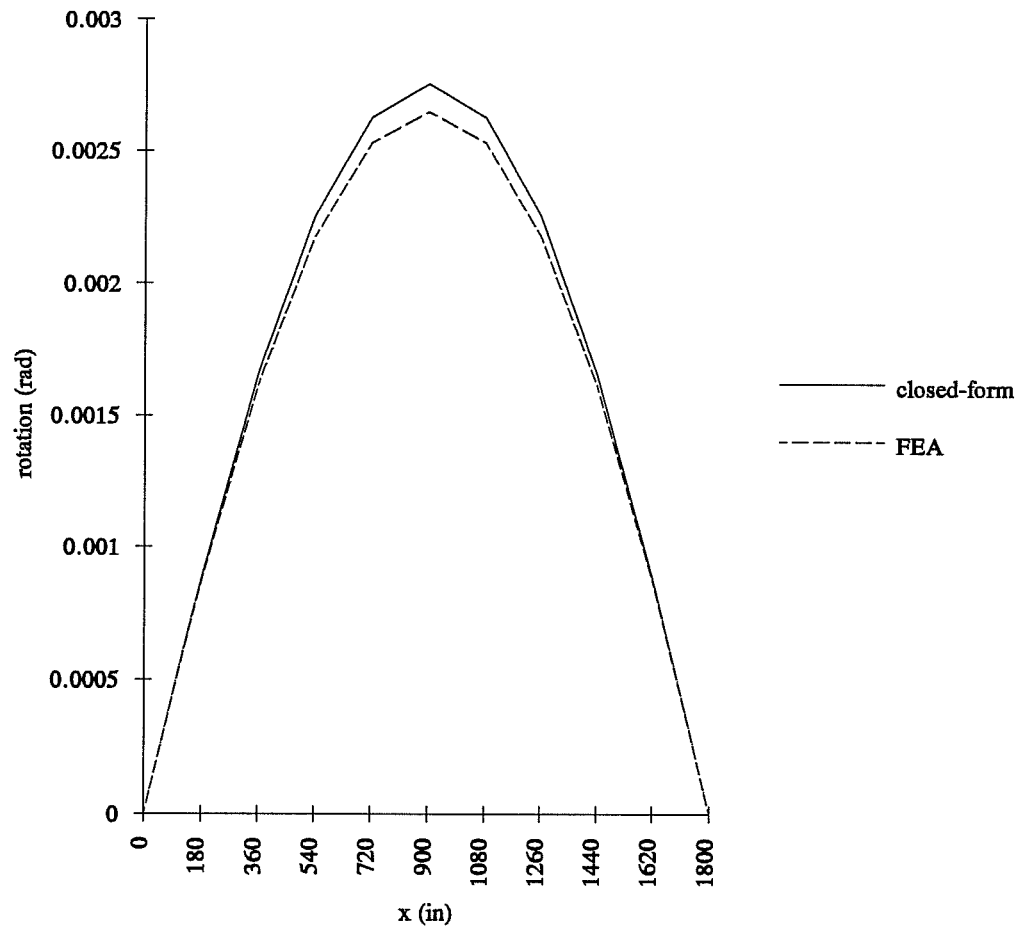
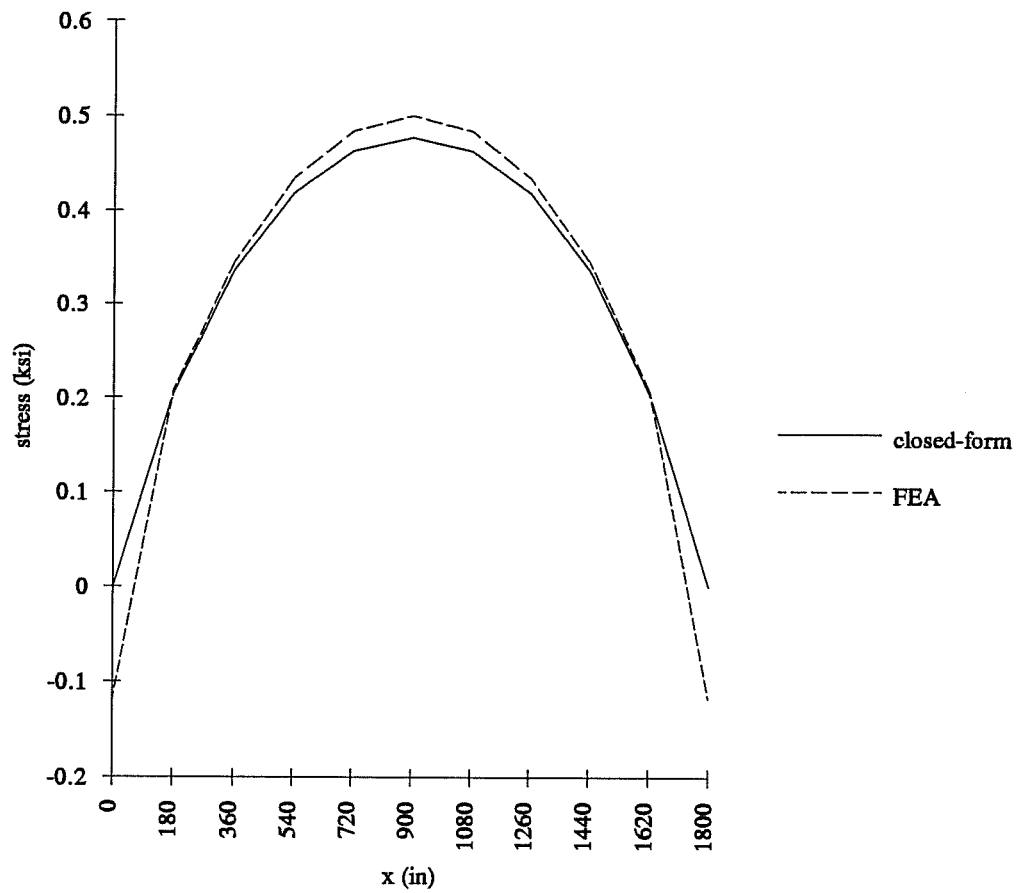


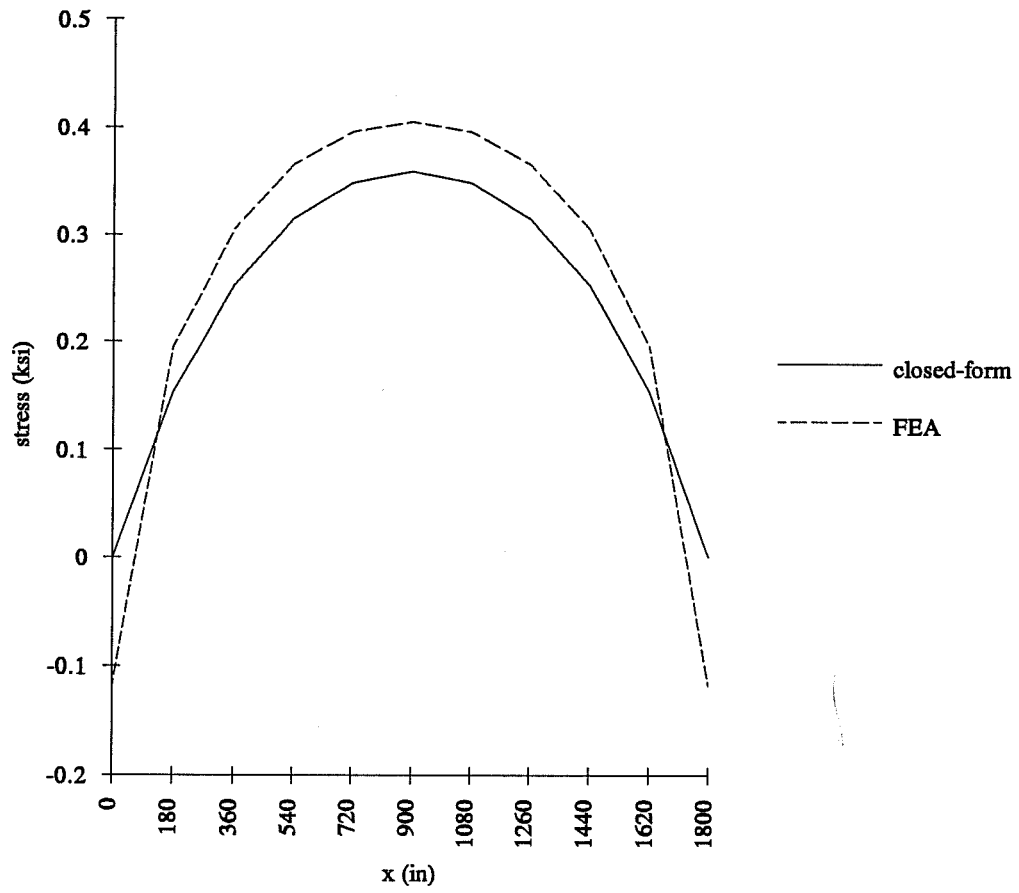
Figure B-8: Bottom Flange Average Warping Normal Stresses Due to Uniform Torque



as they would be in a real bridge rather than at the centroid of the cross-section as assumed by the closed-form solution. Because the finite element model represents the flanges as beam elements rather than plate elements, warping stresses at the flange tips must also be compared to verify that the flanges act like beams in lateral bending. Stresses are not directly available from the finite element model for the flange tips, but rather, the stresses must be calculated from the bending moments in the flanges. A comparison of the bottom flange outer tip warping stresses for the closed-form solution and the finite element model is shown in Figure B-9. Correlation is not as good as for the flange centroid warping stresses. The finite element model predicts noticeably higher stresses than the closed-form solution. Part of this discrepancy could be the result of nonuniform rotation of the cross-section since the webs are able to distort in the finite element model but not in the closed-form solution. In such a case, the finite element model gives a better indication of the flange stresses than the closed-form solution. The discrepancies in flange tip stresses, however, do not appear to contribute significantly to differences in the overall behavior of the section. Consequently, it appears acceptable to model the flanges with beam elements.

Other cases were analyzed using different cross-sections and boundary conditions. The other analyses led to similar conclusions about the viability of this particular modeling method – this particular modeling method produces acceptable results for a bridge subjected to bending and torsion. The model may overpredict stresses in the flange tips relative to the closed-form solution, but such discrepancies do not seem to affect the overall behavior of the cross-section to any significant extent. It should be noted that discrepancies between the finite element method and the closed-form solutions do not necessarily arise because of problems with the finite element models. Rather, the finite element

Figure B-9: Bottom Flange Outer Tip Warping Normal Stresses Due to Uniform Torque



model may produce more accurate results than the closed-form solution. For example, the finite element model predicts warping normal stresses at the center of the bottom flanges at the ends of the girders that do not equal zero because the finite element model applies the supports at the bottom flanges of the girders where they would be in a real bridge rather than at the centroid of the cross-section as assumed by the closed-form solution. Likewise, other assumptions in the closed-form solution, such as the assumption that the elements are composed of thin plates and that these plates connect to the other plates at their centerlines, may not properly reflect the conditions in real bridges. The finite element model is not constrained by these assumptions, so it is possible that the finite element model is producing more accurate results than the closed-form solution.

APPENDIX C

THE V-LOAD METHOD

Introduction

The V-load method is an approximate procedure used for the analysis of horizontally-curved open-framed plate girder bridges. In a 1963 Structural Report [7], United States Steel presented an approximate analysis technique for curved plate girder bridges. This original technique proved cumbersome, so a simplified approach was presented in 1965 [8]. Since the publication of this simplified approach, which has become known as the V-load method, this technique has been shown to give good results for open-framed bridges (plate girders connected by lateral bracing such as floor beams, K-bracing or X-bracing which lie in a vertical plane, but with no lateral bracing lying in a horizontal plane in or near the plane of the bottom flanges of the girders) employing either composite or noncomposite construction and having either radially aligned or skewed supports [9].

The V-load method simplifies the design of curved girders by treating them as isolated straight girders analyzed in the same manner as the girders of straight bridges. In order to incorporate the effects of curvature, the simplified system of straight girders is analyzed twice – first to determine the approximate response due to the vertical loads on the simplified straight system and then to redistribute stresses to reflect the effects of curvature. The simplified straight girders are first analyzed by subjecting them to the vertical loads. The girders,

because they are assumed to be straight, isolated girders, resist the loads only through ordinary bending stresses. From these bending stresses an additional set of artificial loads, the V-loads, are calculated. When applied, these V-loads alter the stresses in the girders so as to approximate the effects of torsion caused by the curvature of the bridge. In order to satisfy static equilibrium, the V-loads are determined such that they are self-equilibrating. This is to say, the V-loads impose no net external vertical, longitudinal or transverse force on the bridge. Rather, the V-loads simply produce redistributions of internal stresses so that the resulting distribution of internal forces approximates the distribution in a curved bridge.

Torsional stresses in curved girders

A vertical load applied to a horizontally curved girder produces a torsional effect in the girder. It can be assumed, approximately, that the moment produced in a beam subject to vertical load is resisted by longitudinal forces in the flanges only. The magnitude of these longitudinal forces equals M , the bending moment at the cross-section, divided by h , the depth between the centroids of the top and bottom flanges, as shown in Figure C-1. Because of the curvature of the girder, the opposing faces of a thin section cut from a curved girder with length dt will not be parallel, as can be seen in Figure C-2. Instead, there will be a slight angle $d\phi$ between the faces, where $d\phi$ equals dt/R and where R is the radius of curvature of the girder, resulting in a net transverse force acting on the flange, where the magnitude of this transverse force is M/hR applied over an arc of length dt . The directions in which these forces act are such that the forces tend to push the compression flange away from – and likewise pull the tension flange toward – the center of curvature. Thus, these forces act as torsional forces on a curved girder, and the distribution of these

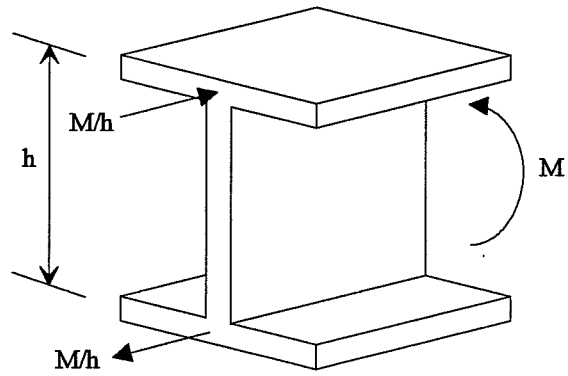


Figure C-1: Approximate internal girder forces due to moment, M

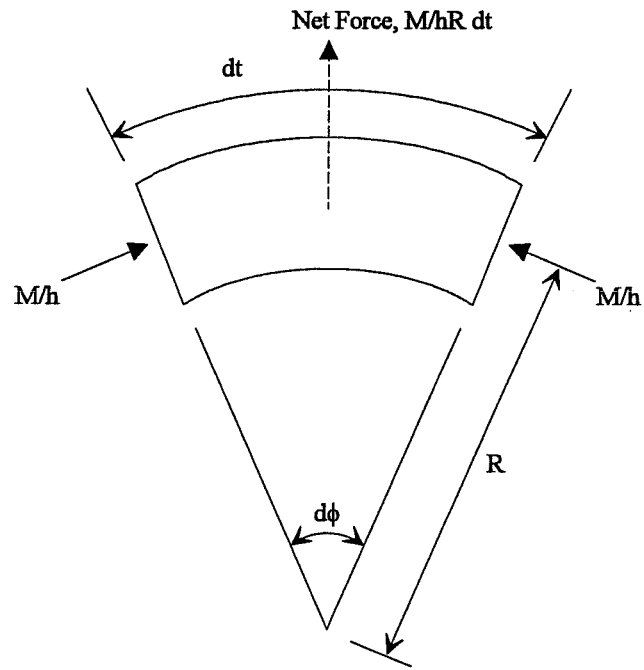


Figure C-2: Unbalanced transverse compression flange force in a differential section of curved girder

forces along the girder will follow directly from the distribution of bending moment due to vertical load.

Development of V-loads

In a curved bridge, diaphragms or cross-braces at regular intervals provide resistance to the torsional forces in the girders. It is assumed that each cross-frame will resist the torsional forces developed over a tributary length of the girder. This tributary length extends from half-way to the previous cross-frame to half-way to the next cross-frame, so for evenly spaced cross-frames, the tributary length equals the cross-frame spacing d . It is further assumed that the bending moment in the girder is constant over this tributary length with a value equal to the moment at the cross-frame. Thus, the total lateral force that the cross-frame must resist for each girder flange is Md/hR , as shown in Figure C-3, where M is the bending moment in the girder at the cross-frame. Since these forces are applied as equal and opposite forces – they are applied as a couple – to the girder flanges to resist the girder torsion, a counterbalancing couple must be generated in the cross-frame to satisfy equilibrium of the cross-frame. This counterbalancing couple consists of vertical shear forces V in the cross-frame. These vertical shear forces are transferred to the girders, which resist these forces in bending, as shown in Figure C-4. Thus, the rigid cross-frames have the effect of transforming torsional forces on the girders into concentrated vertical forces on the girders.

The distribution of the forces is such that the shear forces on the outside girder will tend to increase the moment in that girder, while the shear forces on the inside girder will tend to decrease the moment in that girder. In a two-girder system, the lateral flange forces will equal M_1d/hR and M_2d/hR for the

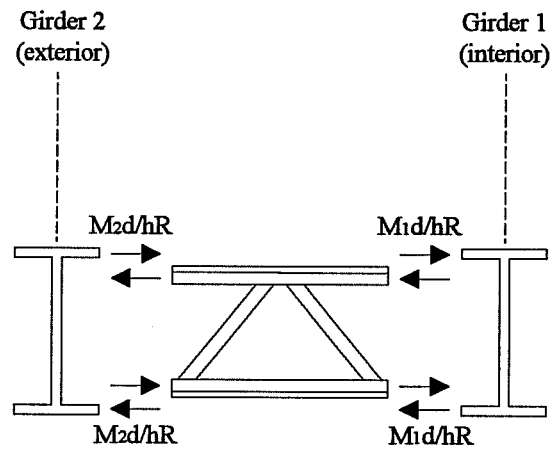


Figure C-3: Distribution of transverse flange forces to the cross-frame

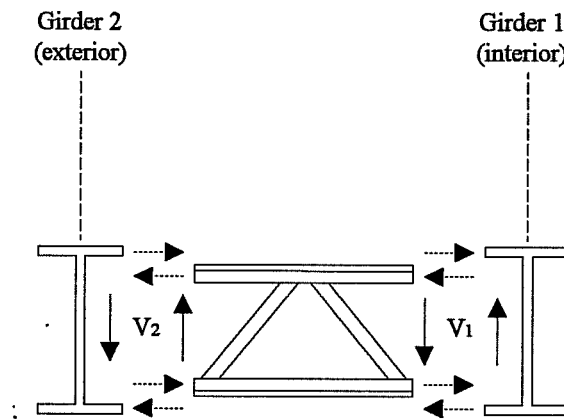


Figure C-4: Equilibrating shear forces between the cross-frame and the girders

inside girder and outside girder, respectively. Moment equilibrium in the cross-frame gives

$$VD = (M_1 d / hR + M_2 d / hR) h \quad (\text{C-1})$$

or

$$V = (M_1 + M_2) / (RD) / d = (M_1 + M_2) / k \quad (\text{C-2})$$

where D is the spacing between the innermost and outermost girders and k equals RD/d . These V -loads are calculated and applied to each girder at each cross-frame with the V -loads applied in such a way so as to increase moment on the outside girder and decrease moment on the inside girder. This means that in the positive moment region, for example, the outside girder is loaded with V and the inside girder is loaded with $-V$, where a downward load is considered positive. Each girder is now analyzed again with the V -loads applied in addition to the vertical bridge loads to produce a new moment diagram. For the two-girder system, each girder must resist half of the torsion imposed in the cross-frame since the system is statically determinate with respect to the distribution of the vertical shear loads between the girders. In multigirder systems, the loads must be distributed based on both equilibrium and compatibility. It is reasonable to assume that the cross-frame rotates essentially as a rigid body. If each girder has approximately the same bending stiffness, then the shear forces will be distributed linearly from one end of the cross-frame to the other. For multigirder systems, then, the V -load formula becomes

$$V = \Sigma M / Ck \quad (\text{C-3})$$

where C is a constant reflecting the effect of distributing V -loads to a number of girders. The values for C are tabulated below in Table C-1 for a few systems with different numbers of girders, where these girders are equally spaced across the cross-section.

Table C-1: Coefficients C for V-load Calculations

No. of Girders	Coefficient, C
2	1
3	1
4	10/9
5	5/4
6	7/5
7	14/9
8	12/7
9	15/8
10	165/81

These coefficients scale the V-loads to the correct magnitude for the outside and inside girders. The V-loads for the interior girders are found from linear interpolation between the exterior and interior girders. For example, for a four-girder system the V-load applied on each girder at a cross-frame in the positive moment region will be, from inside to outside, $-V$, $-V/3$, $V/3$ and V , respectively, as shown in Figure C-5, where a downward force is considered positive.

As an additional note on the V-load method, although this description of the V-load method has assumed noncomposite plate girders, finite element models have shown that the V-load method also produces good results for bridges with composite girders [9], so that this study will not consider composite girders a violation of the assumptions.

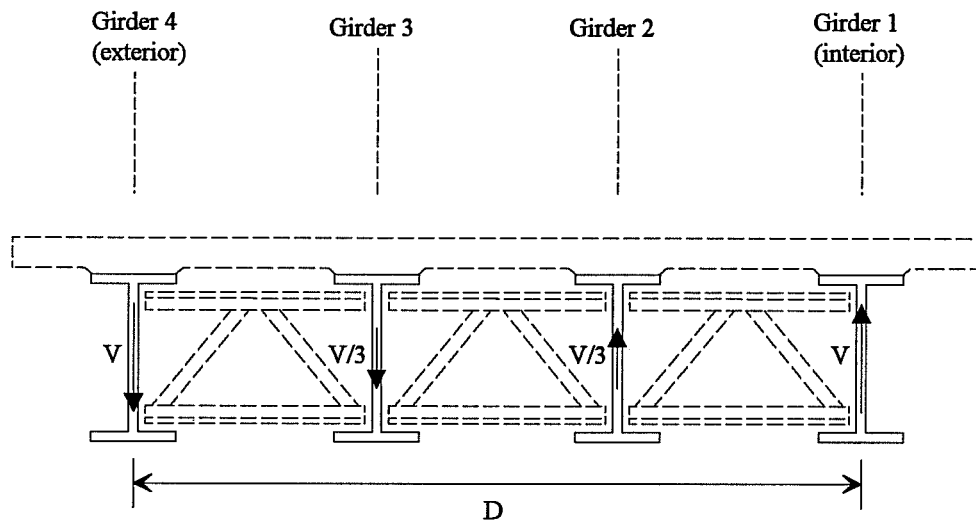


Figure C-5: Distribution of equilibrating V-load vertical shear forces to the girders

BIBLIOGRAPHY

1. *Standard Specifications for Highway Bridges*, Fifteenth Edition, American Association of State Highway and Transportation Officials, Washington, D.C., 1992
2. *Guide Specifications for Horizontally Curved Highway Bridges*, American Association of State Highway and Transportation Officials, Washington, D.C., 1987
3. *Allowable Stress Design*, Ninth Edition, American Institute of Steel Construction, Inc., Chicago, Illinois, 1989
4. *ANSYS User's Manual*, Swanson Analysis Systems, Inc., Houston, Pennsylvania, 1992
5. C.P. Heins, *Bending and Torsional Design in Structural Members*, D.C. Heath and Company, Lexington, Massachusetts, 1975
6. C. Kollbrunner, K. Basler, *Torsion in Structures*, Springer-Verlag, New York, 1966
7. Richardson, Gordon, and associates, "Analysis and Design of Horizontally Curved Steel Bridge Girders," United States Steel Structural Report, 1963
8. *Highway Structures Design Handbook*, Volume 1, Chapter 12, United States Steel Corporation, 1965
9. *Highway Structures Design Handbook*, Volume 1, Chapter 12, United States Steel Corporation, 1984

VITA

Jason Eric Olsen was born in Lodi, California on April 29, 1970 to Robert and Sandra Olsen. In June 1988 he graduated from Alexander Patch American High School in Stuttgart, Germany. He received the degree of Bachelor of Science in Civil Engineering from Rice University in Houston, Texas, in May 1992 . In August 1992 he entered The Graduate School of The University of Texas at Austin.

Permanent Address: 8070 Glen Creek Way
Citrus Heights, California 95610

This thesis was typed by the author.